

**FABRICATION, SURFACE MODIFICATION AND  
GROWTH FACTOR ENCAPSULATION OF  
POLYMERIC MICROSPHERES AS SCAFFOLD FOR  
LIVER TISSUE REGENERATION**

**BY**

**XINHAO ZHU**

**NATIONAL UNIVERSITY OF SINGAPORE**

**2008**



**FABRICATION, SURFACE MODIFICATION AND  
GROWTH FACTOR ENCAPSULATION OF  
POLYMERIC MICROSPHERES AS SCAFFOLD FOR  
LIVER TISSUE REGENERATION**

**BY**

**XINHAO ZHU**

*(M. Eng., B. Eng., TsingHua University)*

**A THESIS SUBMITTED**

**FOR THE DEGREE OF DOCTOR OF PHILOSOPHY**

**DEPARTMENT OF CHEMICAL AND BIOMOLECULAR ENGINEERING**

**NATIOANL UNIVERSITY OF SINGAPORE**

**2008**

*To Wen Lie*

## **Acknowledgements**

I would like to sincerely express my gratitude to my supervisors Professor Yen Wah Tong and Professor Chi-Hwa Wang for their constant guidance, unreserved supports, comments and suggestions throughout my whole Ph.D. studies, which helped me to become a better researcher.

I would like to thank Professor En-Tang Kang and Professor Kai Chee Loh for their valuable comments and suggestions during my Ph.D. qualifying examination, which improved my research proposal greatly. Also, I would like to thank Professor Lin-Yue Yung for sharing his research lab and equipment.

I would like to thank Mr. Jeremy Daniel Lease, Mr. Shih Tak Khew, Mr. Chau Jin Tan, Mr. Nikken Wiradharma, Mr. Wenhui Chen and other group members for helpful technical supports and discussions.

I am grateful to all the technical staff and lab officers for their supports. I would like to thank the Department of Chemical and Biomolecular Engineering, National University of Singapore for providing me the research scholarship. Finally, I would like to thank my family and all of my friends for their supports on my study. Their love and supports help me to focus on this research in the past four years.

## **Table of Contents**

Acknowledgements		i
Table of Contents		ii
Summary		iv
Nomenclature		vii
List of Tables		xi
List of Figures		xii
Chapter 1	Introduction	1
	1.1 Background and Motivation	1
	1.2 Hypothesis	4
	1.3 Objectives	5
Chapter 2	Literature Review	8
	2.1 Tissue Engineering	8
	2.2 Liver and Liver Tissue Engineering	11
	2.3 Biocompatible Scaffold and Biomaterials	14
	2.4 Surface Modification of the Scaffold	21
	2.5 Delivery of Growth Factor for Tissue Engineering	25
	2.6 Vascularization for Tissue Engineering	30
	2.7 Summary	32
Chapter 3	Fabrication and Characterization of PHBV Microsphere scaffold	34
	3.1 Materials and Methods	35

	3.2 Results and Discussion	42
	3.3 Conclusions	58
Chapter 4	Proteins Combination on PHBV Microsphere Scaffold to Regulate Hep3B Cells Activity and Functionality	59
	4.1 Materials and Methods	61
	4.2 Results and Discussion	66
	4.3 Conclusions	87
Chapter 5	Delivery of Hepatocyte Growth Factor from Microsphere Scaffold for Liver Tissue Engineering	88
	5.1 Materials and Methods	90
	5.2 Results and Discussion	96
	5.3 Conclusions	116
Chapter 6	Gelatin Microsphere based <i>In Vitro</i> Vascularization	118
	6.1 Materials and Methods	120
	6.2 Results and Discussion	125
	6.3 Conclusions	141
Chapter 7	Conclusions and Recommendations	142
	7.1. Conclusions	142
	7.2 Recommendations for Future Work	145
	List of Publications	148
	References	150

## Summary

Tissue engineering has emerged as a promising alternative to traditional surgical procedures in regenerating or repairing damaged organs. One of the major strategies of tissue engineering is to culture isolated cells on a three-dimensional scaffold, which will be developed into a functional tissue with proper stimulation. In this study, a novel scaffolding system via polymer microspheres was developed for the purpose of constructing an engineered liver tissue to solve the shortage of liver donors.

Poly (3-hydroxybutyrate-*co*-3-hydroxyvalerate) (PHBV, 8% PHV), a type of microbial polyester, was chosen as the scaffold material due to its biodegradability and biocompatibility. PHBV microspheres with the sizes between 100-300 $\mu$ m were found to be ideal in supporting liver cells growth. Optical and scanning electron microscope images showed that the microspheres were assembled by the cells to form tissue-like constructs after two weeks of culture, while confocal images confirmed that more than 90% of cells were alive. Compared to the cells cultured on positive control, HepG2 cells grown on microsphere scaffold showed a proliferation up to 1.9 times more than that of positive control. HepG2 cells grown on microsphere scaffold secreted albumin 2-4 times more than that on the positive control, which indicated an improved hepatic function.

Three types of extracellular matrix (ECM) proteins, namely collagen, fibronectin and laminin were covalently conjugated onto the surfaces of PHBV microspheres to

improve the biocompatibility of the scaffold. The improved proliferation of cells cultured on mixed protein-conjugated samples, which was around 1.4 times greater than single protein conjugated samples (collagen), suggested that the proliferation of Hep3B cells did not just depend on single protein, but rather, involved complex interactions with all of the ECM components. Furthermore, it was found that hepatocytes with round morphology performed better hepatic functions while having lower proliferation. Thus, during the design of a tissue engineering system, a scaffold showing different surface properties at different cell development stages might be necessary.

One promising feature of microsphere scaffolds is that the growth factors can be encapsulated into the scaffold directly. Three types of polymer microspheres (PHBV, Poly(lactic-co-glycolic acid) PLGA, and PHBV/PLGA) with distinct release profiles of hepatocyte growth factor (HGF) were fabricated. Sustained delivery of HGF from PHBV/PLGA composite microsphere with a core-shell structure was achieved while maintaining bioactivity for at least 40 days. The high encapsulation efficiency (88.62%), moderate degradation rate and well preserved structure after three months of incubation indicated that the composite microspheres would therefore be more suitable as a scaffold. It was also found that bovine serum albumin (BSA) was a suitable model protein for HGF and functioned as stabilizer to prevent the denaturation of HGF during the fabrication process. These were justified by the similar release profiles of BSA and HGF as well as the well-maintained bioactivity of HGF.

Vascularization of the scaffolding system is a prerequisite for the success in engineering large tissues such as the liver. Human umbilical vein endothelial cells



were cultured on gelatin microspheres for the application of *in vitro* vascularization. Basic fibroblast growth factor (bFGF) was then incorporated into the gelatin microspheres based on ionic complexation. Compared to blank microspheres, the proliferation of cells grown on bFGF loaded gelatin microspheres was improved up to 1.3 times, which indicated that the bioactivity of bFGF was well maintained during the incorporation and release process. Capillary-like structure was formed after the incorporation of endothelial cells coated gelatin microspheres into a fibrin gel matrix, and which could be used to prevascularize the engineered liver tissue.

In summary, the viability of using a novel microsphere scaffolding system to regenerate liver tissue was explored in this study. The microsphere scaffold can be easily assembled into various shapes suitable for surgical implantation. It also offers controllable surface modification, growth factor encapsulation properties as well as *in vitro* vascularization, which show great promise for the production of a complete liver tissue engineering system.

**Keywords:** tissue engineering, scaffold, polymeric microsphere, surface modification, growth factor, liver regeneration

## Nomenclature

2D	Two-dimensional
3D	Three-dimensional
Ang-1	Angiopoietins-1
ASGP-R	Asialoglycoprotein receptor
bFGF	Basic fibroblast growth factor
BMP2	Bone morphogenetic protein-2
BSA	Bovine serum albumin
CD	Circular dichroism
CLSM	Confocal laser scanning microscope
CTP	Calcium titanium phosphate
DMEM	Dulbecco's modified eagle's medium
DMSO	Dimethyl sulphoxide
ECGS	Endothelial cell growth supplement
ECM	Extracellular matrix
EDC	N-Ethyl-N'-(3-dimethylaminopropyl) carbodiimide hydrochloride
EDTA	Ethylenediaminetetra-acetic acid
EE	Encapsulation efficiency
EGF	Epidermal growth factor
ELISA	Enzyme-linked immunosorbent assay
EROD	Ethoxyresorufin-o-dealkylase

FBS	Fetal bovine serum
FDA	Food and drug administration
FITC	Fluorescein isothiocyanate
FTIR	Fourier transform infrared spectroscopy
GF	Growth factor
GMs	Gelatin microspheres
GTA	Glutaraldehyde
HBSS	HEPES-buffered saline solution
HCl	Hydrogen chloride
Hep3B	Human hepatoma cell line
HepG2	Human hepatoma cell line
HGF	Hepatocyte growth factor
HPLC	High performance liquid chromatography
HUVECs	Human umbilical vein endothelial cells
IEPs	Isoelectric points
L-929	Mouse fibroblast cell line
LSCM	Laser scanning confocal microscope
MTT	3-(4,5-dimethylthiazol-2-yl)-2,5-diphenyltetrazolium bromide
NaOH	Sodium hydroxide
NC	Negative control
NHS	N-Hydroxysuccinimide
NSF	National science foundation

P-450	Cytochrome P-450
PBS	Phosphate buffer solution
PCL	Poly ( $\epsilon$ -caprolactone)
PDGF	Platelet-derived growth factor
PHB	Poly(3-hydroxybutyrate)
PHBV	Poly(3-hydroxybutyrate- <i>co</i> -3-hydroxyvalerate)
PHBV (8%)	Poly(3-hydroxybutyrate- <i>co</i> -3-hydroxyvalerate) (8% HV content)
PLA	Poly lactide
PLGA	Poly(lactic- <i>co</i> -glycolic acid)
PLG	Poly(lactide- <i>co</i> -glycolide)
PLLA	Poly(L-lactide)
PLL	Poly-L-lysine
PVA	Poly (vinyl alcohol)
RGD	Arg-Gly-Asp
rpm	Revolutions per minute
SD	Standard deviation
SE	Seeding efficiency
SEM	Scanning electron microscope
SF	Serum-free
Sulfo-NHS	N-Hydroxysulfosuccinimide
TCP	Tissue culture plate
Tg	Glass transition temperature

T <sub>m</sub>	Melting temperature
TGF	Transforming growth factor
UV	Ultraviolet
VEGF165	Vascular endothelial growth factor
w/o/w	Water-in-oil-in-water
w/o	Water-in-oil
w/v%	Weight per volume percent
XPS	X-ray photoelectron spectroscopy
YIGSR	Tyr-Ile-Gly-Ser-Arg
ZDBC	Polyurethane film containing 0.25% zinc dibutyldithiocarbamate

## **List of Tables**

Table 2-1	A list of growth factors commonly used in tissue engineering	27
Table 3-1	PHBV microspheres obtained from different homogenizing speeds.	43
Table 4-1	Surface density of proteins conjugation to microspheres	68
Table 4-2	Atomic composition and percentage of C1s in XPS spectra of native and modified PHBV microspheres	69
Table 5-1	PHBV, PLGA and PHBV/PLGA microspheres encapsulated with BSA	97
Table 5-2	Surface chemical composition of PHBV, PLGA and PHBV/PLGA microspheres.	99
Table 5-3	PHBV/PLGA microspheres with BSA and HGF co-encapsulated	101
Table 6-1	Size and swelling ratio of gelatin microspheres	128

---

## List of Figures

Figure 2-1	Schematic representation of tissue engineering approach.	10
Figure 2-2	Liver structure in human body. The highly vascularized system is essential for the liver to perform normal function.	12
Figure 2-3	Molecular structure of PHBV: (a) PHB and (b) PHV.	19
Figure 2-4	Cell adhered on polymer surface mediated by cell adhesive molecules and integrin receptors	23
Figure 3-1	(a) and (b) SEM images of PHBV microspheres with an average diameter of 153.2 $\mu\text{m}$ illustrating their spherical shapes and uniform sizes; (c) magnified image of (b) showing a rough surface with nano-pores; (d) cross-section of the microsphere.	45
Figure 3-2	The seeding efficiency of HepG2 cells on microsphere scaffolds ( $+p < 0.05$ ).	46
Figure 3-3	Optical micrographs of HepG2 cells growth on M1 after (a) 2 days, (b) 4 days, (c) 8 days and (d) 14 days of culture, (e) HepG2 growth on M2 after 14 days of culture, (f) HepG2 growth on M3 after 14 days of culture;	48
Figure 3-4	CLSM images of Hep3B cells grown on M1 after two weeks of culture. (a,b) Cells were stained with live/dead kit. (c,d) Cell actins were dyed with phalloidin-FITC, and the nucleuses were dyed with DAPI.	50
Figure 3-5	SEM images of HepG2 cells seeded on M1 after (a, b) one week; (c, d) two weeks of culture; where b, d, are higher magnifications of a, c respectively.	51

---

Figure 3-6	SEM images of Hep3B cells seeded on M1 after (a, b) one week; (c, d) two weeks of culture; where b, d are higher magnifications of a, c respectively.	52
Figure 3-7	Proliferation of HepG2 cells cultured on positive controls and microspheres as assessed by (a) MTT assay; (b) total DNA quantification. Values represent means $\pm$ SD, n=3.	54
Figure 3-8	Albumin secretion by (a) HepG2 and (b) Hep3B cells cultured on controls and microspheres. Values represent means $\pm$ SD, n=3.	55
Figure 3-9	Cytochrome P-450 activity of Hep3B cells cultured on controls and microspheres. Values represent means $\pm$ SD, n=3.	57
Figure 4-1	CLSM images of surface modified PHBV microsphere grafted with (a) Collagen, (b) Fibronectin, (c) Laminin, (d) RGD, (e) YIGSR, and (f) SEM image of blank microsphere. Proteins and peptides were marked with FITC.	67
Figure 4-2	XPS spectra (C1s) of PHBV microspheres (a) Blank, (b) NaOH treated, and surface conjugated with (c) RGD, (d) YIGSR, (e) Collagen, (f) Fibronectin and (g) Laminin.	70
Figure 4-3	Optical microscope images of cell-microsphere constructs cultured for one week on (a) Blank, (b) NaOH treated, (c) Collagen-conjugated, and (d) Laminin-conjugated PHBV microspheres.	72
Figure 4-4	CLSM images of cell-microsphere constructs cultured for one week on (a) Blank, (b) NaOH treated, (c) Collagen-conjugated, and (d) Laminin-conjugated PHBV microspheres.	73



---

Figure 4-5	SEM images of cell-microsphere constructs cultured for one week on (a) Blank, (b) NaOH treated, (c) Collagen-conjugated PHBV microspheres; (d) higher magnification of (c).	75
Figure 4-6	Proliferation of Hep3B cells cultured on (a) Blank, NaOH treated, Collagen-conjugated, Fibronectin-conjugated, Laminin-conjugated; and (b) proteins combination (Collagen:Fibronectin:Laminin) with a ratio as 1:1:1, 3:1:1, and 1:3:3 PHBV microspheres.	78
Figure 4-7	Albumin secretion by Hep3B cells cultured on (a) Blank, NaOH treated, Collagen-conjugated, Fibronectin-conjugated, Laminin-conjugated; and (b) proteins combination (Collagen:Fibronectin:Laminin) with a ratio as 1:1:1, 3:1:1, and 1:3:3 PHBV microspheres.	80
Figure 4-8	Cytochrome P-450 activity of Hep3B cells cultured on (a) Blank, NaOH treated, Collagen-conjugated, Fibronectin-conjugated, Laminin-conjugated; and (b) proteins combination (Collagen:Fibronectin:Laminin) with a ratio as 1:1:1, 3:1:1, and 1:3:3 PHBV microspheres.	83
Figure 4-9	Proliferation of Hep3B cells cultured on Blank, RGD-conjugated, YIGSR-conjugated, and proteins combination (Collagen:Fibronectin:Laminin) with a ratio as 1:1:1 PHBV microspheres.	85
Figure 4-10	Cytochrome P-450 activity of Hep3B cells cultured on Blank, RGD-conjugated, YIGSR-conjugated; and proteins combination (Collagen:Fibronectin:Laminin) with a ratio as 1:1:1 PHBV microspheres.	86
Figure 5-1	SEM images of PHBV (A), PHBV/PLGA (B), partially dissolved PHBV/PLGA (C), and PLGA (D) microspheres, where panels labeled with 1, 2 and 3 respectively are the general morphology, cross section and close-up on the surface of the microspheres.	98

Figure 5-2	Degradation profiles of microspheres characterized by mass loss up to 110 days for PHBV, PHBV/PLGA, and PLGA. Dotted line shows the degradation profile of PHBV/PLGA microsphere in the presence of Hep3B cells.	103
Figure 5-3	SEM images of PHBV (A) and PHBV/PLGA (B) microspheres after 90 days of degradation, and PLGA (C) microspheres after 30 days of degradation, where panels labeled with 1, 2 and 3 respectively are the general morphology, cross section and close up on the surface of the microspheres.	104
Figure 5-4	Cumulative release of BSA from PHBV, PHBV/PLGA, and PLGA microspheres.	105
Figure 5-5	Actual concentrations of released BSA and HGF from PHBV/PLGA microspheres. Different scales were used to plot HGF and BSA for comparison purposes.	107
Figure 5-6	Hep3B cell proliferations measured by total-DNA assay after incubating the cells in the released HGF and BSA for 24 hours. SF medium was used as the positive control, while SF medium containing 5 ng/mL and 50 ng/mL HGF were used as negative controls.	109
Figure 5-7	Albumin secretions by Hep3B cells after incubating the cells in the released HGF and BSA for 24 hours. SF medium was used as the positive control, while SF medium containing 5 ng/mL and 50 ng/mL HGF were used as negative controls.	111
Figure 5-8	P-450 activity of Hep3B cells after incubating the cells in the released HGF and BSA for 24 hours. SF medium was used as the positive control, while SF medium containing 5 ng/mL and 50 ng/mL HGF were used as negative controls.	112

---

Figure 5-9	Proliferation of primary hepatocytes cultured on PHBV/PLGA microspheres and controls as assessed by total-DNA assay. Cells were cultured on microspheres loaded with HGF, blank microsphere, while cell culture medium supplemented with 50 ng/mL of HGF or without HGF were used as controls.	113
Figure 5-10	Cytochrome P-450 activity of primary hepatocytes cultured on PHBV/PLGA microspheres and controls as assessed by total-DNA assay. Cells were cultured on microspheres loaded with HGF, blank microsphere, while cell culture medium supplemented with 50 ng/mL of HGF or without HGF were used as controls.	115
Figure 5-11	Albumin secretion by primary hepatocytes cultured on PHBV/PLGA microspheres and controls as assessed by total-DNA assay. Cells were cultured on microspheres loaded with HGF, blank microsphere, while cell culture medium supplemented with 50 ng/mL of HGF or without HGF were used as controls.	116
Figure 6-1	SEM images of gelatin microspheres. (A) Non-cross-linked, and Cross-linked with GTA at the concentrations of (B) 5 mM, (C) 10 mM and (D) 20 mM. Light micrographs of (E) Dry and (F) Wet gelatin microspheres cross-linked with 10 mM GTA.	127
Figure 6-2	FTIR spectrum of gelatin microspheres cross-linked with glutaraldehyde.	129
Figure 6-3	Optical micrographs of the morphologies of HUVEC cells grew on gelatin microspheres after (A, D) Three hours (initial adhesion), (B, E) 1 days, and (C, F) 7 days of culture. The right column indicated the cells grew on individual microsphere, while the left column indicated the cell-microsphere clusters. The microspheres were cross-linked with 10 mM GTA.	131

Figure 6-4	SEM (A, B) and CLSM (C, D) images of HUVEC grew on gelatin microspheres after one week. Cell actin was dyed with Phalloidin-FITC, and the nucleus was dyed with DAPI. The microspheres were cross-linked with 10 mM GTA.	133
Figure 6-5	Proliferation of HUVEC cells cultured on gelatin microspheres cross-linked with different concentrations of GTA as assessed by MTT assay. 5 mM, 10 mM, 20 mM. Blank well was used as the control.	134
Figure 6-6	Cumulative release of bFGF from gelatin microspheres cross-linked with different concentrations of GTA. 5 mM, 10 mM, 20 mM.	136
Figure 6-7	Proliferation of HUVEC cells cultured on gelatin microspheres and controls as assessed by MTT assay. Microspheres loaded with bFGF, blank microsphere. Cell culture medium supplement with 60 ng/mL of bFGF or without bFGF were used as controls.	137
Figure 6-8	In vitro formation of capillary network using HUVEC-coated gelatin microspheres (GMs) embedded into a fibrin gel. (A, D) HUVEC grown on blank GMs, (B, E) HUVEC grown on blank GMs with bFGF as supplement of the cell culture medium and (C, F) HUVEC grown on GMs incorporated with bFGF. The left column indicated the cells grew in the gel for 1 day, while the right column indicated the cell grew in the gel for 5 days.	140

# Chapter 1 Introduction

## 1.1 Background and Motivations

Every year millions of people in the world suffer from tissue damage or end-stage organ failure. The traditional procedures to treat these patients include organ transplantation, performing surgical reconstruction and using mechanical devices such as kidney dialyzers. Although there have been tremendous advances in these therapies and countless lives have been saved, the declining availability of compatible donor organs as well as high cost of treatment severely limit their applications. For example, in the United States, about 30,000 people are on the waiting list for liver transplantation each year while only ten percent of them can get a donor liver, and in Singapore alone, around 15 patients die each year while waiting for a liver.

The science of tissue engineering, which aims to develop biological substitutes to maintain or regenerate damaged organs, has therefore emerged from the challenges posed by these limitations, and has turned out to be a promising alternative to regenerate failed organs. One of the major strategies of tissue engineering is to culture isolated cells, either from the patients (autologous) or other sources (allogeneous or xenogeneous), on a three-dimensional (3D) scaffold. Under proper environment and stimulation, a functional engineered tissue will be developed which should be

structurally and functionally integrated into the body upon being grafted into the patient. Important considerations concerning the success of tissue engineering include the biology and spatial organization of the organ to be replaced, the cell source, *in vitro* culture techniques, and the design of the scaffold. Among these numerous factors, 3D scaffolds play a vital role, which provide temporary templates for cells to attach, proliferate and produce extracellular matrix (ECM) proteins, and also to encourage the migration of cells from the surrounding healthy tissue into the scaffold. Scaffolds may also provide a spectrum of bioactive molecules, such as ligands, growth factors, hormones and enzymes to regulate the behaviors of the cells.

Finding appropriate scaffold for a specific organ has always been a significant challenge for tissue engineers. Two-dimensional (2D) polymer films or meshes scaffolds are the simplest forms, and to date, the most successful clinical case is to engineer skin tissues with polymer mesh. However, to some extent, the polymer films or meshes are only suitable for organs with simple structures, while many types of cells would dedifferentiate quickly when being cultured in the 2D environment. Applications of polymer rods, hydrogel and sponges for bone tissue repair and cartilage regeneration have been also extensively investigated. In these cases, the scaffolds are usually fabricated to be similar in shape as the defects for easy implantations. However, for more complex organs, such as the liver, the research is still in its infancy. One big problem is that the quick dedifferentiation of primary hepatocytes (liver cells) to lose the normal liver functions (albumin secretion, detoxification ability) when cultured *in vitro* without the appropriate environment. The lack of sufficient oxygen and nutrient supply may also induce the death of the cells. Therefore, a novel scaffolding system which could provide the proper environment to

preserve the phenotype of the liver cells as well as enough nutrients is necessary for the success of engineering a liver tissue, forming the main motivation for this project.

Microspheres have been traditionally used as drug delivery vehicles or carriers to harvest cells. The unique 3D environment offered by microspheres can improve cell proliferation as well as preserve their differentiated functions. Based on these advantages, we propose to use microspheres as scaffold to regenerate liver tissue. Unlike traditional scaffolds with specific shape or structure, in a microsphere scaffolding system, cells could be first seeded on individual microsphere, and the microspheres could then be assembled into various shapes suitable for different tissue or defects. Microspheres also offer easy and controllable surface modification to enhance cell-scaffold interactions. Furthermore, growth factors and other molecules can be encapsulated into the scaffold to regulate the cell behavior as they are released in a controlled manner. Thus, microsphere scaffolds offer clear cut benefits. However, studies on using microspheres as scaffolds are still limited especially for liver tissue engineering. Therefore, the major incentive of this project is to broaden the application of microspheres as tissue engineering scaffold and design a system with suitable dimension, structure as well as biocompatible surface properties, and controllable delivery of growth factors for the application in liver tissue regeneration.

Besides the structure of the scaffold, the materials are equally important. The scaffold materials should be bio-absorbed over time and the spaces occupied by the scaffolds should be replaced by secreted ECM or regenerated tissue. Biodegradable polymers are the most widely used material which includes natural polymers such as collagen and laminin, and synthetic polymers such as poly(lactic-co-glycolic acid)

(PLGA). The advantage of natural polymers is their good biocompatibility. However, poor control of the mechanical properties, molecular weight and biodegradability in addition to limited supply and high cost are some of their disadvantages. On the other hand, synthetic polymers are becoming more and more popular for use in tissue engineering due to their ease in controlling their chemical and physical properties, degradation rate and relatively low cost. Poly (3-hydroxybutyrate) (PHB) and poly (3-hydroxybutyrate-co-3-hydroxyvalerate) (PHBV), which are polyesters produced by bacteria, have many similar properties to PLGA and have also received much attention in applications for drug delivery and surgical operation. Moreover, as they are bacterially synthesized polyesters, PHB and PHBV could be more biocompatible than the synthesized polyesters and possess controllable mechanical strength which the natural polymers do not have. However, PHBV has been less widely studied for tissue engineering and further studies need to be carried out to verify its viability in this field.

## **1.2 Hypothesis**

It is hypothesized that three-dimensional PHBV microspheres are suitable substrates to guide liver cell growth and to regenerate the liver. Surface modification of the microsphere with ECM proteins can improve the biocompatibility of the scaffold and therefore promote cell adhesion, proliferation and differentiation. Encapsulation of growth factors in the microsphere will further simulate the *in vivo* microenvironment to regulate liver cell behavior and enable the cell-scaffold construct function properly. The overall goal of this research is to design a microsphere scaffolding system and to construct an engineered liver tissue with this system to reduce the cost of implantation and to solve the shortage of donated liver.



### 1.3 Objectives

This project seeks to explore the viability of using polymer microspheres as scaffold to engineer liver tissue. The objectives in this thesis include:

**Objective 1. To fabricate PHBV microsphere scaffolds and to determine the optimum dimension to guide the growth of liver cells.** The microspheres were fabricated by using the emulsion solvent evaporation technique. The morphology and size distributions of the microspheres were characterized by scanning electron microscopy (SEM) and particle size analyzer. Human hepatoma cell lines, Hep3B and HepG2 were cultured on the microspheres with different sizes to determine the optimum dimension of microspheres for the growth of liver cells.

**Objective 2. To modify the surfaces of the microspheres with bioactive molecules to improve their biocompatibility.** The microspheres were conjugated with three types of ECM proteins, collagen, laminin and fibronectin, and the surface densities of proteins and atomic composition were characterized by using Micro BCA<sup>TM</sup> protein assay and X-ray photoelectron spectroscopy (XPS) respectively. Hep3B cells were cultured either on microsphere conjugated with single protein type or a mixtures of microspheres individually conjugated with three types of proteins respectively, to study the interactions between various proteins and cells to regulate cell activity and functionality.

**Objective 3. To encapsulate growth factors in the microsphere scaffold to regulate the cell behaviors.** PHBV and PLGA were chose as the microsphere scaffold materials for the encapsulation of bovine serum albumin (BSA) and hepatocyte growth factor (HGF). The release of BSA served as the model for HGF since both proteins

have similar molecular weights and hydrophilicity, and the co-encapsulation of BSA with HGF were believed to be able to preserve the bioactivity of the growth factor by reducing its exposure to organic solvents. The effects of polymers on the morphologies, release and degradation profiles of the microsphere scaffolds were studied and the bioactivity of released HGF was assessed by using Hep3B cells and primary hepatocytes.

**Objective 4. To culture endothelial cells on gelatin microspheres for a preliminary study of *in vitro* angiogenesis.** Gelatin microspheres were fabricated using a water-in-oil emulsion technique and cross-linked with glutaraldehyde (GTA). Basic fibroblast growth factors (bFGF), which can improve angiogenesis *in vivo*, were incorporated into the gelatin microspheres by electrostatic interactions. The gelatin microspheres pre-seeded with human umbilical vein endothelial cells (HUVECs) were embedded into a fibrin gel to stimulate the formation of capillary-like structure *in vitro*.

This study involves the design of a novel tissue engineering system with polymer microsphere as scaffold, which could be applied to regenerate liver tissue and other similar soft tissues, like the kidney and the heart, to solve the shortage of organ donors. Furthermore, the results of surface modification will improve our understanding on the synergistic effects of ECM proteins on cells, and the growth factor delivery system can be developed as a feasible way in the application of soluble growth factors for tissue engineering. The preliminary study on *in vitro* angiogenesis could be used to pre-vascularize the scaffold for the purpose of providing oxygen, blood and nutrient to the cells growing in the deeper sections the scaffold.

Although the final purpose of this study is to regenerate a defective liver tissue, no *in vivo* animal experiments will be included in this thesis. All tests are based on *in vitro* cell culture experiments. Since the objectives of this thesis are to prove the viability of microsphere as scaffold for liver tissue engineering and to study the response of the liver cell in this microsphere scaffold system, *in vitro* cell culture is adequate for this purpose in addition to having some advantages, for example, relative easier to characterize and analyze, repeatable and low cost. Therefore, *in vivo* implantation is out of the scope of this thesis and can be considered as the future work.

In the next chapter, a literature review on liver tissue engineering will first be given, followed by discussions on the biomaterials and scaffolds for tissue engineering. Surface modification of scaffold, the application of drug delivery technique for tissue engineering and *in vitro* angiogenesis process will be also reviewed in detail. All these literature review will provide the theoretical basis for this study.

## Chapter 2 Literature Review

### 2.1 Tissue Engineering

Organ transplantation, surgical reconstruction and the use of mechanical devices are the main medical procedures used currently to treat patients with tissue damage or organ loss. Although these procedures have saved countless lives, they are imperfect with inherent limitations. Liver and kidney are among the commonly transplanted organs today. The successful application of organ transplantation is limited not by the surgical technique but by the declining availability of compatible donor organs, as well as high cost. Furthermore, long-term and massive drug administration is often required to maintain the normal function of the transplanted organ and to protect it from immune rejection. Surgical reconstruction often involves grafting tissues from one part of the patient to another part (autograft) which may result in donor site morbidity. Mechanical devices such as kidney dialysers are still not good enough to perform integrated functions of whole organs. Most of them can only serve as a temporary treatment to sustain the patient until a donated organ is available. Other devices, such as artificial heart valves, which are integrated into the patients for long-term applications, are subjected to mechanical failure (Langer and Vacanti, 1993; Hubbell and Langer, 1995).

The limitations of the current therapies encourage researchers to find alternatives, such as regeneration of failed organs. The science of tissue engineering, which combines the disciplines of engineering and life science to create functional tissue substitutes for the failed organs, therefore emerged from the challenges and advances a promising way to improve the health of human beings. The term “Tissue Engineering” was initially coined by National Science Foundation (NSF) in 1987 and defined as “the application of the principles and methods of engineering and life sciences toward the fundamental understanding of structure-function relationships in normal and pathological mammalian tissues, and the development of biological substitutes to restore tissues” (\*).

In tissue engineering, three general strategies are commonly used to create a functional tissue: (1) use of isolated cells or cell substitutes; (2) use of tissue-inducing substances; and (3) use of cells cultured on or within polymer matrices (Langer and Vacanti, 1993). All of these methods have shown some promising results, but only the third approach holds the promise of generating new tissue or organ *in vitro* and has thus become the major strategy for tissue engineering. Figure 2-1 is a typical schematic diagram for this strategy (Marler et al., 1998). Cells isolated from the patients (autologous) are seeded on or into three-dimensional (3D) scaffolds fabricated from natural or synthetic polymers. The cell-scaffolds are then cultured in static or dynamic environments to promote cellular remodeling and tissue formation. A functional engineered tissue will be thus developed, which would be structurally and functionally integrated into the body upon being grafted back to the patients. As the cells grow, they will secrete their own extracellular matrix (ECM). The scaffold should therefore

---

\* [http://www.nsf.gov/od/lpa/nsf50/nsfoutreach/htm/n50\\_z2/pages\\_z3/45\\_pg.htm](http://www.nsf.gov/od/lpa/nsf50/nsfoutreach/htm/n50_z2/pages_z3/45_pg.htm)

be biocompatible and biodegradable at a suitable rate so that the space occupied by the scaffold initially is eventually replaced by the regenerated natural tissue.

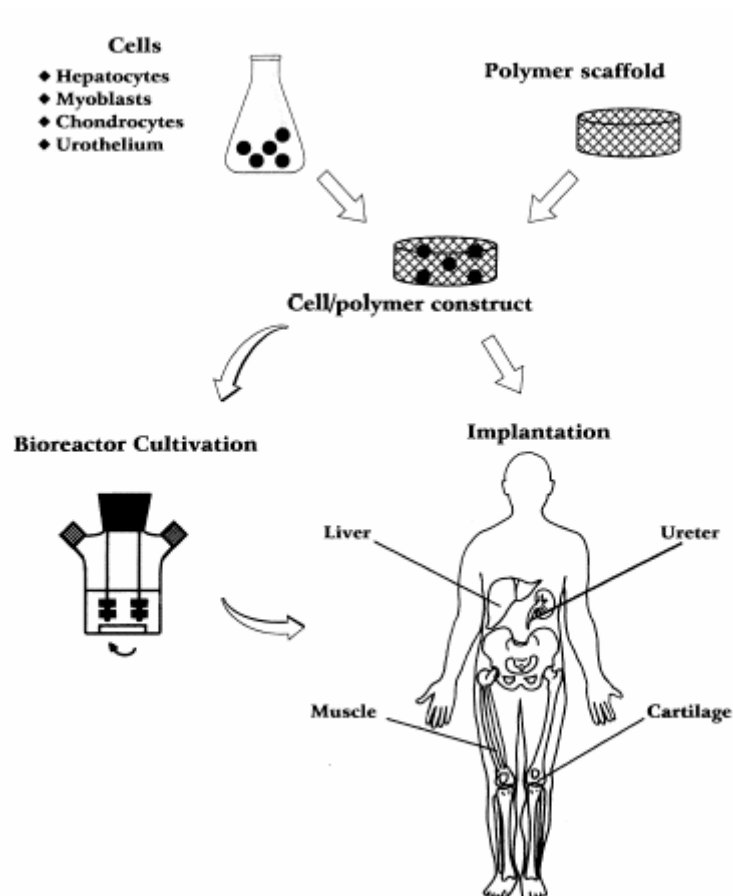


**Figure 2-1.** Schematic representation of the tissue engineering approach (Adapted from Marler et al., 1998).

Meeting the challenges of engineering tissue substitute means answering the question of how to imitate nature accurately. To do so, researchers should address at least three issues: (1) cell-related considerations such as cell source (autologous, allogeneic, xenogeneic and stem cell), and manipulation of cell proliferation and functions; (2) designing a 3D substrate which allows the cells to organize and remodel to develop into tissue-like constructs; and (3) integration of the tissue-like constructs into the living system (Nerem, 2000). Therefore, scientists from various fields

including biologists, material (especially polymer) experts, biomedical specialists and surgeons need to work together to meet the challenge and make tissue engineering a successful therapy for regenerating defective tissues.

Investigators have attempted to engineer virtually every mammalian tissue including nerve, cornea, skin, cartilage, bone, tendon, muscles, liver, pancreas, and heart valves (Langer and Vacanti, 1993). To date, engineered skin tissue is the most successful in clinical application, and the efforts on engineering bone and cartilage tissues also show promising results. However, research on complex organs engineering, such as the liver, is still in its infancy and will be the object of discussion for this project.

## **2.2 Liver and Liver Tissue Engineering**

### **2.2.1 Liver**

The reddish brown, wedge-shaped liver is one of the most sophisticated and complicated organs in the human body (Figure 2-2) (\*). The liver performs a variety of metabolic and synthetic functions which are crucial for life. It secretes bile for digestion and synthesizes plasma proteins (albumin, globulin etc.), which are essential components of blood. Another important function of the liver is to detoxify xenobiotic and endogenous toxins. The liver also functions as a center of storage for glycogen and vitamins A, B, D and K (\*). The liver consists of multiple types of cells, such as hepatocytes, sinusoidal endothelial cells, stellate cells, and kupffer cells (Gumucio et

---

\* <http://www.cincinnatichildrens.org/svc/alpha/l/liver/liver-anatomy.htm>

al., 1996). Among them, hepatocytes make up more than 70% of the liver and perform most of the liver-specific functions mentioned above.

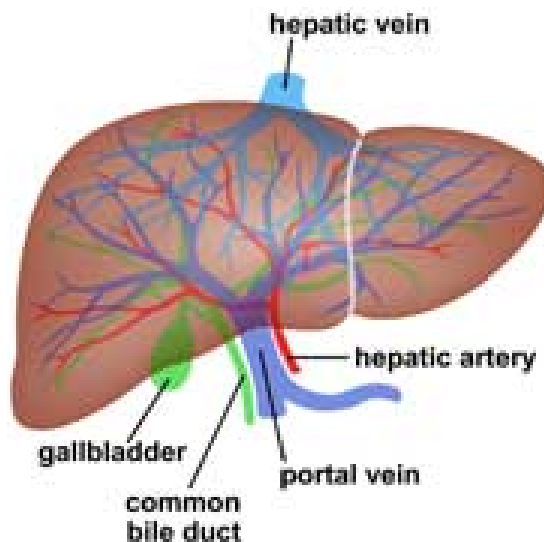


**Figure 2-2.** Liver structure in human body. The highly vascularized system is essential for liver to perform normal function \*.

Acute and chronic hepatitis, cirrhosis and liver cancer kill thousands of people every year. Currently, the main surgical treatment of severe end-stage liver disease is liver transplantation. However, the declining availability of donor livers and high medical cost led to patients losing their lives while waiting for liver donation. This situation is getting worse every year (Langer and Vacanti, 1993). Alternative therapies are urgently needed to overcome the shortage, and tissue-engineered liver is one candidate.

### **2.2.2 Liver tissue engineering**

The research on liver tissue engineering can be traced back to more than 20 years ago when the use of injected hepatocytes to replace hepatic functions was investigated (Davis and Vacanti, 1996). In this strategy, isolated hepatocytes were injected into the



defects directly with the hope that they can perform and restore the normal hepatic functions. However, necrosis and granuloma formation were frequently observed and it was difficult to distinguish injected hepatocytes from the host's. As an improvement, hepatocytes were attached onto micro-carriers or encapsulated into biocompatible membranes before the injection. The micro-carrier/membrane allowed incorporation of ECM proteins into the substrate to prolong the survival of the cells and to stimulate cell organization. However these are only effective in providing short-term replacement of the hepatic functions. Development of implantable engineered live tissue for long-term hepatic support still requires much work.

The various physiological functions and metabolic activities of the liver pose significant challenges to the engineering of implantable engineered liver tissue. Important considerations include the biology and spatial organization of the liver, the cell source, *in vitro* culture techniques, and the design of the scaffold. To date, culturing hepatocytes on biodegradable polymer scaffolds under proper microenvironment is believed to be a promising method to develop an implantable liver tissue (Davis and Vacanti, 1996). The scaffold acts as substrate to guide cell proliferation and functionality as well as to promote recombination of the ECM. Furthermore, the scaffold can be modified to incorporate ligands for cell receptors and release soluble stimuli such as growth factors, to regulate cell proliferation and differentiation (Jagur-Grodzinski, 2006). The scaffold is so important for the success of tissue engineering that finding an appropriate scaffold for specific tissue regeneration has always been one of the primary tasks for tissue engineers. Therefore, a detailed literature review on the biocompatible scaffold and the biomaterials used to fabricate the scaffold is given in next section.

## 2.3 Biocompatible Scaffold and Biomaterials

### 2.3.1 Biocompatible scaffold

As a temporary replacement of the ECM, the polymer scaffold plays an essential role in tissue engineering. It guides the growth of seeded cells *in vitro* as well as encourages migration of cells from surrounding healthy tissue into the scaffolds after implantation. The scaffold must therefore satisfy the following requirements: (1) suitable structure and shape, (2) large surface to volume ratio and porosity, (3) appropriate mechanical and surface properties, and (4) biodegradability (Freed and Vunjak-Novakovic, 1998; Thomson et al., 2000). A large surface area is preferred so that a high number of cells can seed on/in the scaffold. A highly porous structure with interconnected pores can enhance cell migration and ingrowth from the local tissues. It can also promote the formation of vasculature into the scaffold to allow the exchange of oxygen, nutrients and removal of metabolic wastes. This is essential in engineering thick tissue since diffusion is not enough to provide oxygen and nutrients to the cells growth inside the scaffold. Mechanical properties of the scaffold are often critical for hard tissue (such as cartilage and bone) regeneration. The roughness, wettability and charge of the scaffold surface are also reported to affect cell attachment, proliferation and functionality. Last but not least, the scaffold should ideally be biodegradable over time allowing ECM proteins or regenerated tissue to replace the space it occupied initially.

Various types of scaffolds have been studied for tissue engineering purpose in the last decade. Two-dimensional (2D) scaffolds such as polymer films or meshes made from nano-fibers are the simplest forms commonly used in preliminary experiments to

test the biocompatibility of the scaffold materials (Carlisle et al., 2000; Khang et al., 2002; Kim et al., 2003; Majima et al., 2005). To date, the best clinical success is with engineered skin tissues using polymer mesh. However, to some extent, the polymer films or meshes are only suitable for organs with simple structures and organization. Moreover, many types of cells would dedifferentiate quickly when cultured in a 2D environment. 3D substrates are necessary to promote cell proliferation as well as to preserve the phenotype. Applications of polymer rods, hydrogel and sponges for bone tissue repair and cartilage regeneration have therefore been extensively investigated (Köse et al., 2003; Lin and Yen, 2004; Stevens et al., 2004; Wayne et al., 2005). Stevens et al developed a rapid-curing alginate gel system which was capable of supporting the growth of chondrocytes. When whole-tissue explants of periosteum were cultured in the gel for six weeks, significant expansion of periosteal explants were observed, which could be transplanted for the treatment of partial or full-thickness defects in articular cartilage (Stevens et al., 2004). Lin et al fabricated alginate/hydroxyapatite (HAP) sponge for bone tissue engineering. The improved mechanical and cell-attachment properties suggested a promising approach to engineer bone tissue (Lin and Yen, 2004).

In these cases, for easy implantations, the scaffolds are usually fabricated to match only the architectures, structures and mechanical properties of defect sites. However, for more complex and highly vascularized organs such as the liver, this is insufficient. Besides the irregular shapes of the defects which limit the use of conventional scaffolds, another challenge is the quick dedifferentiation of primary hepatocytes leading to loss of the normal liver functions (such as albumin secretion, detoxification ability and etc). This occurs when the hepatocytes are cultured on polymer substrates

without an appropriate stimulation (Davis and Vacanti, 1996). Furthermore, when engineering thick tissue equivalents, diffusion alone would not be sufficient to provide oxygen and nutrients to cells growing in the deeper sections of the scaffolds (Griffith et al., 2005). Therefore, a novel scaffolding system which could preserve the phenotype of primary hepatocytes as well as allow enough nutrient exchange, in addition to being able to match the defect site physically, is necessary for the success of engineering a liver tissue.

### **2.3.2 Microsphere scaffold**

Microspheres have been traditionally used as drug delivery vehicles or carriers to harvest cells (Jacobson and Ryan, 1982; Cao and Shoichet, 1999; Malda et al, 2003). The unique 3D environment offered by microspheres can improve cells' proliferation and preserve their differentiated functions. However, using microspheres as a scaffold for tissue engineering is a new idea reported so far in only a few studies (Barrias et al., 2005; Mercier et al., 2005; Sahoo et al., 2005). Mercier et al. (2005) demonstrated the successful application of poly(lactide-*co*-glycolide) (PLG) microspheres as a moldable scaffold for cartilage repair. They reported that the cartilagenous tissue formed maintained thickness, shape, and chondrocyte collagen type II phenotype. According to Barrias, calcium titanium phosphate (CTP) microspheres improved bone marrow stromal cells' spread and proliferation, as well as expression of osteoblastic phenotype (Barrias et al., 2005). Sahoo et al. (2005) prepared various porous PLGA and polylactide (PLA) microspheres containing hydrophilic polymers poly(vinyl alcohol) (PVA) and evaluated their physical properties. Their results indicated that the cells showed better adhesion and growth on PLA-PVA microspheres due to the compatible

structure. Taken together, microsphere scaffolds made from synthetic polymers are good substrates to support cell growth and preserve the specific phenotypes. However, most synthetic polymers lack the ability to interact with cells specifically. Surface conjugation with extracellular matrix proteins and peptides are effective approaches to improve the surface biocompatibility. Hong et al. (2005) prepared PLA microspheres with larger amount of collagen on their surfaces by a method of aminolysis and grafting-coating. *In vitro* chondrocyte culture demonstrated that this surface modification is effective in making the microsphere more conducive to chondrocyte cells. Instead of natural proteins, Chen et al. (2006) modified poly(L-lactide) (PLLA) microspheres with RGDDSPK, a short peptide chain which can bind with the integrin receptors on cell membrane. Their results showed improved cell-matrix interactions.

In summary, the microsphere is a versatile scaffold which can assemble into various shapes suitable for different tissue applications, and it also offers easy and controllable surface modification for enhanced cell-scaffold interaction. However, the studies of microspheres as scaffold are still quite limited, especially on liver tissue engineering. Therefore, the use of microspheres to engineer liver tissue will be further explored in this project.

### **2.3.3 Biomaterials for scaffold**

#### **2.3.3.1 Natural and synthetic polymers**

Besides the scaffold's bulk physical properties, the scaffold material is equally important. A variety of materials have been studied for tissue engineering purpose, including degradable polymer (Langer, 1999; Pachence and Kohn, 2000) and non-

degradable ceramic materials (Rodriguez-Lorenzo and Ferreira, 2004). Among them, biodegradable polymers are the most widely used.

Biodegradable polymers can be gradually degraded through hydrolysis of the polymer backbone with the help of water or enzymes secreted by cells. They are broadly classified as synthetic and natural polymers.

Natural polymers widely used in tissue engineering scaffolds include collagen (Wallace and Rosenblatt, 2003), chitosan (Li et al., 2003), alginate (Dvir-Ginzberg et al., 2003), PHB and PHBV (Hu et al., 2003). One advantage of natural polymers is good biocompatibility. For example, as the major ECM component, collagen-derived scaffolds improve cell adhesion and functionality (Pachence and Kohn, 2000). The degradation products of natural polymers are non-toxic small molecules which can be converted into carbon dioxide and water over a period of time and removed by metabolic activity. However, poor control over the mechanical properties, molecular weight and biodegradability in addition to limited supply and high cost are the disadvantages for using natural polymer.

Synthetic polymers, on the other hand, are becoming increasingly popular in tissue engineering due to the ease of controlling the chemical and physical structure, degradation rate, and hydrophobicity, as well as low cost. Furthermore, they can be processed into scaffolds with complex shapes easily, and the surface or porosity of the scaffold can be modified without changing the polymer properties. The disadvantages are lack of intrinsic biological activity and possible production of toxic degradation products. The products may also change the local microenvironment dramatically, such as lowering the pH, which can affect cell growth and function. Some widely used

synthetic polymers in tissue engineering are poly ( $\epsilon$ -caprolactone) (PCL) (Coombes et al., 2004), PLA (Sahoo et al., 2005), and copolymer (PLGA) (Newman and McBurney, 2004; Mercier et al., 2005; Sahoo et al., 2005). PLA and PLGA have been the most widely used synthetic aliphatic polyesters in medical applications since they received the approval from the US Food and Drug Administration (FDA).

### 2.3.3.2 PHB and PHBV

Poly (3-hydroxybutyrate) (PHB) and poly (3-hydroxybutyrate-*co*-3-hydroxyvalerate) (PHBV) are microbial polyesters produced by bacteria (Avella et al., 2000). The molecular structures of PHB and PHBV are shown in Figure 2.3. As natural polymers, PHB and PHBV received great interests in medical applications because of their biocompatibility, biodegradability and non-cytotoxicity (Sendil et al., 1999; Köse et al., 2003).

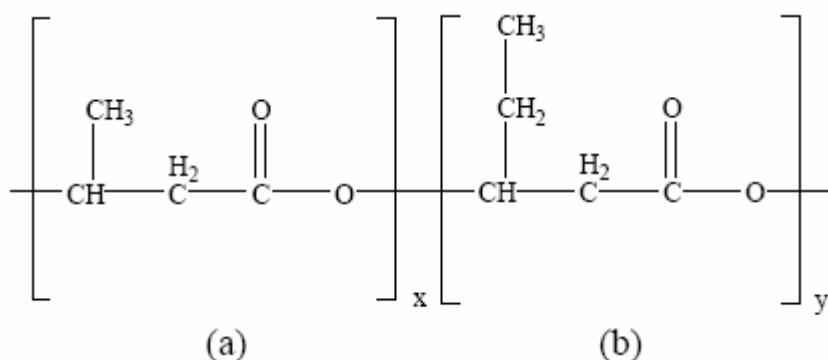


**Figure 2-3.** Molecular structure of PHBV: (a) PHB and (b) PHV.

Unlike other natural polymers, the physical properties of PHBV can be controlled by varying the fractions of HV, which can be achieved easily by adjusting the growth environment of bacteria (Avella et al., 2000). For example, with the increase of the

PHV composition, the glass transition temperature ( $T_g$ ), melting temperature ( $T_m$ ) and crystallinity of PHBV decrease. By varying copolymer composition, the molecular weight and degradability were found to vary widely too (Thwin, 2004). Compared with the widely used synthetic copolymer PLGA (50:50), the degradation rate of PHBV is slower. Both of PLGA and PHBV are polyesters which will produce organic acids as degradation products, which will lower the pH value around the tissue dramatically and kill healthy cells. Lower degradation rate may allow the exchange of the acids by the metabolic system in time and keep the local pH unchanged.

A number of studies have shown that PHB and PHBV are suitable materials for drug delivery and biomedical application. Sendil et al. (1999) loaded tetracycline, an antibiotic, into PHBV microspheres of three valerate contents (7, 14, and 22% molar ratio) using a water in oil in water (w/o/w) double emulsion technique. The encapsulation efficiency (EE), drug loading, release characteristics, and morphology were investigated. They concluded that the EE of neutralized tetracycline was much higher than in acidic conditions and the release behavior fitted Higuchi's approach for microsphere release well. Doyle et al. (1991) evaluated degradation properties and biocompatibility of PHB and PHB reinforced by hydroxyapatite both *in vitro* and *in vivo*. They reported that the degradation rate was a function of the composition and the materials did not cause any undesirable chronic inflammatory response after implantation in rabbits for up to 12 months. PHBV rods encapsulated with antibiotics did not elicit an inflammatory response when implanted into rabbit tibia, which indicated good *in vivo* biocompatibility (Gürsel et al., 2001). PHB patches were reported to promote the regeneration of atrial septum at defect sites after the patches were implanted into six calves for 12 months. In addition, no shunt or signs of



infection were found (Malm et al., 1992). Despite all these studies, compared to the more commonly used polyester PLGA, PHBV has many similar properties but has been less studied for use as tissue engineering scaffolds.

## **2.4 Surface Modification of the Scaffold**

Surface modification of the scaffold can improve its biocompatibility and create appropriate biomimetic environment to regulate cell growth, which is crucial for the success of tissue engineering.

### **2.4.1 Cell interaction with the surface of the scaffold**

For anchorage-dependent cells, adhesion to the surface of scaffold is critical because it precedes other events such as cell proliferation, migration and function (Saltzman, 2000). The mechanism of cell adhesion to substrates has been explained by two theories: (1) physicochemical theory which refers to passive adhesion including hydrophobic interaction, electric and ionic interaction; and (2) biological theory which refers to active adhesion mediated by receptors on cell membranes and cell adhesive molecules on the substrates (Curtis and Lackie, 1991). Cell aggregation is also important in tissue engineering because it can promote cell-cell interaction which often enhances cell function and viability. It has been reported that certain surface modification method resulted in the formation of hepatocytes aggregates, which resemble what cells form *in vivo*, and thus exhibit cell specific functions (Li et al., 2003).

Many studies were done on surface modification techniques to change surface properties such as wettability (Khang et al., 2002), surface charge (Wan et al., 2003),

functional groups (Li et al., 2003; Chua et al., 2005), as well as to introduce cell-adhesive ligands (Jun and West, 2004; Bartolo et al., 2005; Biltresse et al., 2005).

## **2.4.2 Surface modification of polymeric substrate**

### **2.4.2.1 Surface oxidation to change the wettability**

Hydrophilicity is one of the most important factors which determine cell adhesion to surfaces. It is believed that cell adhesion appears to be optimal on surfaces with intermediate wettability (Saltzman, 2000). Surface oxidation by acids or bases can introduce oxygen-based functional groups such as carboxyl, carbonyl and hydroxyl groups, which have been demonstrated to enhance hydrophilicity effectively. Also, the introduced functional groups have the potential to react with other bioactive molecules such as Arg-Gly-Asp (RGD) and Tyr-Ile-Gly-Ser-Arg (YIGSR) to further enhance surface biocompatibility. Khang et al. (2002) investigated the effect of chemical (chloric acid, sulfuric acid, and sodium hydroxide) and physical treatments (corona and plasma discharge) on PLGA (75:25) films. The results indicated that the water contact angles of surface-treated PLGA films decreased from 73° to 50°–60°.

### **2.4.2.2 Immobilization of cell adhesive proteins and peptides onto the surface**

Essential ECM proteins such as collagen, laminin, fibronectin and vitronectin, are referred to as cell adhesive proteins because they can interact with the integrin receptors on cell membranes (Figure 2-4). These proteins can be immobilized on the scaffold surface by simple coating or covalent grafting, providing cells with a mimetic microenvironment (Hubbell, 2000; Ku et al., 2005). Sanchez et al (2000) investigated how different ECM proteins affect the morphology, growth and differentiation of rat hepatocytes. They found that all of the proteins improved cell attachment to a similar

extent while cells exhibited a cord-like structure only when cultured on fibronectin coated petri-dishes. The cells also expressed liver specific genes to greater extents. However, Mooney believed that regardless of the type of ECM proteins, the densities at which they were presented to the cells might be the key in controlling hepatocytes' phenotype (Mooney et al., 1992).

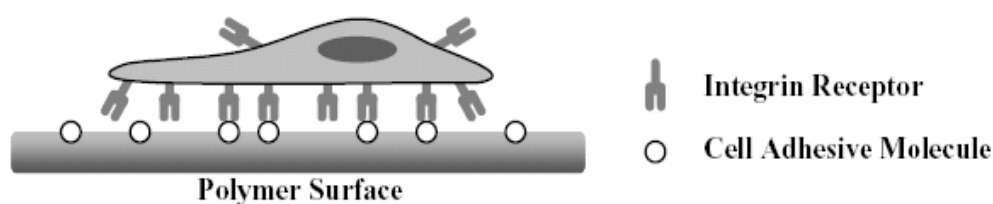


**Figure 2-4.** Cell adhered on polymer surfaces mediated by cell adhesive molecules and integrin receptors.

Although grafting ECM proteins onto the scaffold surface is an effective way to mediate cells attachment, several reports have demonstrated that the integrin receptors bind specific sequences in the cell adhesive proteins, such as the tripeptide RGD and the pentapeptide YIGSR, which are called the cell adhesive peptides (Bhadriraju and Hanse, 2000; Massia and Stark, 2001; Merrett et al., 2001). Compared with the proteins, short cell adhesive peptides can be coupled at high density onto the scaffold surface, are easier to characterize, and are available at a lower cost. Carlisle et al. (2000) grafted RGD and YIGSR peptides onto the surfaces of PCL and PLLA substrates by the pulsed plasma deposition technique. Surface density, quantified by radio-iodinated tyrosine in YIGSR, were  $158 \text{ fmol/cm}^2$  on PLLA and  $425 \text{ fmol/cm}^2$  on PCL surfaces. Hepatocytes adhesion was significantly enhanced on both RGD and

YIGSR modified PCL surface, while only RGD-modification improved cell adhesion on PLLA surface. Massia et al. (2001) covalently immobilized three synthetic peptides, GRADSP (inactive control), GRGDSP (linear) and GpenGRGDSPCA (cyclic) on surface-grafted dextran by a nontoxic aqueous method. *In vitro* endothelial cell, fibroblast and smooth muscle cell attachment results indicated that surface-grafted cyclic RGD peptides promoted cell adhesion while inactive peptides did not. According to Reznia et al. (2000), a surface density higher than 0.62 pmol/cm<sup>2</sup> of a fifteen amino acid peptide (containing RGD) significantly enhanced the mineralization of ECM by osteoblasts.

#### **2.4.2.3 Immobilization of carbohydrates onto the surface**

Besides the integrin receptors, hepatocytes have a specific asialoglycoprotein receptor (ASGP-R), which promotes the removal of glycoproteins from the blood circulating in the liver (Watanabe et al., 2000). ASGP-R can recognize several carbohydrate-based substances such as galactose, lactose and fructose in a calcium ion-dependent manner. Therefore galactose or fructose moiety immobilized onto polymer surfaces as specific ligands to hepatocytes has been widely investigated in liver tissue engineering to enhance liver cell adhesion and promote hepatic functions. Li et al. (2003) investigated rat hepatocytes growth in fructose-modified chitosan scaffold. They found a much larger number of hepatocytes attaching onto the modified scaffold and the cells exhibited a round cellular morphology. Scanning electron microscope (SEM) images confirmed the observation of cellular aggregates formation on the modified chitosan scaffold. In addition, albumin secretion and urea synthesis were significantly increased when the cells were cultured on the fructose-modified scaffold.

The advantages of using carbohydrates include a much lower cost, no risk of viral transfer and more permanent activity. However, it is also reported that the binding forces between receptors and carbohydrates are much weaker than those of peptides (Hersel et al., 2003).

## **2.5 Delivery of Growth Factor for Tissue Engineering**

In tissue engineering, growth factors are essential to promote cell proliferation, differentiation and to induce vascularization. However, direct administration of these molecules is not always applicable due to poor *in vivo* stability as a result of proteolysis (Babensee et al., 2000; Tabata, 2000; Saltzman and Olbricht, 2002; Chen and Mooney, 2003). A localized delivery system which can maintain the bioactivity of growth factors as well as provide to the cells with the molecules without the dilution effect in solution is therefore necessary.

### **2.5.1 Growth factors and criteria for delivery systems**

Growth factors are small molecular proteins which are secreted by various types of cells. Through binding to receptors on the target cells, growth factors can regulate cell migration, differentiation and proliferation. Growth factors act in a concentration, spatial and time dependent manner and have been widely applied in surgical procedures including skin regeneration, bone induction and vascularization.

Skin and wound healing was the first area where growth factor-based pharmaceutical therapy was applied. The growth factors which have been identified as mediators of skin and wound regeneration include platelet-derived growth factor (PDGF), epidermal growth factor (EGF) and transforming growth factor (TGF- $\alpha$ , TGF- $\beta$ ) (Deuel and Zhang, 2000). Other growth factors such as bone morphogenetic

protein-2 (BMP-2) and osteogenic proteins (OP-1 or BMP-7) can induce the infiltration of the osteoblasts from the surrounding healthy tissues into the implanted devices and have been clinically used to treat patients with bone diseases. Furthermore, vascular endothelial growth factor (VEGF<sub>165</sub>), basic fibroblast growth factors (bFGF), angiopoietins-1 and 2 (Ang-1 and Ang-2) play a key role in the formation of new blood vessels which are critical for curing vascular diseases in tissue engineering. A list of commonly used growth factors in tissue engineering and their known activities is given in Table 2-1 (Chen and Mooney, 2003).

Although growth factors clearly play an important role in tissue regeneration, it is a challenge to deliver the molecules to the desired sites in an appropriate mode. Direct injection is not always feasible because the half-life (several minutes to several hours) of most growth factors in the human body is too short for them to exhibit their effects. Moreover, the distribution of the growth factors throughout the body, resulting from bolus delivery, may lead to undesirable side effects (Tabata, 2000; Chen and Mooney, 2003). Researchers should keep several important considerations in mind when designing a growth factor delivery system for tissue regeneration: (1) identifying the biologic activities of the growth factors for a particular tissue application; (2) delivering the molecules to desired cells or tissues and avoiding signal propagation to non-target cells; (3) long-term delivery with well-maintained bioactivity of the growth factors; and (4) delivery with a temporal and spatial mode (Babensee et al., 2000).

**Table 2-1.** A list of growth factors commonly used in tissue engineering\*

<b>Growth Factor</b>	<b>Abbreviation</b>	<b>Molecular Weight (kDa)</b>	<b>Known Activities</b>
Epidermal growth factor	EGF	6.2	Proliferation of epithelial, mesenchymal, and fibroblast cells
Platelet-derived growth factor	PDGF-AA	28.5	Proliferation and chemoattractant agent for smooth muscle cells;
	PDGF-AB	25.3	extracellular matrix synthesis and deposition
	PDGF-BB	24.3	
Transforming growth factor- $\alpha$	TGF- $\alpha$	5.5	Migration and proliferation of keratinocytes; extracellular matrix synthesis and deposition
Transforming growth factor- $\beta$	TGF- $\beta$	25.0	Proliferation and differentiation of bone forming cells; chemoattractant for fibroblasts
Bone morphogenetic protein	BMP-2	26.0	Differentiation and migration of bone forming cells
	BMP-7	31.5	
Basic fibroblast growth factor	bFGF/FGF-2	17.2	Proliferation of fibroblasts and initiation of angiogenesis
Vascular endothelial growth factor	VEGF <sub>165</sub>	38.2	Migration, proliferation, and survival of endothelial cells

\* Adapted from (Chen and Mooney, 2003)

### 2.5.2 Polymeric delivery system for growth factor

The use of polymeric particles for localized delivery of anti-cancer drugs has been widely studied for many years (Langer, 1999; Wang et al., 2002) and it has also been proved to be able to deliver growth factors at an appropriate time profile to stimulate cell growth for the tissue regeneration (Cao and Shoichet, 1999; Holland et al., 2005; Defail et al., 2006).

Ishihara et al. (2003) incorporated FGF-1, FGF-2, VEGF165 and HB-EGF into photo-crosslinked chitosan hydrogels. The *in vitro* release results indicated that 10-25% of growth factors were released within the first day while no further substantial release took place. The growth factors interacted with the chitosan hydrogel to form polyion complexes, and could not be released without degradation. They also observed that addition of heparin with either FGF-1 or FGF-2 resulted in a significantly enhanced and prolonged vascularization effect. According to Perets et al. (2003), releasing of bFGF from PLGA microspheres largely induced the penetration of capillaries into the porous alginate scaffolds, which was shown by the massive layer of mural cells surrounding endothelial cells. Peters et al. (1998) also demonstrated that VEGF released from alginate microspheres stimulated endothelial cell growth effectively *in vitro*. Oe et al. (2003) injected hepatocyte growth factor (HGF)-incorporated gelatin microspheres into the livers of rats. Compared with free HGF and HGF-free gelatin microsphere, gelatin microspheres incorporating HGF effectively promoted the rats' recovery from liver fibrosis as well as liver regeneration.

However, one big challenge of growth factor delivery technology is the loss of biological activity caused by protein denaturation and deactivation during their



incorporation into the polymer matrix (Tabata and Ikada, 1998). High temperatures, strong mechanical mixing and use of organic solutions are potential factors which contribute to the loss of activity of proteins. Therefore, it is necessary to employ a feasible way to enhance the encapsulation efficiency as well as minimize denaturation of growth factors. Tabata et al. (1999a, 1999b, 1999c) prepared bFGF-incorporated gelatin microspheres using a surfactant-free process. Based on different isoelectric points (IEPs), positively or negatively charged gelatin molecules interacted with oppositely charged protein molecules to form a polyion complex. The bFGF-incorporated gelatin microspheres effectively promoted the formation of new blood vessels and accelerated bone regeneration after implantation, which proved the maintenance of biological activity of the growth factor.

In a tissue engineering system, it would be ideal if the scaffold which functions as a substrate for cell to attach could be able to simultaneously deliver suitable growth factors in a controlled manner to stimulate cell growth and new vessel formation at the implantation sites. However, it is not always possible to encapsulate growth factors directly into the scaffolds due to the complex structures and fabrication process. One solution is to initially encapsulate the growth factors into microspheres, and the microspheres can then be incorporated into the scaffolds (Holland et al., 2005; Defail et al., 2006). Among the many types of scaffolds studied, microspheres have been found to offer a number of exciting advantages for tissue regeneration (Barrias et al., 2005; Mercier et al., 2005; Sahoo et al., 2005). Microspheres provide 3D environments which can better preserve the phenotype of the cells (Malda et al., 2003). Also, growth factors can be encapsulated into the microspheres and released with controllable delivery profiles. Therefore, the use of polymeric microsphere as a scaffold, which can

deliver growth factor directly to the cells grown on it, could be advantageous to producing a viable tissue engineering system.

## **2.6 Vascularization for Tissue Engineering**

One of the major obstacles in engineering large tissues *in vitro* is the insufficient supply of nutrients and oxygen to the cells growing inside the scaffold (Griffith et al., 2005). Vascularization of the scaffolding system, which can maintain the viability of the cells as well as improve the structural integrity of the engineered tissue, is a prerequisite for the success of engineering large tissues (Frerich et al., 2001; Levenberg et al., 2005).

### **2.6.1 Microvasculature and *in situ* remodeling**

Microvasculature begins with arteries dividing consecutively into smaller branches consisting of meta-arterioles (80-100  $\mu\text{m}$ ) and capillaries (10-15  $\mu\text{m}$ ). These vessels serve to distribute blood and nutrients whilst lowering the pressure head. In addition, the system allows for a more efficient exchange of metabolites (Levick, 2000).

The vascular tree is formed during early gestation. Angiogenic cells form clusters which coalesce to form solid tubes, and eventually canalize to form blood vessels (Buschmann and Schaper, 2000). The outer ring consists of angioblasts which form the vessel walls. The subsequent differentiation of these precursor angioblasts into endothelial cells and the *de novo* formation of a vascular network are termed “vasculogenesis”. These vessels are capillary-like initially and eventually differentiate into either arteries or veins (Murohara, 2001). The adult vascular network remodels itself by arteriogenesis with enlargement of existing collaterals, as well as formation of completely new vessels from existing vessels (Peirce and Skalak, 2003). Micro-

vascular remodeling is a mechanistic process which frequently occurs in a fibrin-rich extracellular matrix. Through binding with the ligands (RGD) on the  $\alpha$ -chain of fibrinogen, endothelial cells adhere and spread on the matrix to form capillary-like tubules (Nehls and Herrmann, 1996). It is believed that the new capillaries induced from the microvascular network play a crucial role in organ development and wound healing.

### **2.6.2 Vascularization of scaffold-based system**

Although tissue engineering shows great potential to restore function to almost every tissue, the most successful applications to date have been limited to thin tissue equivalents such as skins in which nutrients could be delivered by diffusion (Frerich et al., 2001). For thick and more complex tissue equivalents such as muscles and liver, diffusion alone would not be sufficient to provide oxygen and nutrients to cells growing in the deeper sections of the scaffolds, thus resulting in the ultimate failure of the engineered tissue (Levenberg et al., 2005). For example, the lack of sufficient blood supply is believed to be the primary reason for cell death that occurs in hepatocyte transplantation. Therefore, a vascularized scaffold-based system which can provide nutrient and oxygen to maintain cell viability might be a prerequisite for the success of engineering large tissues.

Vascularization of engineered tissue constructs *in vivo* can be achieved by implanting the scaffold into the body and permitting the growth of blood vessels into the matrix. This can be further stimulated with the administration of angiogenic factors, such vascular endothelial cell growth factor (VEGF) and basic fibroblast growth factor (bFGF) (Tabata and Ikada, 1998; Riley et al., 2006). However, it is more complicated

to vascularize the scaffold *in vitro*, and this is perhaps the biggest challenge faced by tissue engineers. Frerich and co-workers developed a soft tissue model consisting of micro-carriers covered with adipose tissue stromal cells which were then mixed with endothelial cells in a fibrin matrix *in vitro*. Capillary-like structures were observed under confocal microscope after 8 days of culture (Frerich et al., 2001). In a recent work, Levenberg and co-workers added embryonic fibroblasts into a co-culture system consisting of myoblasts and endothelial cells on porous PLGA scaffold. The addition of fibroblast promoted the formation of vessels *in vitro*, and the prevascularized scaffold improved *in vivo* vascularization after transplantation (Levenberg et al., 2005). Although there are many factors affecting the formation of blood vessels *in vitro*, culturing endothelial cells on appropriate 3D scaffolds is believed to be the basis and premise for the success of vascularization (Nehls and Herrmann, 1996). Furthermore, it is well known that several growth factors such as bFGF, VEGF<sub>165</sub> and platelet-derived growth factors can stimulate the rapid formation of capillary vessels (Babensee et al., 2000; Tabata, 2000). However, the effects of the growth factors by direct administration or injection were found to be insignificant because of their poor stability resulting from proteolysis (Chen and Mooney, 2003). Therefore, a localized delivery system which can maintain the bioactivity of growth factors for an extended period of time might be necessary in promoting the formation of blood vessels.

## 2.7 Summary

Tissue engineering shows great promise to regenerate damaged tissues and solve the problem of organ donation shortage. Although investigators have attempted to

engineer various mammalian tissues such as skin, bone, cartilage, tendon and muscles, the research on complex organs such as the liver is still in its infancy. The biggest challenges are the quick dedifferentiation of primary hepatocytes resulting in the loss of normal liver functions, and the death of the cells due to the lack of sufficient oxygen and nutrient supply when cultured *in vitro*. Therefore, a novel scaffolding system which could provide proper environment (3D environment, biocompatible surface, growth factors release and vascular networks) to preserve the phenotype as well as provide enough nutrients to the cells the maintain their viability is necessary for the success of engineering a liver tissue, which is the motivation of this project.

## **Chapter 3 Fabrication and Characterization of PHBV Microsphere Scaffold**

As temporary replacement of extracellular matrix (ECM) to support the growth of the cells, polymer scaffolds play an essential role in tissue engineering. The scaffold should not only act as a substrate for cells to attach, but also provide desirable microenvironment such as biocompatible surface and controllable delivery of growth factors to improve the proliferation as well as preserve the phenotype of the cells. The scaffold should also provide flexible structures for easy implantation and match the irregular shapes of defects or complex architecture of organs. Microspheres have been traditionally used as drug delivery vehicles or carriers to harvest cells. The unique three-dimensional (3D) environment offered by microspheres can improve cells' proliferation and preserve their differentiated functions. Microspheres have also been demonstrated for application in tissue engineering to deliver bioactive molecules such as growth factors and genes. However, using microspheres as scaffold for tissue engineering is a new idea which needs further exploration. Poly (3-hydroxybutyrate) (PHB) and poly (3-hydroxybutyrate-co-3-hydroxyvalerate) (PHBV) are microbial polyesters produced by bacteria. PHB and PHBV received great interests in the

applications for drug delivery and tissue engineering because of their biocompatibility, biodegradability and non-cytotoxicity.

In this chapter, PHBV microspheres with three size distributions were fabricated using an emulsion solvent evaporation technique. The fabricated microspheres were characterized by particle size analyzer and a scanning electron microscope (SEM). Human hepatoma cell lines, HepG2 and Hep3B which were chosen as models of primary human hepatocytes, were cultured on the microsphere scaffold. The proliferation of the cells and two liver functions, albumin secretion and cytochrome P-450 activity were quantitatively measured. The objectives were to determine the optimum scaffold dimension to guide the growth of liver cells and also to compare the functions of the two human hepatoma cell lines cultured on the scaffold.

### **3.1 Materials and Methods**

#### **3.1.1 Materials**

Poly(3-hydroxybutyrate-*co*-3-hydroxyvalerate) copolymer (PHBV, 8% PHV), Tween<sup>®</sup>80, Tween<sup>®</sup>20, sodium pyruvate, antimycotic solution, poly(L-lysine), Phosphate-buffered saline (PBS) (pH=7.4), HEPES-buffered saline solution (HBSS) (pH=7.4), paraformaldehyde, saponin, phalloidin-FITC, DAPI, glutaraldehyde (GTA), dimethyl sulfoxide (DMSO), 3-(4,5-Dimethyl-2-thiazolyl)-2,5-diphenyl-2H-tetrazolium bromide (MTT), bisbenzimidazole (Hoechst 33258), trypsin, Tris-HCl (pH=7.4), sodium chloride, ethylenediaminetetraacetic acid (EDTA), bovine serum albumin (BSA), 7-ethoxyresorufin, dicumarol, sodium resorufin, ethanol, and trapan blue were purchased from Sigma-Aldrich (St. Louis, MO, USA). Chloroform was purchased from Fluka (Steinheim, Germany). Poly (vinyl alcohol) (PVA) (MW 6000)

was purchased from Polysciences (Warrington, PA, USA). Dulbecco's modified eagle medium (DMEM) was purchased from Gibco (USA). Fetal bovine albumin (FBS) was purchased from Hyclon (UT, USA). Laminin was purchased from Invitrogen (USA). Live/dead kit was purchased from Molecular Probes (Eugen, OR, USA). Lysis buffer was from Promega (San Luis Obispo, CA, USA). Human albumin enzyme-linked immunosorbent assay (ELISA) quantification kit was purchased from Bethyl (Texas, USA). HepG2 and Hep3B cells were purchased from American Type Culture Collection (ATCC, Virginia, USA). All chemicals were used directly without further purification.

### **3.1.2 Fabrication of microspheres**

A water-in-oil-in-water (w/o/w) emulsion solvent evaporation technique was used to fabricate PHBV microspheres (Yang, et al., 2000). Briefly, 0.6 g of PHBV (8%) powder was dissolved in 12 mL of chloroform, and then 1 mL of phosphate-buffered saline (PBS) (pH=7.4) with 0.05 w/v% poly(vinyl alcohol) (PVA) was added. Emulsification was subsequently carried out using a homogenizer (T25B, Ika Labortechnik, Staufen, Germany) for 15s. Several homogenizing speeds, 16000 rpm, 19000 rpm and 22000 rpm were applied to get different size distributions of microspheres. The homogenized mixture was immediately poured into 300 mL of PBS with 0.05 w/v% PVA. The solution was then placed under continuous mechanical stirring (RW20, Ika Labortechnik, Staufen, Germany) at 300 rpm for 3h to evaporate the organic solvent. The temperature was maintained at 37°C with a magnetic hotplate stirrer (Cimarec2, Barnstead/Thermolyne, IA, USA). The microspheres fabricated were washed with deionized water 5 times and transferred into a 15 mL glass vial and



placed in a freeze dryer (Alpha 1-4, Martin Christ, GmbH, Germany) for 36 hours to remove any remaining solvent and water droplet and to get a constant weight of porous microspheres.

### **3.1.3 Characterization of microspheres**

The size distributions of microspheres produced by different homogenizing speeds were measured by a particle size analyzer (Coulter LS-230, FL, USA). Tween<sup>®</sup>80 was used to disperse the microspheres into the water evenly. The external surface morphologies of the microspheres were characterized by a scanning electron microscope (SEM) (JSM-5600VL, JEOL, Tokyo, Japan). To observe the internal structure of the microspheres, samples were sectioned with a cryostat microtome (Leica CM3050S, Germany) with blade step setting at 30  $\mu\text{m}$  and air dried. The intact microspheres and cross-sectioned samples were mounted onto brass stubs using double-sided adhesive tape and vacuum-coated with a thin layer of platinum using the Auto Fine Coater (JFC-1300, JEOL, Tokyo, Japan) for 40 seconds prior to examination. The diameters of the internal pores were estimated using a software Smile View.

### **3.1.4 Cell culture and cell seeding on microspheres**

Human hepatoma cell lines, HepG2 and Hep3B (American Type Culture Collection, ATCC), were selected as models for the culture of primary hepatocytes. The cells were cultured in DMEM medium supplemented with 10% FBS, 110 mg/L sodium pyruvate and 1% antimycotic solution. The cells were maintained in T-75 flasks in an incubator at 37°C in the presence of 5% CO<sub>2</sub> and 95% relative humidity. The medium was renewed every 3 days.

Five milligrams of microspheres with a total surface area around  $2.5 \text{ cm}^2$  were sterilized in a 2 mL centrifuge tube using 70% ethanol followed by completely washing with sterilized PBS. The tube was then placed in an incubator with culture medium for 3 hour at  $37^\circ\text{C}$  to let the microspheres stabilize at the bottom. Cells were subsequently seeded at  $2.5 \times 10^4$  cells/mL into the tube, or approximately  $1 \times 10^4$  cells/ $\text{cm}^2$  of microsphere surface. The microspheres with attached cells were transferred to 24-well tissue culture plates after 1 hr incubation. The cells attached on the microspheres were counted by a trypan blue exclusion method to estimate the seeding efficiency (Jacobson and Ryan, 1982).

To prepare the positive control, 200  $\mu\text{L}$  of 1 mg/mL poly(L-lysine) aqueous solution was added to each well of a 24-well plate and the plate was incubated for 2 days at room temperature. Then, 100  $\mu\text{L}$  of a 0.5 mg/mL aqueous solution of laminin was added and incubated overnight at  $37^\circ\text{C}$ . Polyurethane film containing 0.1% zinc diethyldithiocarbamate (ZDBC) was used as the negative control.

### **3.1.5 Morphology of cell-microsphere constructs**

**Optical microscope:** The morphologies of cells and cell-microsphere construct were observed under optical microscope (Leica DMIL, GmbH, Germany). Images were taken by a digital camera (OICAM Fast 1394, OIMAGING, Canada) connected with the microscope at different days of culture.

**CLSM images:** (1) Live/Dead assay: The viability of cells cultured on microsphere scaffold was assessed using a live/dead kit which contains two components, SYTO 10 green fluorescent nucleic acid stain and DEAD Red (ethidium homodimer-2) nucleic acid stain. Briefly, the cell-microsphere constructs were washed

with HBSS buffer and incubated in 200  $\mu$ L of live/dead solution in dark for 30 min at room temperature. The dye solution was then removed. The cell-microsphere constructs were washed with fresh HBSS and fixed with 4 v/v% glutaraldehyde in HBSS (freshly prepared) for at least 15 minutes before observation. A confocal micrograph was obtained by using a confocal laser scanning microscope (CLSM) (Leica, DM-IRE 2, Germany). The fluorescent green-colored indicated live cells while the fluorescent red-colored cells were dead cells.

(2) Nucleus/Actin double staining: The cell-microsphere constructs were washed twice with PBS and fixed with 4 v/v% paraformaldehyde in PBS for 30 min. The samples were then washed with PBS and the cells were permeabilized with 0.2% saponin for 15 mins. After being washed with PBS, the cell-microsphere constructs were stained with phalloidin-FITC (1:200) for 1 hour. The samples were washed three times with PBS and counter stained with DAPI (1: 10,000) for 5 minutes. A confocal micrograph was obtained by using a CLSM (Leica, DM-IRE 2, Germany). The fluorescent green-color indicated actin of the cells while the fluorescent blue-color was the nucleus.

**SEM images:** For SEM imaging, cell-microsphere constructs were washed twice with PBS and fixed with 2.5 v/v% glutaraldehyde (GTA) in PBS in a 24-well plate for 1 hr. The samples were then washed twice with PBS and dehydrated using a graded series of ethanol (50%, 60%, 70%, 80%, 90%, and 100 v/v%) (Jacobson and Ryan, 1982). Samples were air dried and mounted onto an aluminum stub and sputter-coated with platinum for 40 s before viewing under SEM.

### **3.1.6 Cell proliferation and functionality**

#### **3.1.6.1 MTT quantification**

The MTT assay is based on the cleavage of a water-soluble yellow methylthiazol tetrazolium (MTT) salt to water-insoluble purple formazan crystals by the action of dehydrogenase enzymes, which are produced by living cells. The amount of the formazan formation can be measured spectrophotometrically, where the absorbency measurement is directly proportional to the number of living cells (Carlisle et al., 2000). At different days of incubation, the MTT assays were carried out to measure the cells viability. Briefly, the cell culture medium was removed firstly. The cell-microsphere constructs were then washed with sterilized PBS. 0.9 mL of serum-free cell culture medium and 0.1 mL of MTT solution (5mg/mL) were added into each well and incubated at 37°C for 4 hours. The culture medium was removed and washed with PBS. The formazan was then dissolved in DMSO and the absorbance was measured at wavelength of 560 nm as measurement and 620 nm as reference by a Microplate Reader (Tecan GENios, Switzerland).

#### **3.1.6.2 Total DNA quantification**

Cellular DNA content was quantified using bisbenzimidide (Hoechst 33258) fluorescence assay (Rago et al., 1990). Briefly, cell-microsphere constructs were rinsed twice with PBS solution and were lysed for two hours in 200  $\mu$ L of a lysis cocktail containing 0.25 v/v% trypsin and 2.5 v/v% lysis buffer in ultra-pure water followed by three freeze-thaw cycles. The cell lysates were mixed with 1  $\mu$ g/mL bisbenzimidide in 10 mM Tris-HCl (pH 7.4), 1 mM EDTA and 0.2 M NaCl fluorescence assay buffer and were incubated in dark for 30 minutes. The fluorescence was read using a

microplate reader (Tecan GENios) with 360 nm as excitation wavelength and 465 nm as emission wavelength.

### **3.1.6.3 ELISA assay to quantify albumin secretion**

The albumin secretion of liver cells was measured by ELISA, which is based on the antibody-sandwich mechanism (Glicklis et al., 2000). Since the Hep3B cells are of human origin, the bovine albumin from the serum media should not react with the anti-human albumin affinity. According to the protocol of the ELISA, blocking solution (50 mM Tris, 0.14 M NaCl, 1% BSA, pH 8.0) was used to block the non-specific area and sample diluent (50 mM Tris, 0.14 M NaCl, 1% BSA, 0.05% Tween 20, pH 8.0) was used to dilute the samples. Since both of these two solutions contain 1% BSA, the BSA from cell culture medium was believed to have no cross reactivity in the ELISA assay and will not affect the final results. At the desired days of culture, 0.5 mL of the supernatant was aspirated from the wells and centrifuged at 13000 rpm for 5 min, filtered with 0.25  $\mu$ m millipore filter and stored at  $-20^{\circ}\text{C}$  until required for analysis.

### **3.1.6.4 Cytochrome P-450 activity by EROD assay**

The P-450 (CYP1A1/2) activity represents the detoxification ability of liver cells, which was measured by an ethoxyresorufin-o-dealkylase (EROD) assay (Bhandari et al., 2001). At the desired days of culture, after the culture medium was aspirated and stored for ELISA test, the cell-microsphere constructs were rinsed twice with sterilized PBS solution. One milliliter of PBS solution containing 5  $\mu$ M 7-ethoxyresorufin and 10  $\mu$ M dicumarol was then added into each well and incubated for 3 hours at  $37^{\circ}\text{C}$  in the dark. The fluorescence of the supernatant was measured using a microplate reader

(Tecan GENios) with 535 nm as excitation wavelength and 595 nm as emission wavelength. The standard curve was obtained from resorufin sodium salt solutions.

### 3.1.7 Statistical analysis

All data are presented as mean  $\pm$  standard deviation and were analyzed by a one-way ANOVA test, where the symbol “\*” on the bars of the positive control indicate significant difference with all of the samples to the positive control. Student’s t-test was also carried out to do statistical comparisons between pairs of samples. Differences between the groups were considered statistically different when  $p < 0.05$ .

## 3.2 Results and Discussion

The use of micro-carriers to harvest cells has been studied widely since the 3D environment offered by micro-carriers can improve cell proliferation as well as preserve the differentiated functions. However, using microspheres as scaffold for tissue engineering is a new and different idea which so far only a few studies have reported. For tissue engineering purposes, the microspheres firstly act to provide a surface to support cell growth *in vitro*. When a tissue-like cell-microsphere construct is formed with certain functions, it will be implanted into the defect tissue to recapitulate the desired function and regenerate the defect as the microspheres degrade. Therefore, the *in vivo* degradation profile of the microsphere scaffold should match with the regeneration rate of the defect otherwise the scaffold would become a hindrance to the formation of new tissue.

HepG2 and Hep3B are well developed liver cell-like cell lines and are widely used to model *in vitro* culture of primary human hepatocytes. Both of these two lines show epithelial morphology when adherent growth on solid surface. Besides high

proliferation rates, the cells possess biological functions similar to human primary hepatocytes and can secrete many hepatocellular products, such as albumin, transferrin, alpha fetoprotein and so on (ATCC).

### 3.2.1 Fabrication and characterization of PHBV microspheres

Three size distributions of microspheres were fabricated using different homogenizing speeds to study the effects of size and shape of microspheres on liver cell proliferation and functions. The mean diameters are 153.2, 242.5 and 361.8  $\mu\text{m}$  respectively, and small standard deviations (SD) indicate narrow distributions (Table 1). It was shown that a faster homogenizing speed yielded much smaller microspheres while a slower speed yielded larger ones (Table 3-1). A possible explanation for this could be that a higher homogenizing speed mixed the emulsifier (0.05 w/v% PVA) with the polymer molecules more thoroughly. Since surfactant micelles acted as the repulsive steric entropic force among the molecules, larger relative contact between emulsifier and polymer molecule isolated them into smaller microspheres.

**Table 3-1.** PHBV microspheres obtained from different homogenizing speeds

Homogenizing Speed (rpm)		Diameter		Internal Pore Size	
		Mean ( $\mu\text{m}$ )	SD ( $\mu\text{m}$ )	Mean( $\mu\text{m}$ )	SD ( $\mu\text{m}$ )
<b>M1</b>	22000	153.2	31.6	16.3	2.1
<b>M2</b>	19000	242.5	38.2	17.5	3.2
<b>M3</b>	16000	361.8	40.1	13.2	1.8

Figure 3-1 shows the internal and external morphologies of PHBV microspheres. It can be seen that the microspheres have spherical shapes with uniform sizes, and the

surfaces have rough topography with nano-pores. The porous structure of the microspheres was induced by the removal of internal water droplets through lyophilization, and the average sizes of the internal pores are around 10-20  $\mu\text{m}$ . The highly porous structure is a crucial feature of tissue engineering scaffold because the pores will benefit the exchange of nutrient, oxygen, cellular signals as well as removal of metabolic wastes. Since PHBV is relative hydrophobic, adding 1 mL of PBS (0.05 w/v% PVA) into the polymer solution following by high speed homogenizing resulted in evenly distributed water droplets among the organic phase, and homogeneous pores were formed after microspheres were freeze dried [Figure 3-1 (d)]. Although the pores are not clearly observed to be interconnected, the nano-pores on the walls of the pores would make the exchange of nutrients possible [Figure 3-1(e)].



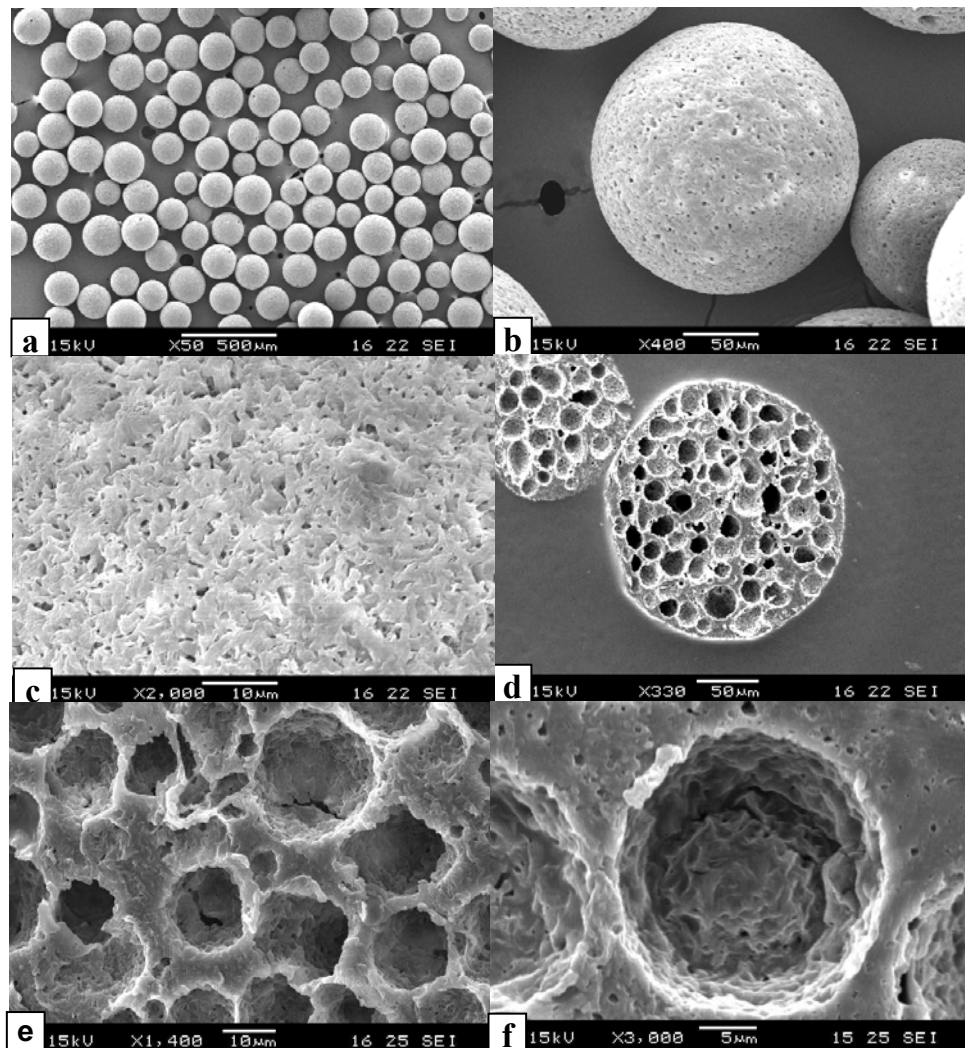


**Figure 3-1.** (a) and (b) SEM images of PHBV microspheres with an average diameter of  $153.2 \mu\text{m}$  illustrating their spherical shape and uniform size; (c) magnified image of (b) showing a rough surface with nano-pores; (d) cross-section of the microsphere. (e) and (f) magnified images of (d).

### 3.2.2 Seeding efficiency of HepG2 cells on PHBV microspheres

The seeding efficiency (the ratio of cells attached onto microspheres to the initial seeded cells) was investigated using trypan blue exclusion method (Figure 3-2). Approximately 20-30% of cells attached onto the microsphere scaffold and the highest seeding efficiency was found on the smallest microsphere ( $p < 0.05$ ). As HepG2 cells are anchorage-dependent, the initial cell adhesion on microspheres is a critical stage

because it precedes other events, such as cell spreading, proliferation and differentiation. Compared to 2D scaffolds such as polymer films, seeding efficiency on most 3D scaffolds is generally lower and it is difficult to distribute the cells uniformly within the scaffolds (Barrias et al., 2005). In this study, about 20-30% cells were seeded onto the microspheres and the cells were distributed relatively uniformly onto the scaffolds.

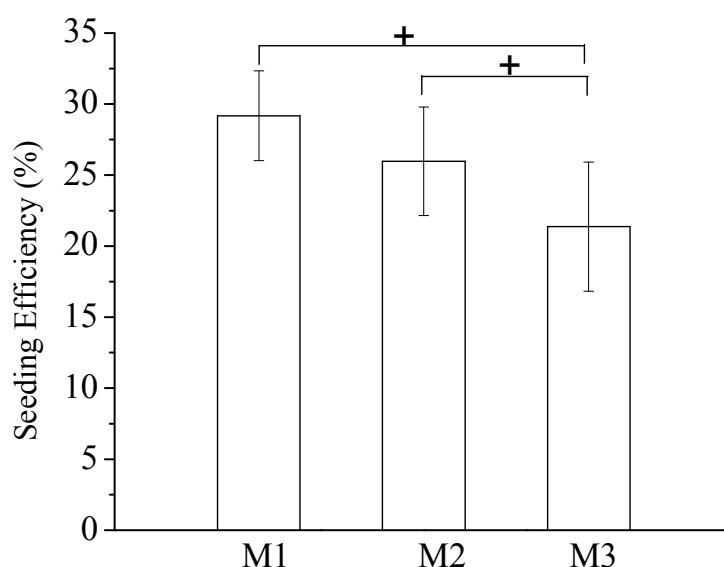


**Figure 3-2.** The seeding efficiency of HepG2 cells on microsphere scaffolds (+ $p < 0.05$ ).

### 3.2.3 Morphology of cell-microsphere constructs

#### 3.2.3.1 Optical micrographs

Optical micrographs of HepG2 or Hep3B cells cultured on PHBV microspheres are shown in Figure 3-3. It can be seen that the cells attached and spread on the microspheres after two days of culture [Figure 3-3 (a)]. The cells spread over the surface of single microspheres and began to bridge adjacent microspheres together

after 4 days of culture [Figure 3-3 (b)]. From day 8 onwards, the cells bridged more and more microspheres together. At the same time, the cells stretched to fill the gaps between the microspheres to form multilayers of cells. After two weeks of culture, cells were seen to become confluent on the microsphere scaffolds and cell-polymer aggregates started to form [Figure 3-3 (d)]. The cell growth on M2 showed a similar profile. After two weeks of culture, the cells have spread completely on the microspheres and formed multilayers of cells among the microsphere scaffolds as well as deposited an abundant amount of ECM-like structures [Figure 3-3 (e)]. However, HepG2 growth on M3 were not adequate as the formation speed of tissue-like structure was slower than on M1 and M2 and no confluent tissue-like structures were formed after two weeks of culture [Figure 3-3 (f)].

Although cell growth on M3 showed a similar trend to M1 and M2, the formation speed of tissue-like structure was slower. One possible reason for this could be that the size of M3 was too big for HepG2 cells (10-20  $\mu\text{m}$  in diameter) to bridge the adjacent microspheres together to form aggregates. However, it does not mean that the smaller microspheres were better. Microspheres which were too small easily settled to the bottom of the plates. This allowed the cells to extend to the bottom of plates from the microspheres and fix them onto the surface. As a result, no microspheres could be bridged together (data not shown). Accordingly, 3D PHBV microspheres, especially the size range between 100  $\mu\text{m}$  to 300  $\mu\text{m}$ , are suitable adhesive substrates for *in vitro* culturing HepG2 cells.

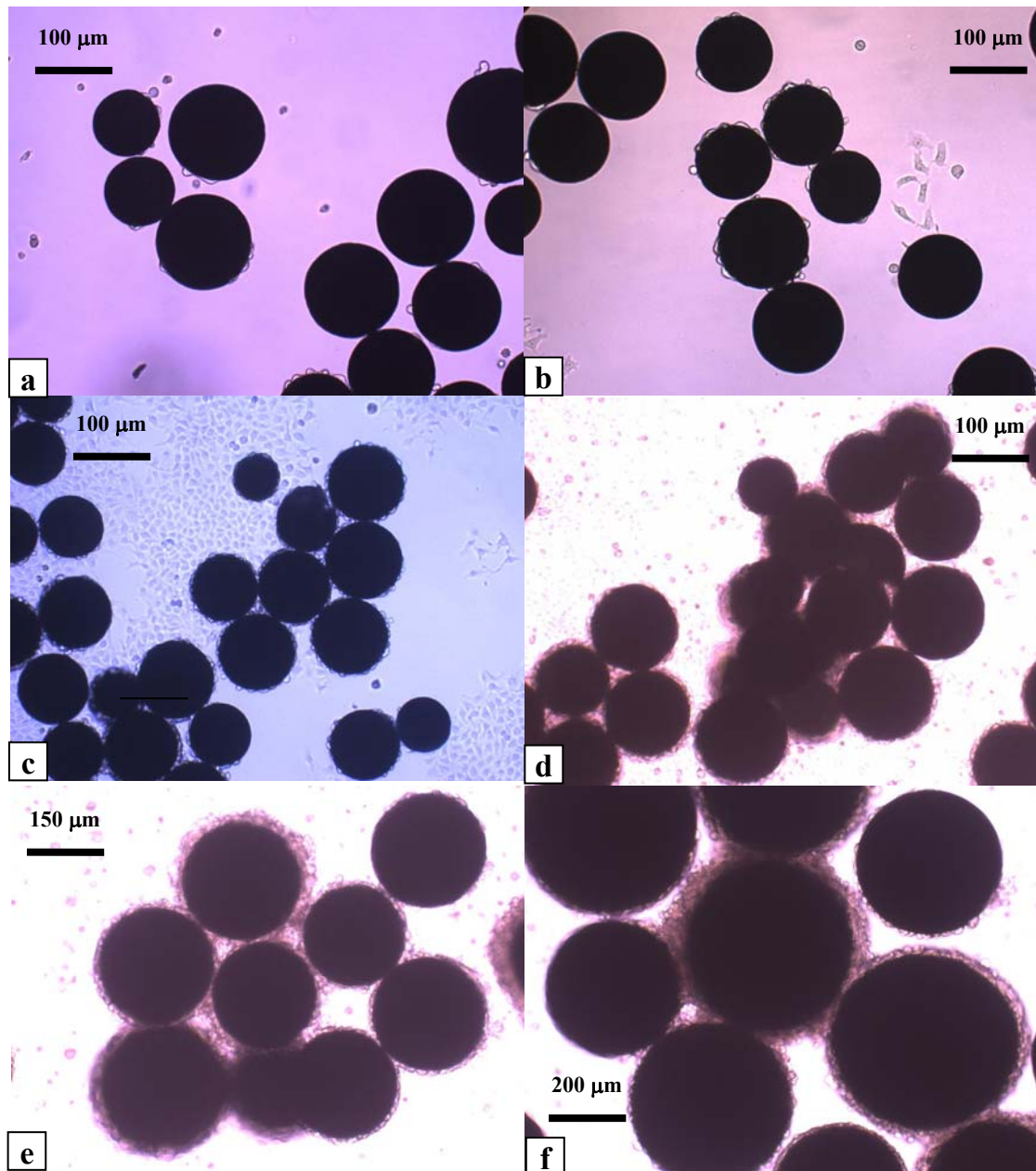


**Figure 3-3.** Optical micrographs of HepG2 cells grown on M1 after (a) 2 days, (b) 4 days, (c) 8 days and (d) 14 days of culture, (e) HepG2 grown on M2 after 14 days of culture, (f) HepG2 grown on M3 after 14 days of culture.

### 3.2.3.2 Confocal laser scanning micrographs (CLSM)

The viability of Hep3B cells cultured on microsphere scaffold was assessed using a live/dead assay. The fluorescent green-colored indicated live cells while the

fluorescent red-colored cells were dead cells [Figure 3-4 (a) and (b)]. It can be seen that most of the Hep3B cells grown on microspheres were viable although multilayers of cells were formed on the scaffold. However, necrosis could occur if cellular regions become even thicker. Diffusion alone will not be efficient to provide nutrients and oxygen to the cells grown on the deeper sections of the scaffold. Therefore, pre-vascularization within the scaffolds should be considered to help the exchange of nutrients as well as removal of wastes (Perets et al., 2003).

The actins and nucleuses of the cells were further stained with phalloidin-FITC and DAPI to get detail images on how the cells grown on the microsphere scaffolds [Figure 3-4 (c) and (d)]. As can be seen, the cells distributed quite evenly on the microsphere surface and secreted abundant extracellular matrix components. The confocal images indicated that the PHBV microspheres are well-suited in guiding the growth of Hep3B liver cells *in vitro*.

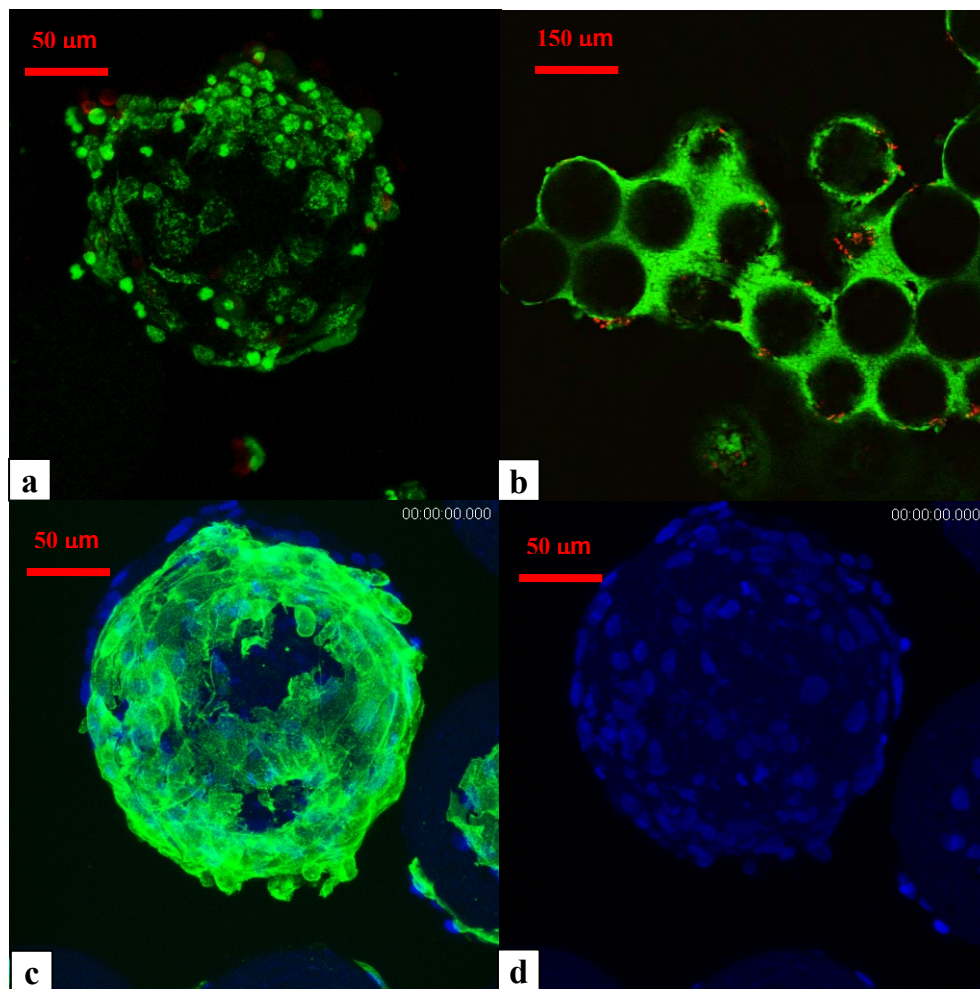


**Figure 3-4.**CLSM of Hep3B cells grown on M1 after two weeks of culture. (a,b) Cells were stained with live/dead kit. (c,d) Cell actins were dyed with phalloidin-FITC, and the nucleuses were dyed with DAPI.

### 3.2.3.3 Scanning electron micrographs

SEM images of HepG2 and Hep3B cells cultured on M1 as a function of time are presented in Figure 3-5 and Figure 3-6. The images show that the surfaces of microspheres were covered by cell layers which deposited an abundant amount of extracellular matrix components. The arrows indicated that there existed strong cell-

cell interaction and cell-substratum interaction between cells and the microspheres. Similar to the optical micrographs, multilayer of cells formed to bridge the microspheres as well as stretched to fill the gaps, producing tissue-like structures. Although both HepG2 and Hep3B are liver cell lines, the morphologies of these two lines were observed to be slightly different when cultured on PHBV microsphere scaffold. HepG2 tended to form multilayer of cells in the gaps between microspheres in bridging the microspheres together [Figure 3-5 (c,d)] while Hep3B cells tended to spread on the surface and formed confluent monolayer [Figure 3-6 (c,d)]. These could be due to the different morphology properties of the two types of cell lines.

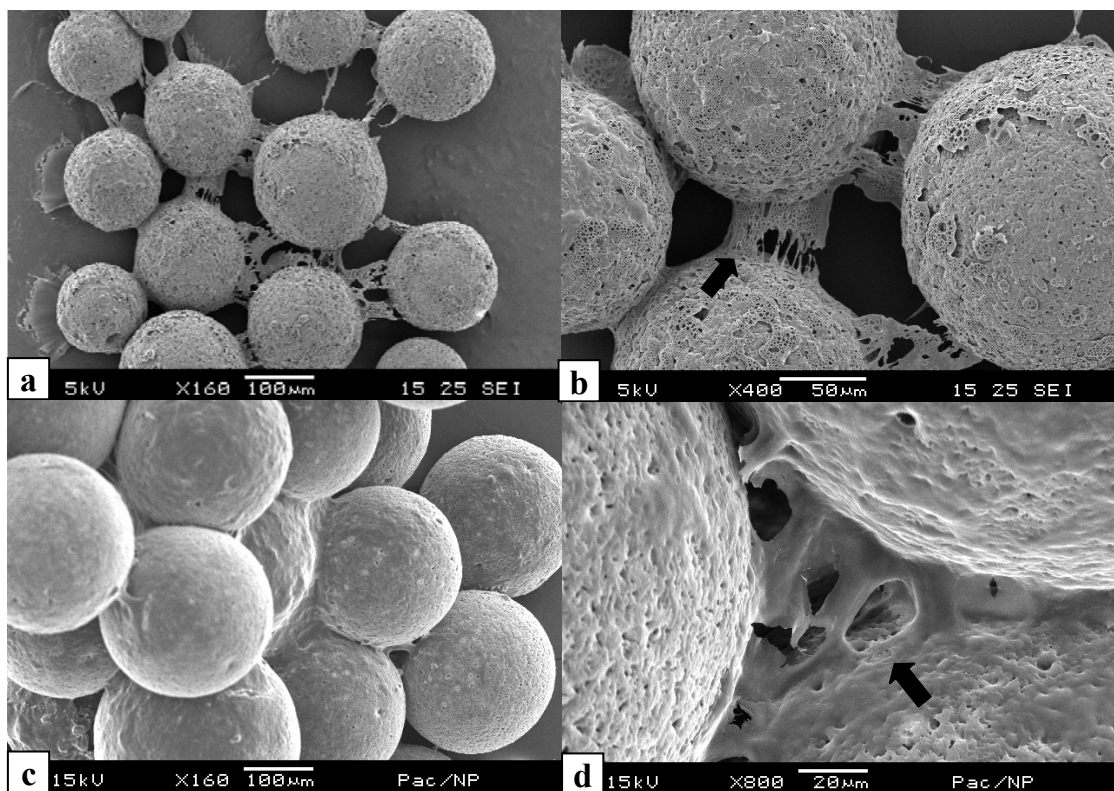


**Figure 3-5.** SEM micrographs of HepG2 cells seeded on M1 after (a, b) one week; (c, d) two weeks of culture; where b, d, are higher magnifications of a, c respectively.



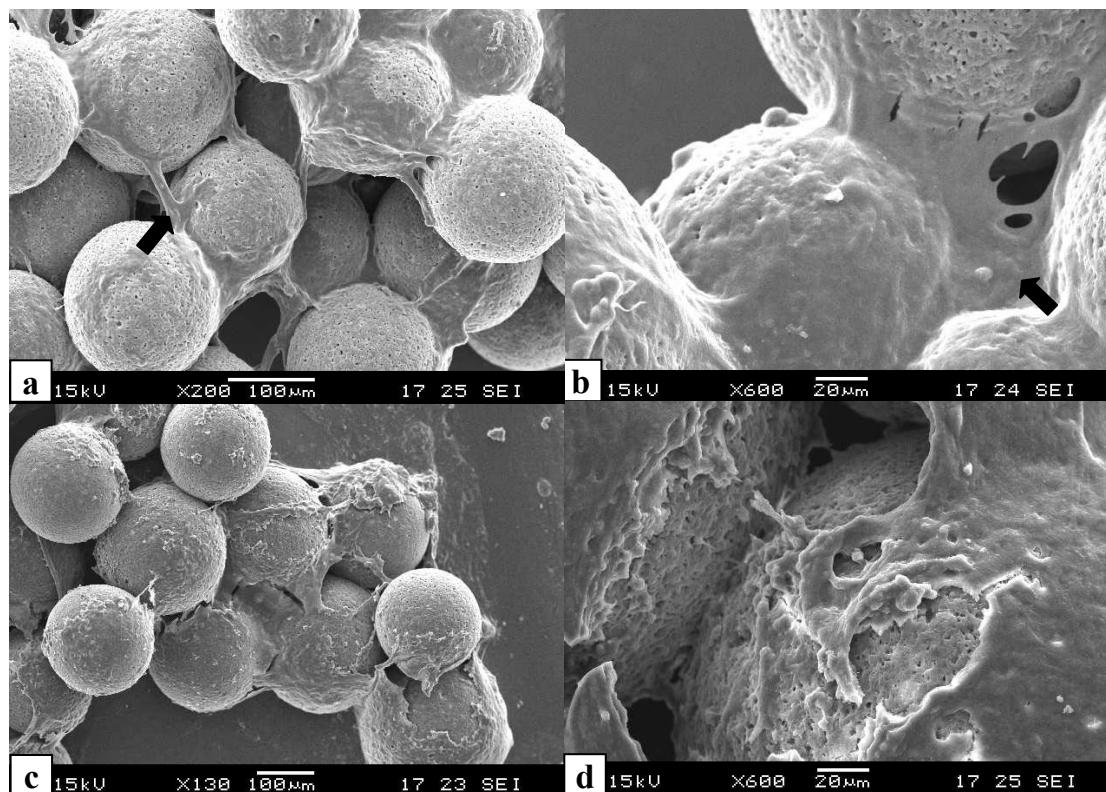


**Figure 3-6.** SEM micrographs of Hep3B cells seeded on M1 after (a, b) one week; (c, d) two weeks of culture; where b, d are higher magnifications of a, c respectively.

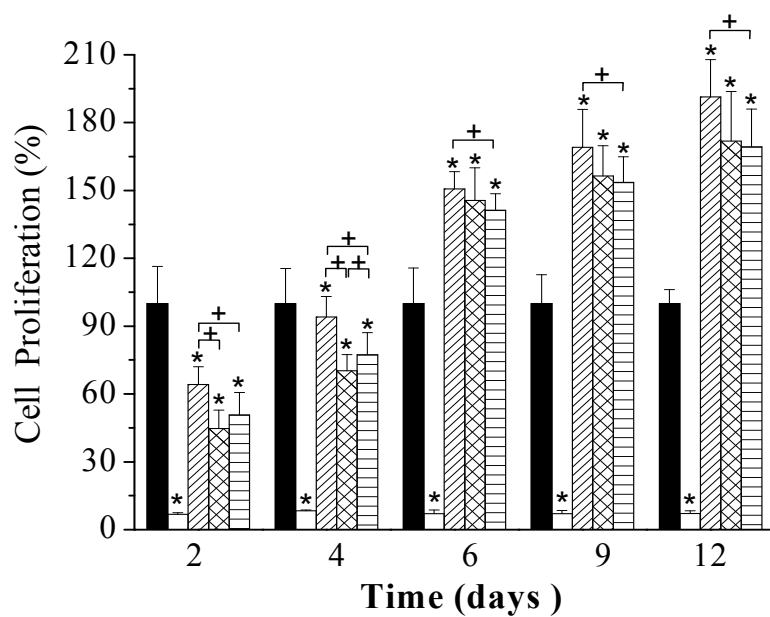
### 3.2.4 Proliferation of HepG2 cells grown on PHBV microsphere scaffold

The proliferation of HepG2 cells grown on PHBV microspheres as well as the positive control (laminin coated PLL films) and negative control (ZDBC films) were quantitatively evaluated by MTT and total DNA quantification during the 12 days of culture as shown in Figure 3-7 (a,b). For each time point, absorbance of MTT solution from positive control was set as 100%. The ratios of absorbance of MTT solution from microspheres or negative control to that of the positive control were used to evaluate cell proliferation on the corresponding substrates. It can be seen that the cell

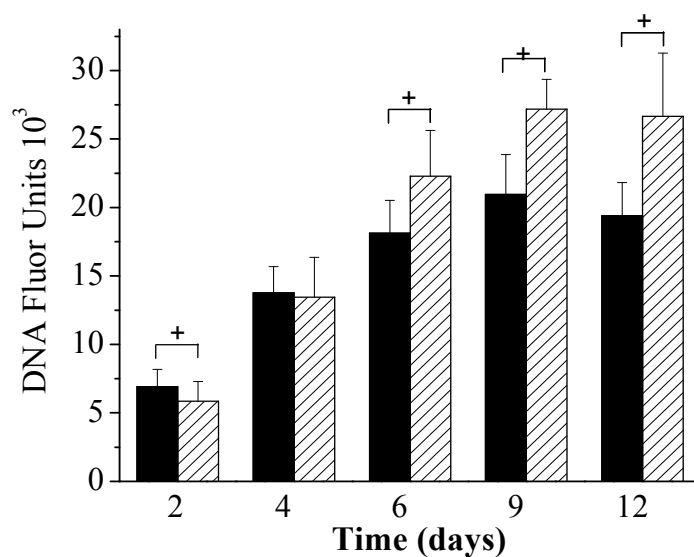


proliferation on the three types of microspheres were lower than that of the positive control at day 2 and day 4 of culture, while after 6 days, the proliferations of the cells on three types of microspheres were significantly increased to 150.7%, 145.5% and 141.3% respectively. From day 6 onwards, cell proliferations increased steadily on the microsphere scaffolds. By the last day of culture, the cell proliferations on M1, M2 and M3 reached 191.3%, 171.9% and 169.3%. One reason for this is that compared to 2D positive control, microspheres have a larger surface area, which allow larger number of cell to grow on it. More importantly, it is believed that the shape of the scaffold affects cell adhesion, proliferation and function greatly (Malda et al., 2003; Barrias et al., 2005). Smaller microspheres improved cell-cell interaction and cell-substrate interaction (Figure 3-3 to Figure 3-6), which may stimulate cell proliferation. The cells would also be more active in aggregate forms. Figure 3-7(a) also indicated that HepG2 showed much lower proliferation rate on the negative control, where all values was lower than 10%. The proliferation of Hep3B cells showed a similar profile (data not shown).

To more accurately quantify the cell proliferation, a total DNA assay was conducted. Figure 3-7(b) shows a similar profile of an increase in cellular DNA which is indicated by the fluorescence intensity as the MTT results for the cells grown on 2D positive control and the M1 samples. T-tests between these two samples show a significantly greater amount of cell growth on M1 which confirmed that cell proliferation was improved when cultured on 3D microsphere scaffolds.



(a)



(b)

**Figure 3-7.** Proliferation of HepG2 cells cultured on positive control (■), negative control (□), M1 (▨), M2 (▩) and M3 (▤) as assessed by (a) MTT assay; (b) total DNA quantification. Values represent means  $\pm$  SD,  $n=3$  ( $*p<0.05$  as compared to the positive control by ANOVA,  $^+p<0.05$  by t-test comparison between the two samples).

### 3.2.5 Albumin secretion and P-450 activity of the cells grown on microsphere scaffold

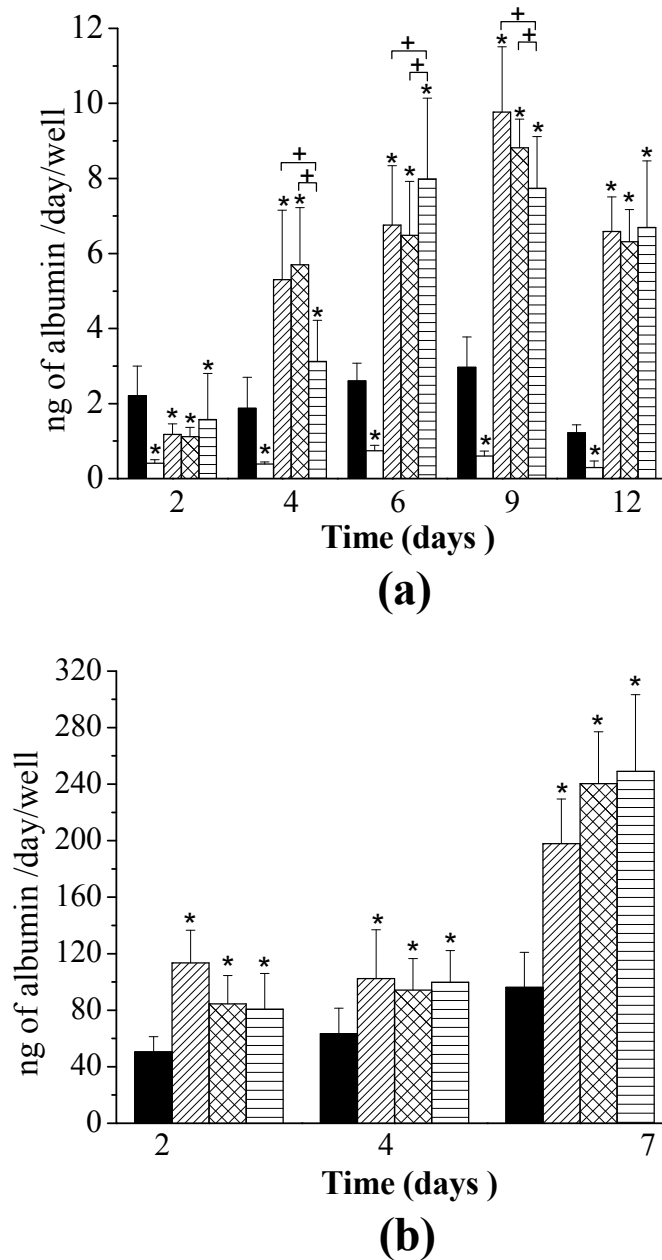


**Figure 3-8.** Albumin secretion by (a) HepG2 and (b) Hep3B cells cultured on positive control (■), negative control (□), M1 (▨), M2 (▩) and M3 (▤). Values represent means  $\pm$  SD,  $n=3$  ( $*p<0.05$  as compared to the positive control by ANOVA,  $^+p<0.05$  by t-test comparison between the two samples).

Albumin production by HepG2 and Hep3B cells cultured on controls and microspheres were assessed by ELISA and the results are shown in Figure 3-8 (a) and Figure 3-8 (b) respectively. HepG2 cells cultured on microspheres maintained a steady increase of albumin secretion throughout the study although there was a slight drop at 12 days of culture. No significant increases of albumin secretion were found on the positive controls. It can be seen that Hep3B cells seeded on microspheres secreted albumin 2-4 times more than that on the positive control after 7 days of culture, which indicated that this hepatic function was greatly improved by the aggregation of cells on microspheres.

HepG2 and Hep3B cells secreted significantly more albumin when cultured on microspheres than on positive control. The results from cell proliferation assays indicated that HepG2 cells proliferated faster on microspheres than on the positive control (Figure 3-7), and the larger number of cells might secrete a higher amount of albumin [Figure 3-8 (a)]. More importantly, it is believed that the cell-scaffold aggregate can improve the hepatic functions of liver cells (Bhandari et al., 2001). From 4 days onwards, HepG2 attached onto microspheres secreted albumin 2-4 times more than that on the positive control. However, the proliferation was only 0.8-1.9 times of the positive control (Figure 3-7), so the higher level albumin secretion could be attributed mainly to the improvement of hepatic function by the cell-scaffold aggregation. Compared to HepG2, Hep3B cells expressed much higher levels of albumin secretion. After 7 days of culture, Hep3B cells grown on microspheres secreted albumin up to 30 times more than that by HepG2 cells. According to the results obtained by ELISA, it can be seen that albumin secretion by HepG2 and Hep3B

cells were well preserved on microsphere scaffolds and the levels were much higher than that on the positive control.

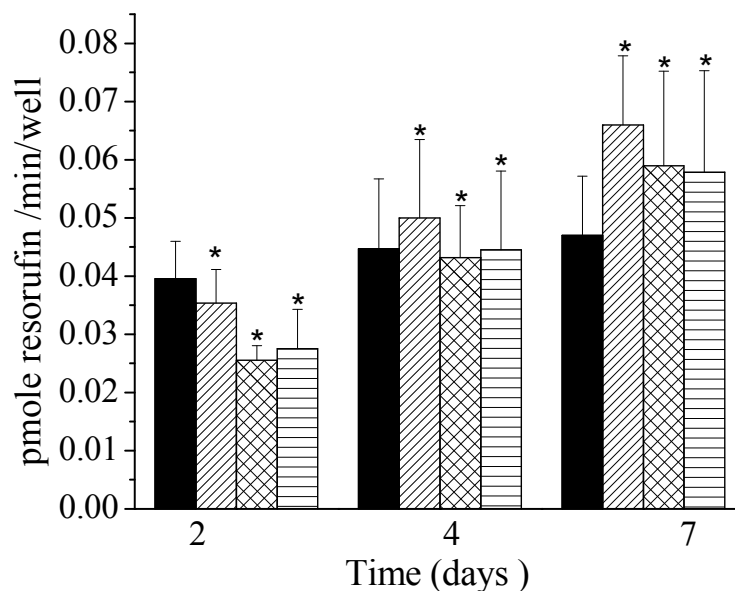


**Figure 3-9.** Cytochrome P-450 activity of Hep3B cells cultured on positive control (■), M1 (▨), M2 (▩) and M3 (▤). Values represent means  $\pm$  SD,  $n=3$  ( $*p<0.05$  as compared to the positive control by ANOVA).

Our experiments indicated that HepG2 cells could not express P-450 functions. Therefore only Hep3B cells were used to test this hepatic function. The cytochrome P-450 enzyme activities of Hep3B grown on the positive control and microsphere scaffolds were measured over one week in culture and the results are shown in Figure 3-9. Although there are no statistically significant differences among the three different sizes of microsphere scaffold ( $p>0.05$ ), the P-450 activities of Hep3B cultured on microspheres were significantly higher than the positive control. The higher P-450 activity which Hep3B cells performed on 3D microsphere scaffold than on positive

control again proved that the aggregation of cells on microspheres can improve hepatic cellular functions. Taken together, 3D microsphere scaffolds are proved to be suitable substrates to guide liver cell proliferation and function, with a potential role in regenerating liver tissue *in vitro*.

### **3.3 Conclusions**

In this chapter, polymeric microspheres fabricated from poly(3-hydroxybutyrate-co-3-hydroxyvalerate) (PHBV, 8% PHV), were explored as novel scaffold for liver tissue regeneration. Compared to cells cultured on 2D controls, cells grown on microsphere scaffold showed higher proliferation rates as well as improved hepatic functions. This could be attributed to the large surface area provided by the microspheres, which allowed larger number of cell to grow. More importantly, it is believed that the spherical shape of the scaffold affects cell adhesion, proliferation and function greatly. Smaller microspheres improved cell-cell interaction and cell-substrate interaction which can stimulate cell proliferation and function. It was found that PHBV microspheres with the size range between 100-300 $\mu$ m were suitable for supporting the growth of the liver cells. Light and SEM images showed that the microspheres were assembled by the cells into various shapes after two weeks of culture, which would be desirable for the regeneration of irregular shaped defects or complex organs. Although multilayers of cells was formed among the cell-scaffold constructs, the viability of the cells was well preserved as confirmed by live/dead imaging assay. All of these indicated that the PHBV microsphere is a promising scaffold for liver tissue regeneration and further investigation should be carried out.

## **Chapter 4 Proteins Combination on PHBV Microsphere Scaffold to Regulate Hep3B Cells Activity and Functionality**

In the previous chapter, PHBV microspheres have been shown to be well suited for liver cell growth, judging from the high cell proliferation as well as improved hepatic functions. For the successful engineering of liver tissue, the creation of a proper biomimetic environment for hepatocytes growth and functionality are equally important. Extracellular matrix (ECM) proteins and peptides are believed to be able to regulate the attachment, migration and growth of cells by binding to the integrin receptors on cellular membranes. Therefore, immobilization of these cell adhesive molecules onto the scaffold surface is hypothesized to be a mean of mimicking the *in vivo* environment, and therefore had been widely studied for tissue engineering application (Carlisle et al., 2000; Hong et al., 2005; Ku et al, 2005).

The ECM of hepatocytes *in vivo* is a dynamic structure having different compositions during the different developmental phases of the liver. In fetal

developing livers, hepatocytes are surrounded mainly by basement membrane components such as laminin while collagen is sparsely distributed. Sinusoidal laminin is also present in large amounts in the regenerating liver. This suggests that laminin plays a part in the growth stimulation of hepatocytes. On the other hand, during liver cirrhosis, collagen type I amounts are relatively increased, which suggests that higher collagen levels are inhibitive of cell growth (Clement et al., 1992). Sanchez et al (2000) investigated how different ECM proteins affect the morphology, growth and differentiation of rat hepatocytes. They found that all of these proteins improved cell attachment to a similar extent while cells exhibited cord-like structure and expressed higher liver specific genes only when cultured on fibronectin coated petri-dishes. However, Mooney believed that instead of the type of ECM proteins, the densities at which they were presented to the cells could be the key to switch the hepatocytes from differentiation to growth state (Mooney et al., 1992). Similarly, peptide sequences derived from these proteins have been commonly studied to replace the functions of the whole proteins themselves. However, the synergistic effects of combination ECM proteins on polymeric scaffolds have not been widely studied for tissue engineering purpose.

Although the effects of ECM proteins on hepatocytes have not been fully characterized, there is sufficient data showing that ECM proteins do affect hepatocyte growth and function. In this chapter, we aim to demonstrate the versatility of microspheres as tissue engineering scaffold through simple modification of the scaffold surfaces in a controllable manner. The surfaces of PHBV microspheres were modified with collagen (type I), fibronectin and laminin. These proteins are the major ECM components. With the ultimate aim to mimic the *in vivo* conditions of the body,



we have cultured a model liver cell line, Hep3B, either on microspheres grafted with single protein type or on mixtures of microspheres individually grafted with one of the three proteins. The proliferations and functions of Hep3B cells grown on the mixture samples were further compared with the cells grown on microspheres grafted with two types of cell adhesive peptides, Arg-Gly-Asp (RGD) and Tyr-Ile-Gly-Ser-Arg (YIGSR). The aim of this work is to show that various ECM proteins do interact with Hep3B cells in a synergistic manner to regulate cell activity and functionality.

## **4.1. Materials and Methods**

### **4.1.1 Materials**

Collagen (type I), fibronectin and laminin were purchased from BD Biosciences (San Jose, CA, USA). Arg-Gly-Asp (RGD), Tyr-Ile-Gly-Ser-Arg (YIGSR), N-Ethyl-N'-(3-dimethylaminopropyl) carbodiimide hydrochloride (EDC), N-Hydroxysulfosuccinimide sodium salt (Sulfo-NHS), MES buffer (pH=6.0), fluorescein isothiocyanate (FITC), hydrogen chloride (HCl) and pluoronic-127 were purchased from Sigma-Aldrich (St. Louis, MO, USA). Sodium hydroxide (NaOH) was purchased from Merck. Micro BCA™ Protein Assay Kit was purchased from Pierce (Rockford, USA). AccQ • Tag amino acid analysis kit was purchased from Waters (Milford, USA). The information of the chemicals which were used in this chapter but not listed in this section can be found at section 3.1.1 in Chapter 3. All chemicals were used directly without further purification.

### **4.1.2 Microsphere fabrication and surface hydrolysis**

The PHBV microspheres were fabricated using an established method (rf. 3.1.2 in Chapter 3). The PHBV microspheres obtained were separated by using standard sieves

to get a diameter of 100-300  $\mu\text{m}$  and used for the following studies. The external surface morphologies of the microspheres were characterized by a scanning electron microscope (SEM) (JSM-5600VL, JEOL, Tokyo, Japan).

In order to introduce functional groups, PHBV microspheres were hydrolyzed in 6 M NaOH solution for 15 min at room temperature with shaking at 130 rpm (Unimax 1010, Heidolph Instruments, Germany). The NaOH solution was aspirated out and replaced with distilled water, followed by shaking for 1 min to wash off residual solutes. This washing process was repeated five times.

#### **4.1.3 Proteins/peptides conjugation on the surface of PHBV microspheres**

The hydrolyzed microspheres were re-suspended into MES buffer (pH=6.0) containing 10 mM EDC and 10 mM sulfo-NHS to activate the carboxyl groups on the surfaces, and shaken at 130 rpm during the reaction for 6 hours. The surface-activated microspheres were washed five times with distilled water to remove the un-reacted EDC and sulfo-NHS, and subsequently immersed in PBS buffer (pH=7.4) containing 0.05  $\mu\text{M}$  proteins or 0.6 mM peptides and shaken at 130 rpm for 24 hr at room temperature. The supernatant was aspirated out and the microspheres obtained were washed five times. The modified microspheres were then dried in the freeze dryer and stored at  $-20^{\circ}\text{C}$  freezer. Three sets of microspheres conjugated with different types of ECM proteins (Collagen, Laminin or Fibronectin) respectively were obtained through this way. The mixtures of these three sets of microspheres in different mass ratios (Collagen: Laminin: Fibronectin at 1:1:1, 3:1:1 and 1:3:3) were also used for cell culture.

In order to get a qualitative understanding on how the conjugated molecules distributed on the surface, proteins and peptides-modified microspheres were dyed with FITC which is widely used to attach a fluorescent label to proteins via amine group. The labeled microspheres were observed under a confocal laser scanning microscope (CLSM, Leica, DM-IRE 2).

#### **4.1.4 Determination of surface conjugation density**

The protein quantity on the microsphere surface was determined using a Micro BCA<sup>TM</sup> Protein Assay Kit according to the manufacturer's instruction. Briefly, 30 mg of each microsphere samples were immersed in 1 mL of ultra-pure water followed by the addition of 1 mL of the Micro BCA working solution. The resulting solution was incubated at 60°C in a water bath for 1hr. After being cooled to room temperature, the developed solution was transferred to a cuvette and the absorbance was measured by a spectrophotometer at a wavelength of 562 nm. Blank microspheres were used as the control. Triplicate samples were prepared for testing purposes.

The peptide densities on the modified microspheres surface were measured using an AccQ • Tag amino acid analysis kit (Waters) followed by a high performance liquid chromatography (HPLC) test. Briefly, 10 mg of peptide-modified microspheres were immersed in a glass vial containing 0.5 mL of 6 M HCl and hydrolyzed at 115°C for 24 hour. After the solution was cooled to room temperature, the vial was dried under vacuum. The residual was reconstituted by adding 100 µL of 20 mM HCl, 300 µL of AccQ • Tag buffer and derivated with 20 µL of AccQ • Fluor Reagent. The concentrations of amino acid derivatives were measured using HPLC (Shimadzu,

Japan) with a fluorescence detector. Blank microspheres were used as the control. Triplicate samples were prepared for testing purposes.

#### **4.1.5 Atomic composition of microsphere surface**

The chemical structure and atomic composition of the blank and surface-modified microspheres were characterized using X-ray photoelectron spectroscopy (XPS, VG ESCALAB 220I-XL, Thermo VG Scientific, UK), with the data processing performed using XPSPEAK (Raymond, W.M. Kwok, Hong Kong). Wide scan (0-1000eV) and high-resolution (C1s, O1s and N1s) spectra were acquired respectively.

#### **4.1.6 Cell culture and seeding on microspheres**

Human hepatoma cell line Hep3B cells (ATCC) were cultured in DMEM supplemented with 10 v/v% FBS, 110 mg/L sodium pyruvate and 1% antimycotic solution. The cells were maintained in T-75 flasks in an incubator at 37°C in the presence of 5% CO<sub>2</sub> and 95% relative humidity. The medium was renewed every three days.

Microspheres were sterilized using 70 v/v% ethanol followed by washed with sterilized PBS for three times. To prevent cells from attaching to the bottom of the wells, a 24-well plate was coated with 1% w/v pluronic-127 (Caldwell, 1997) (Control experiments indicated that more than 90% cells were prevented from attaching to the bottom of the wells coated with pluronic-127) and a glass ring with 9 mm diameter was attached on the center of each well before use. Five milligram of sterilized microspheres was transferred to the glass rings in each well to form monolayer, and cells were subsequently seeded at  $3 \times 10^4$  cells/well. In order to further mimic the *in vivo* environment, individual protein conjugated microspheres were added in the mass

ratios of 1:1:1, 3:1:1 and 1:3:3 (Collagen : Fibronectin : Laminin) to form the mixed protein conjugated samples. The glass rings were taken out and the plate was topped up to 1 mL of DMEM per well after 1.5 hour of incubation.

#### **4.1.7 Cell morphology and viability**

The morphologies of cells and cell-microsphere constructs were observed under an optical microscope and images were taken at different days of culture (rf. 3.1.5 in Chapter 3).

The viability of Hep3B cells cultured on the surface modified microspheres was assessed using a live/dead assay (rf. 3.1.5 in Chapter 3).

Clear and more detail images of cell-microsphere constructs were obtained by fixing the cells with 2.5 v/v% glutaraldehyde and observed under SEM (rf. 3.1.5 in Chapter 3).

#### **4.1.8 Cell proliferation and functionality**

The proliferations of the cells grown on surface modified microspheres were quantified by using MTT assay. Two liver functions, albumin secretion and cytochrome P-450 activity, were quantified by using ELISA and EROD assays. The detailed description of these assays can be found at 3.1.6 in Chapter 3.

#### **4.1.9 Statistical analysis**

All data are presented as mean  $\pm$  standard deviation. One-way Analysis of Variance (ANOVA) followed by Tukey's Honestly Significant Difference (HSD) post hoc analysis were carried out to do the statistical comparison and  $*p < 0.05$  was considered as significant difference.

## **4.2 Results and Discussion**

### **4.2.1 Surface coverage of protein-modified microsphere**

The surface modified microspheres which were labeled with FITC were observed under confocal laser scanning microscope and the images were shown in Figure 4-1. The successful conjugation of protein and peptide molecules was verified by the presence of a completely fluorescent green surface of the PHBV microspheres. The stronger fluorescence on peptide-conjugated microspheres (Figure 4-1d and 4-1e) indicated that larger numbers of peptide molecules were grafted which was consistent with the surface density assay (Table 4-1). The possible reason for this is that the RGD and YIGSR molecules were much smaller than proteins molecules which resulted in lower steric hindrance during the conjugation process and thus a higher grafting density.

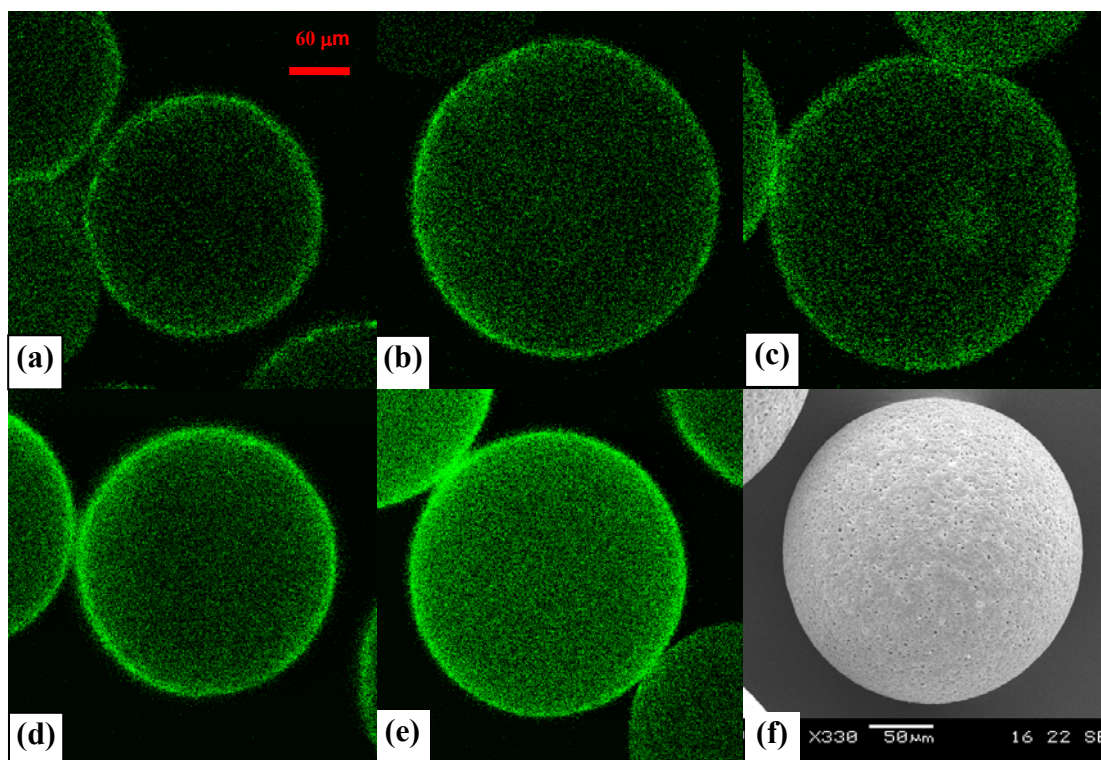


**Figure 4-1.** CLSM images of surface modified PHBV microsphere grafted with (a) Collagen, (b) Fibronectin, (c) Laminin, (d) RGD, (e) YIGSR, and (f) SEM image of blank microsphere. Proteins and peptides were labeled with FITC.

#### 4.2.2 Surface density of conjugated molecules

The surface densities of conjugated proteins were quantified using micro BCA™ protein assay and the results were shown in Table 4-1. It was observed that the surface density of conjugated collagen was higher than that for laminin and fibronectin. This could be due to the larger conformational size of laminin (900,000 Daltons) and fibronectin (440,000 Daltons) molecules resulting in greater steric hindrance during grafting. It was also believed that self-assembly of fibronectin into fibrils may occur during the conjugation process and decrease the amount of fibronectin grafted onto the surface (Hynes, 1990).

**Table 4-1:** Surface density of proteins conjugation to microspheres

<b>Samples</b>	<b>Surface Density (pmol/cm<sup>2</sup>)</b>
<b>Collagen</b>	2.193 ±0.355
<b>Laminin</b>	0.704±0.181
<b>Fibronectin</b>	0.670 ±0.135
<b>RGD</b>	36.92±12.68
<b>YIGSR</b>	16.24±5.21

\* MW of collagen, Lamin and Fibronectin was 300,000, 900,000 and 440,000 Daltons, respectively.

As explained in the previous section, peptides with shorter chains were conjugated to the surface with a much higher densities as compared to proteins due to the lower steric hindrance of smaller peptides molecules.

#### 4.2.3 XPS spectra of modified surface

X-ray photoelectron spectroscopy analysis was performed to monitor the changes of the surface composition during the modification process. The successful conjugation of proteins and peptides on microsphere surfaces were verified by the presence of nitrogen (N1s) peaks at 398.1 eV from the XPS spectra (Table 4-2). There were no nitrogen peaks from the XPS spectra of intact PHBV and NaOH treated microspheres. The NaOH-treated surfaces showed a decrease of oxygen concentration. However, the decreasing trend does not necessarily mean that the number of hydroxyl and carboxyl groups on the surface has been reduced. This is because the XPS probes a layer of about 4-7 nm thick (Merrett et al., 2001; Gan et al., 2003), which includes the bulk polymer, thus the total peaks from both terminal hydroxyl or carboxyl groups that



has been created and ester bonds in the bulk PHBV cannot be distinguished in the XPS spectra. Several previous works have proved that carboxyl groups could be introduced by NaOH hydrolysis of the ester bond of PGA and PHB films (Yang et al., 2002; Lee et al., 2004). Therefore, it can be postulated that the number of carboxyl groups was increased by the surface hydrolysis, but the relatively more methyl groups present due to the slower degradation of monomer units would have lead to higher peak areas of the methyl carbon.

**Table 4-2:** Atomic composition and percentage of C1s in XPS spectra of native and modified PHBV microspheres

samples	Atomic Conc. %			Peak Ratio (%) of C1s			
	N 1s	O 1s	C 1s	<u>C</u> -C	<u>C</u> -N	<u>C</u> -O	O- <u>C</u> =O
				285.1eV	285.9eV	286.6eV	289.1eV
<b>Untreated</b>	-	32.54	67.46	50.66	-	28.66	20.68
<b>NaOH</b>	-	27.52	72.48	46.52	-	33.51	19.97
<b>Collagen</b>	7.22	21.24	71.54	37.66	19.12	31.88	11.34
<b>Fibronectin</b>	3.95	26.30	69.75	46.33	16.53	21.47	15.66
<b>Laminin</b>	2.79	24.86	72.35	44.23	13.60	23.97	18.19
<b>RGD</b>	2.06	22.83	75.11	35.60	19.35	28.87	16.18
<b>YIGSR</b>	3.18	26.21	70.61	40.66	14.35	25.43	19.56

Figure 4-2 shows the XPS spectra of C1s peaks with the detailed values of peak ratios summarized in Table 4-2. The NaOH-treated microspheres showed a decrease in the area of peak for C-C, while an increase for hydroxyl carbon, C-O. The increase of hydroxyl carbon is related to the oxygen insertion from water by nucleophilic attack of water molecules during the hydrolysis process to form carboxyl groups. It can also be seen that a new carbon bond, C-N, was introduced for proteins and peptides grafted

microspheres (Figure 4-2c to 4-2g). The higher percentages of  $\underline{C}$ -N peak areas were consistent with higher nitrogen atomic concentration as indicated in Table 4-2.

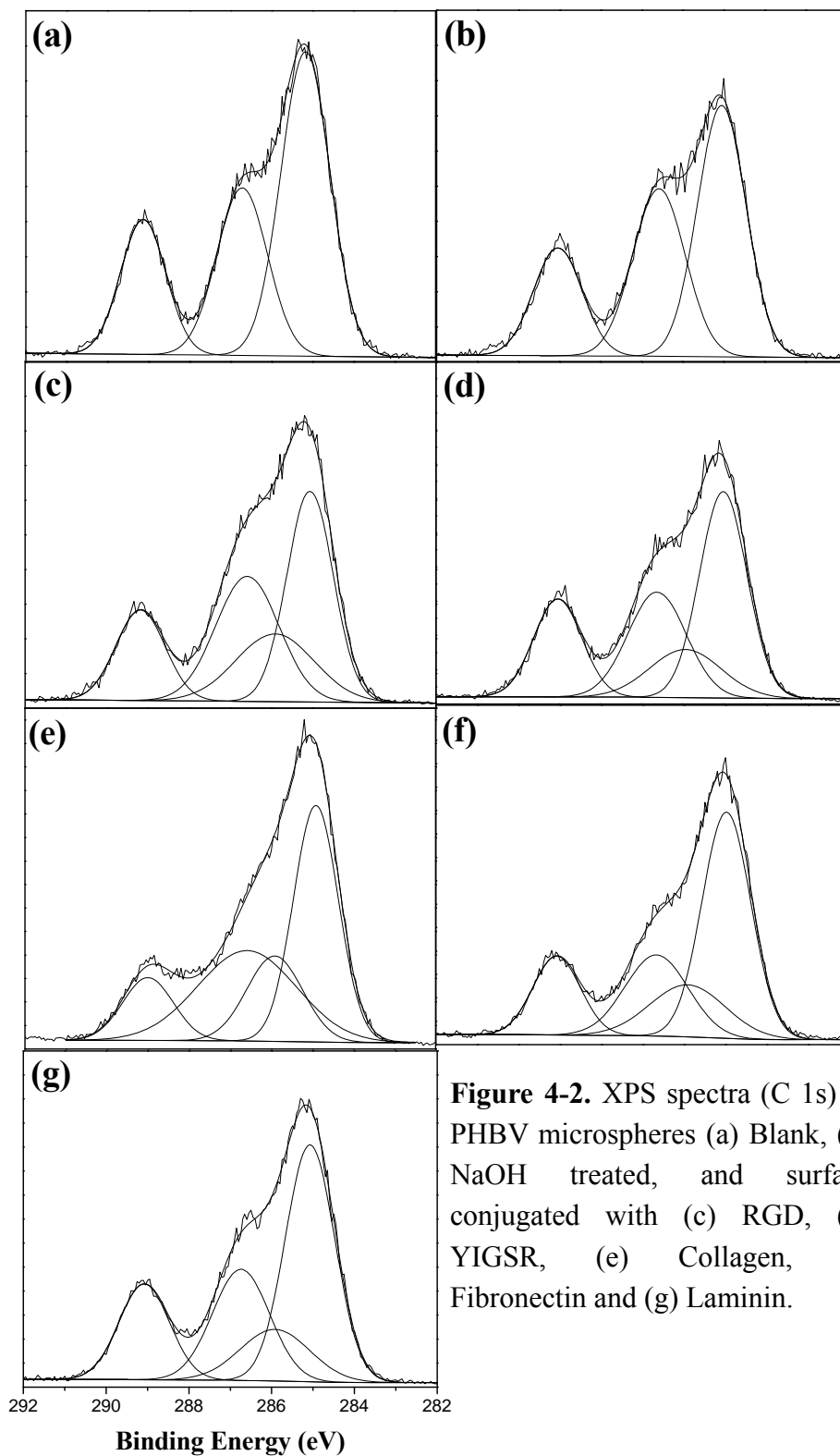


**Figure 4-2.** XPS spectra (C 1s) of PHBV microspheres (a) Blank, (b) NaOH treated, and surface conjugated with (c) RGD, (d) YIGSR, (e) Collagen, (f) Fibronectin and (g) Laminin.

#### **4.2.4 Morphologies of Hep3B cells grown on surface-modified microspheres**

A human hepatoma cell line Hep3B was used as model liver cells to study the effects of the modified microspheres on liver cell proliferation and function. Cells were cultured either on single proteins grafted microspheres (Collagen, Laminin, and Fibronectin), or on mixtures of microspheres individually grafted with the three types of proteins respectively in different mass ratios (Collagen: Laminin: Fibronectin at 1:1:1, 3:1:1 and 1:3:3).

##### **4.2.4.1 Optical micrographs**

No significant differences in the morphologies of the Hep3B cells cultured on the blank, protein-conjugated and mixed protein-conjugated samples were observed under optical microscope [Figure 4-3 (a), (c) and (d)]. Only the cells cultured on NaOH-treated microspheres showed a different morphology [Figure 4-3 (b)]. Images taken at a residence time of one week were used as representatives. It was observed that the cells spread and flattened on blank and protein-grafted microspheres, and many microsphere-aggregates were virtually encapsulated by the cells and formed a three-dimensional tissue-like structure (Figure 4-3). Although there were no significant differences in the morphology of the Hep3B cells cultured on the blank and protein-conjugated microspheres, the cells spread more extensively when cultured on protein-conjugated samples and more microspheres were bridged together to form thicker tissues. Studies by others have also indicated that hepatocytes exhibited a flat and extended morphology when cultured on ECM proteins coated substrates with certain densities (Benzeev et al., 1988; Mooney et al., 1992). It was believed that ECM

proteins coated on rigid, planar surfaces could stimulate the gene expression of major cytoskeletal proteins through binding to specific integrin receptors and therefore regulated the morphology of the cells (Mooney et al., 1992). However, for NaOH samples, cells were absent on large portion of the microspheres and many cells that remain attached were round in shape (indicated by arrows at Figure 4-3b), which in general, could be associated with partial cellular degeneration. These images have shown that the surface-modified microspheres were conducive towards the attachments and spreading of the Hep3B cells. The morphologies of Hep3B cells grown on fibronectin, mixed protein-conjugated samples, RGD and YIGSR grafted microspheres were similar to the cells grown on collagen-grafted microspheres (images not shown).

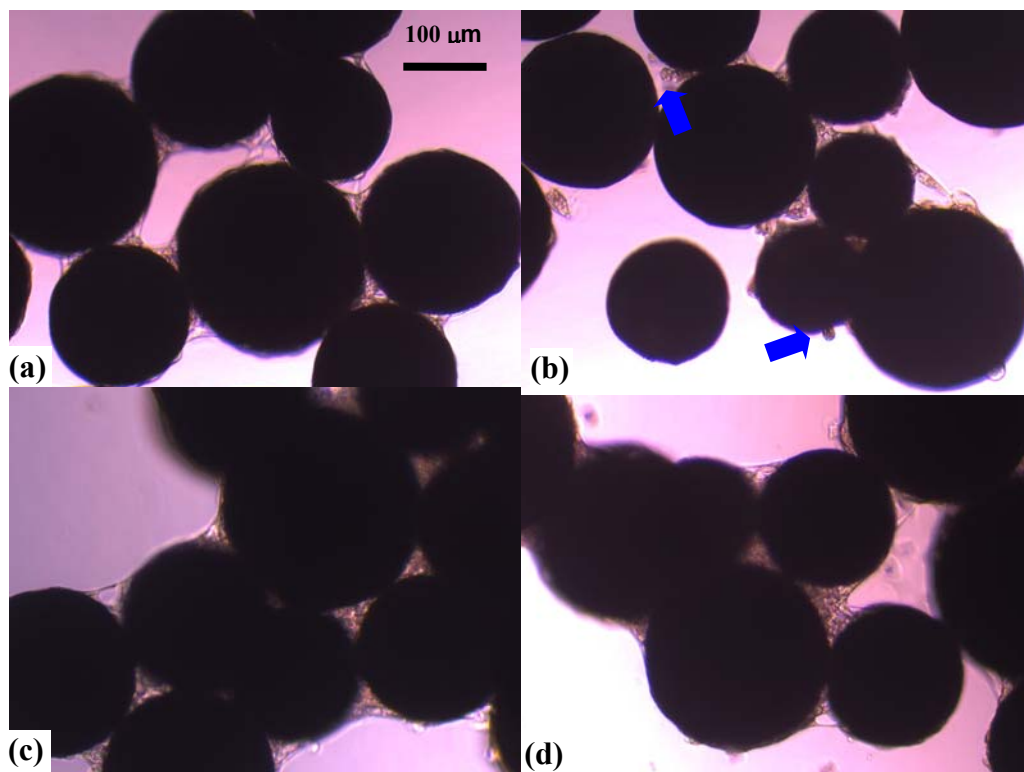


**Figure 4-3.** Optical microscope images of cell-microsphere constructs cultured for one week on (a) Blank, (b) NaOH treated, (c) Collagen-conjugated, and (d) Laminin-conjugated PHBV microspheres.

#### 4.2.4.2 Confocal laser scanning micrographs

The cells were stained with a live/dead kit (Molecular Probes) to examine their viability grown on surface modified microsphere scaffold. The fluorescent green-colored indicated live cells while the fluorescent red-colored were dead cells. CLSM images proved that most of the cells grown on blank and treated microspheres were viable. Cells were found to be better distributed on protein-conjugated microspheres [Figure 4-4(c) and (d)] as compared to the blank and NaOH-treated microspheres [Figure 4-4 (a) and (b)], which indicated that the immobilization of these bioactive molecules improved the biocompatibility of PHBV microspheres.

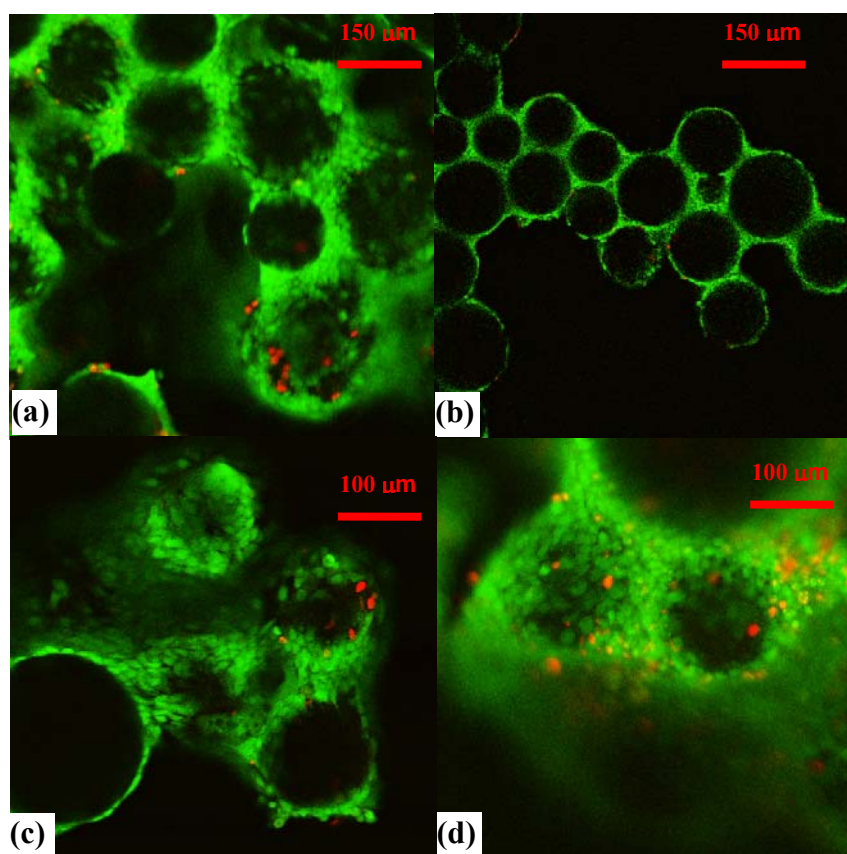


**Figure 4-4.** CLSM images of cell-microsphere constructs cultured for one week on (a) Blank, (b) NaOH treated, (c) Collagen-conjugated, and (d) Laminin-conjugated PHBV microspheres.

#### **4.2.4.3 Scanning electron micrographs**

SEM images of Hep3B cells after one week of culture on blank and surface modified PHBV microspheres are shown in Figure 4-5. It was observed that the cells had encapsulated the microspheres and aggregated them into 3D clumps. This suggested that the microspheres were good substrates for Hep3B cells, and thus also hepatocytes, to grow on by allowing extensive cell-cell and cell-substrate interactions to occur. Similar to optical and confocal micrographs (Figure 4-3 and Figure 4-4), cells were found to be better distributed on protein-conjugated microspheres as compared to the blank and NaOH-treated microspheres. The cells covered the whole surfaces of the microspheres and strong cell-substrate interactions were found on protein-conjugated samples [Figure 4-5 (d)].

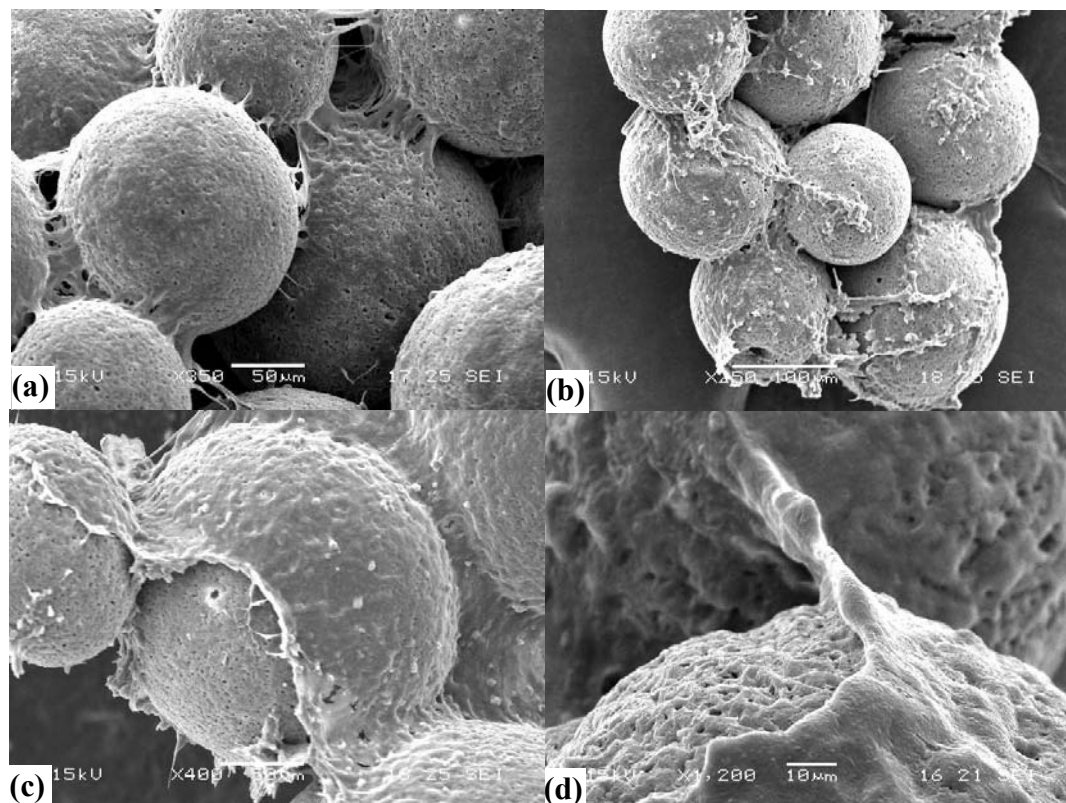


**Figure 4-5.** SEM images of cell-microsphere constructs cultured for one week on (a) Blank, (b) NaOH treated, (c) Collagen-conjugated PHBV microspheres; (d) higher (1200X) magnification of (c).

#### 4.2.5 Proliferation activity of Hep3B cells grown on microsphere scaffold

The proliferation activities of Hep3B cells grown on the blank as well as on the surface modified microspheres were quantitatively evaluated by MTT assay during the two weeks of culture (Figure 4-6). As shown in Figure 4-6 (a), the cells cultured on single protein conjugated microspheres showed no significant improvements of proliferation over the blank after two days of culture. A study by Tomomura indicated that different types of ECM protein coated substrates have no significant effects on the DNA synthesis of liver cells in 24 hr to 48 hr as the cells were in the lag growth phase

(Tomomura et al., 1987). From day 4 onwards, the cells showed improved proliferation activities when cultured on protein conjugated microspheres, especially on laminin conjugated sample over the blank, while no significance differences were found among the three protein conjugated samples [Figure 4-6 (a)]. According to Mooney, high ECM density activated hepatocytes spreading and proliferation, regardless of the type of ECM molecules used. Since the surface densities of the three proteins on the microspheres were in the range of 200-600 ng/cm<sup>2</sup>, it was believed that the cells had been stimulated into the S phase with higher proliferation activities (Mooney et al., 1992). Studies by others suggested that growth and gene expression of hepatocytes were dependent on the interactions of cells with different ECM substrates, however these effects were absent at high cell density (Bissell et al., 1987; Tomomura et al., 1987). Taken together, the three types of proteins might be different in terms of improving cell proliferation but the differences could have been diminished by the naturally high proliferation rate of the Hep3B cell line and strong cell-cell interactions induced by the tissue-like constructs.

Compared to the other samples, the cells cultured on NaOH sample exhibited the lowest proliferation rate, which was consistent with what was observed using the optical microscope (Figure 4-3). The reduced proliferation activity could probably be attributed to the more hydrophilic surface formed by the surface hydrolysis process using NaOH, which introduced carboxyl and hydroxyl groups to the surface. It has been reported that cells would have the maximum adhesion on surfaces with an intermediate hydrophilicity (Saltzman, 2000). In this regard, a more hydrophilic surface may inhibit cell attachment. Furthermore, the significant improvement of overall protein-conjugated samples as compared to the NaOH samples indicated that



the conjugation process was successful in making the microspheres more conducive to cell proliferation.

In an attempt to develop an improved liver tissue engineering system, we hypothesized that culturing Hep3B cells onto microsphere scaffolds with combinations of different ECM proteins on the surface would improve cell proliferation activity and functionality. From the MTT results [Figure 4-6 (b)], it is interesting to note that the mixed protein-conjugated samples produced a significant improvement in proliferation of Hep3B cells. It can be observed that mixtures of 1:1:1, 3:1:1 and 1:3:3 (Collagen: Laminin: Fibronectin) microspheres showed an average of 1.4 times greater cell proliferation activity than collagen conjugated microspheres and around 1.6 times greater than the blank from day 7 onwards. The three types of ECM molecules used in this work contain distinct peptide sequences which can bind with different integrin receptors on the membranes of hepatocytes. When microspheres conjugated with different proteins were bridged together (Figure 4-3 to Figure 4-5), the Hep3B cells would have chances to interact with different proteins through multiple ECM receptors. These interactions might function to re-organize the cytoskeletons of the cells, which were associated with the regulation of gene expression and DNA synthesis. Studies by others showed that the response of hepatocytes cultured on a complex substratum (EHS gel, an ECM derived from EHS tumor) were strikingly different from that on individual matrix proteins like type I collagen gel (Bissell et al., 1987; Benzeev et al., 1988). The results presented here were consistent with these findings in term of the synergistic effects of various proteins, but our results also demonstrated that the combination of proteins on rigid polymer surface could improve the cell extension as well as stimulate cell proliferation activity.

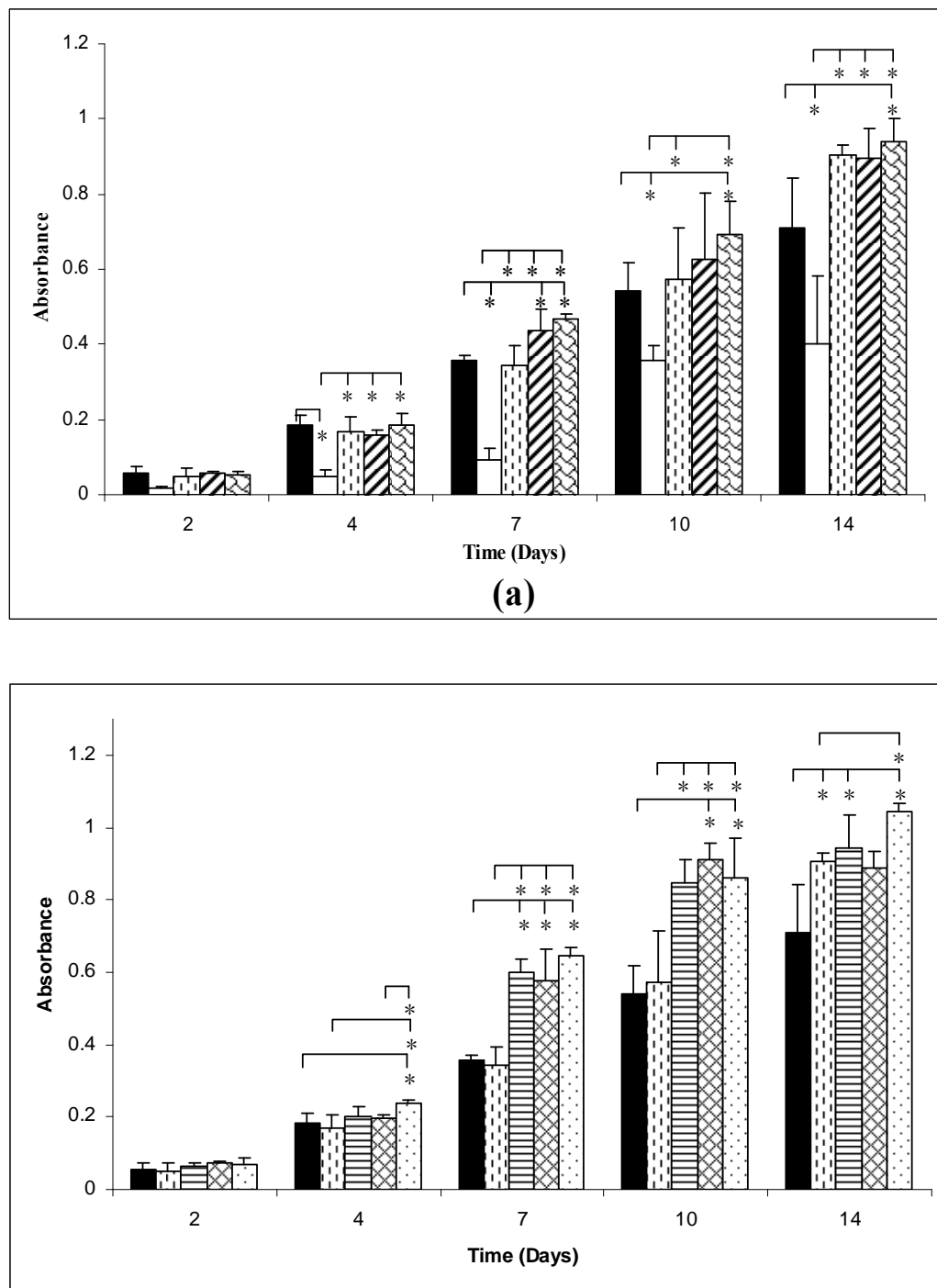


**Figure 4-6.** Proliferation of Hep3B cells cultured on (a) Blank (■), NaOH treated (□), Collagen-conjugated (▤), Fibronectin-conjugated (▨), Laminin-conjugated (▩); and (b) proteins combination (Collagen:Fibronectin:Laminin) with a ratio as 1:1:1 (▤), 3:1:1 (▨), and 1:3:3 (▩) PHBV microspheres. Values represent means±SD, n=3. Statistical significance ( $*p<0.05$ ) was determined by one-way ANOVA with Tukey's HSD post hoc analysis.

#### **4.2.6 Albumin secretion by Hep3B cells grown on microsphere scaffold**

Albumin secretion is an important indicator of hepatic function for normal primary hepatocytes, and can be similarly modeled by the Hep3B cells. In general, there was a trend of increasing albumin secretion with time elapsed for all samples (Figure 4-7). This was expected as it was known from the MTT data that cell proliferation activity increased and thus, the greater number of living cells present would have secreted more albumins. It is interesting to note that the cells cultured on mixed protein-conjugated microspheres did not show improved albumin secretion ability although they had a much higher proliferation rates, which indicated that the synergistic effect of combination ECM proteins on rigid polymer surface functioned more for improving cell proliferation. On the other hand, the blank samples showed higher albumin secretion over most of the other samples while they showed lower proliferation rates. As discussed in section 4.2.5, the high surface densities of proteins may have stimulated the higher percentage of cells into S phase with a concomitant down-regulation of differentiated functions. Our results are consistent with the findings by others that hepatocytes could be switched from differentiation to proliferation cycle through binding with different ECM molecules (Mooney et al., 1992; Rana et al., 1994; Brieva and Moghe, 2004).

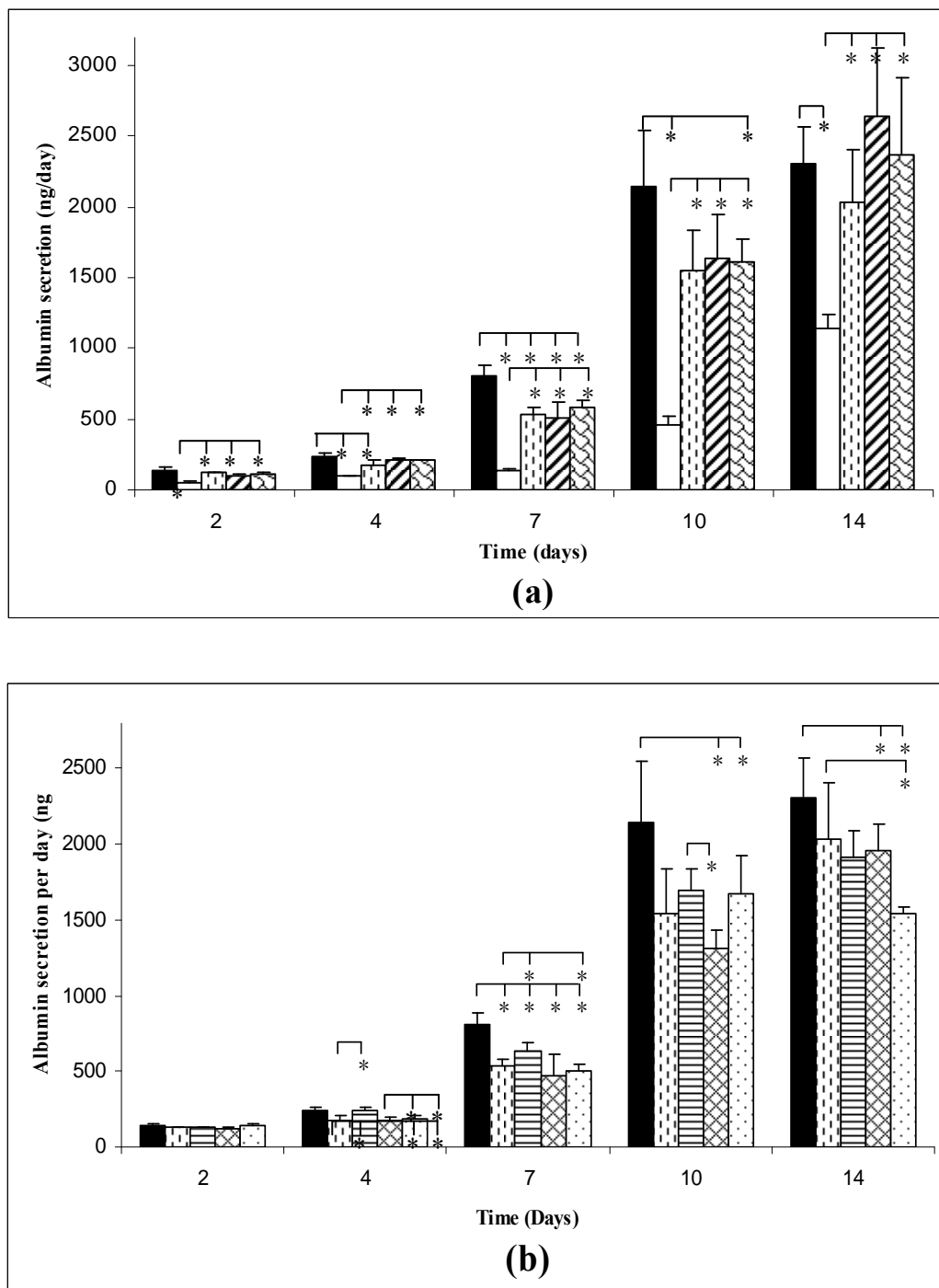


**Figure 4-7.** Albumin secretion by Hep3B cells cultured on (a) Blank (■), NaOH treated (□), Collagen-conjugated (▣), Fibronectin-conjugated (▤), Laminin-conjugated (▥); and (b) proteins combination (Collagen:Fibronectin:Laminin) with a ratio as 1:1:1 (▨), 3:1:1 (▩), and 1:3:3 (▪) PHBV microspheres. Values represent means±SD, n=3. Statistical significance ( $*p<0.05$ ) was determined by one-way ANOVA with Tukey's HSD post hoc analysis.

Albumin secretion by the cells cultured on the NaOH samples was significantly lower than other samples. This is very likely to be caused by a low population of cells present, as indicated by the poor proliferation shown in the MTT results. However, the difference is not proportional to the proliferation results. For example, by the last day of culture, the sample with the highest proliferation (mixture sample, collagen: laminin: fibronectin=1:3:3) was around 3 times of NaOH samples, while albumin secretion for this case was only around 1.2 times. There are two possible explanations. Firstly, the spherical shape of cells grown on NaOH samples [Figure 4-3 (b)] may suggest partial cellular degeneration which resulted in the release of intracellular albumin into the medium. Secondly, the rounded cell shape may also suggest elevated differentiated hepatic functions (Bhadriraju and Hansen, 2000). The study by Mooney indicated that low density proteins did not promote cell spreading, and the cells that remained spherical expressed higher liver specific functions (Mooney et al., 1992).

#### **4.2.7 P-450 activity of Hep3B cells grown on microsphere scaffold**

Another important indicator of liver hepatocyte function that can be modeled by Hep3B cells is the cytochrome P-450 enzyme activity. The P-450 activities of Hep3B cells grown on microsphere scaffolds are shown in Figure 4-8, which indicated the detoxification ability of Hep3B cells over 3 hours at the test day. Similar to the ELISA results, the blank samples had higher P-450 activity over most of the other samples, which suggested that cells with lower proliferation rate may have higher differentiated functions. As explained above, combination of proteins did not show a conclusive enhancement to the P-450 activity. By the last day of culture, the P-450 activity of samples with the highest proliferation rate (3 times more than that of NaOH samples)

was only around 1.5 times more than that of NaOH samples. Since decomposed cells could not perform P-450 activity, this interesting result suggested that Hep3B with round morphology [Figure 4-3 (b)] may perform higher hepatic functions while lower proliferation.

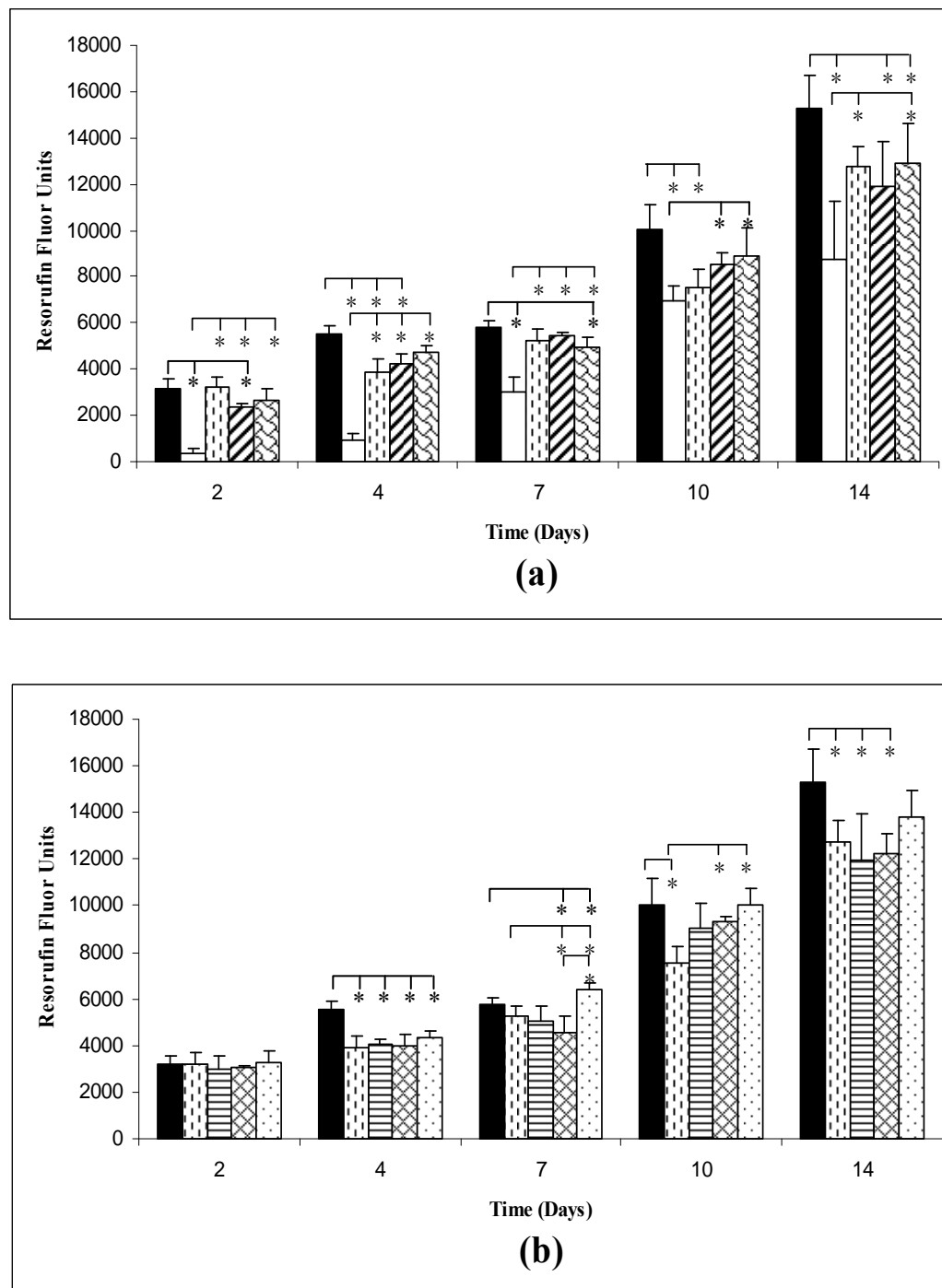


**Figure 4-8.** Cytochrome P-450 activity of Hep3B cells cultured on (a) Blank (■), NaOH treated (□), Collagen-conjugated (▣), Fibronectin-conjugated (▤), Laminin-conjugated (▥); and (b) proteins combination (Collagen:Fibronectin:Laminin) with a ratio as 1:1:1 (▨), 3:1:1 (▩), and 1:3:3 (▪) PHBV microspheres. Values represent means±SD, n=3. Statistical significance (\* $p$ <0.05) was determined by one-way ANOVA with Tukey's HSD post hoc analysis.

#### **4.2.8 Hep3B cells grown on peptide-grafted microsphere scaffold**

We have demonstrated that the conjugation of ECM proteins on the microsphere surfaces was an effective way to improve the biocompatibility of the scaffold. It was also reported that the integrin receptors on the cell membranes bind to specific sequences in the ECM proteins, which are called cell adhesive peptides. Compared with the whole protein, short cell adhesive peptides can be coupled in high densities onto the scaffold surfaces (rf. Table 4-1), and are available at a lower cost. In order to further investigate the synergistic effects of the ECM proteins, the proliferation and P-450 activity of Hep3B cells grown on the proteins mixture samples were compared with the cells grown on microspheres conjugated with two types of cell adhesive peptides, RGD and YIGSR.

The proliferation of Hep3B cells grown on blank, peptide-conjugated microspheres and the proteins mixture sample were quantitatively evaluated by MTT assay during the two weeks of culture. For convenient comparison, the absorbance of MTT solution from blank microsphere at day 2 was set as a benchmark. The ratios of absorbance of MTT solution from other samples to the benchmark were used to evaluate cell proliferation on the corresponding substrates as shown in Figure 4-9. As expected, the mean proliferation rates of the Hep3B cells grown on peptides conjugated samples were higher than the blank samples from day 7 onwards. It was also slightly higher than the single protein conjugated samples (rf. Figure 4-6). This could be attributed to the higher densities of the peptides onto the scaffold surface which improved the cell attachment as well as DNA synthesis. However, the cells grown on the proteins



mixture samples showed much higher proliferation rate than the cells grown on peptide conjugated samples. This further validated our previous finding that the combination of three ECM proteins produced a synergistic effect on all of the cell surface receptors to enhance cell proliferation activity.

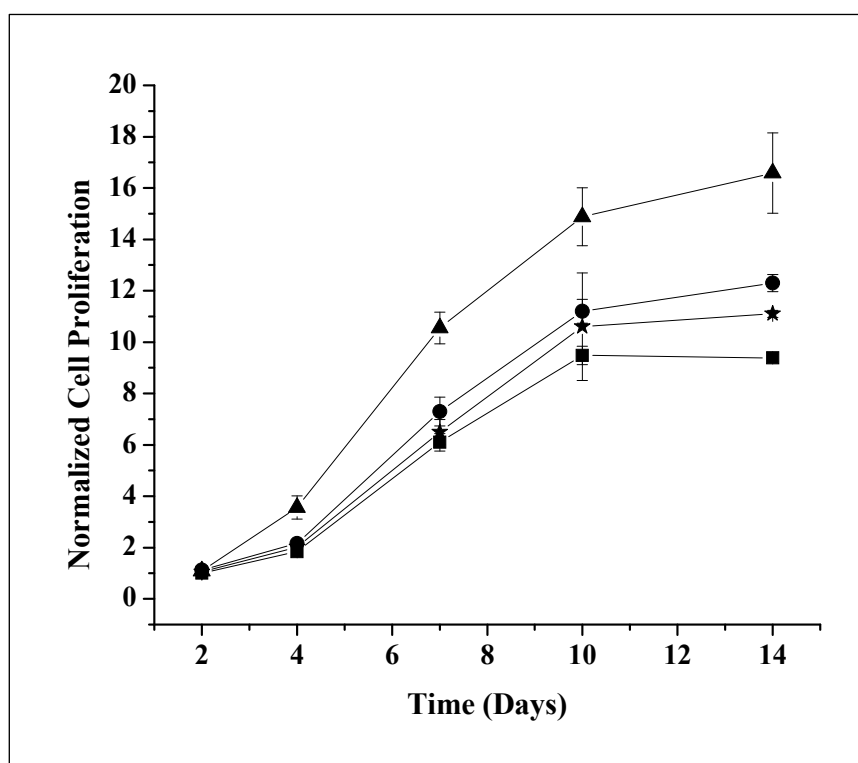


**Figure 4-9.** Proliferation of Hep3B cells cultured on Blank (■), RGD-conjugated (★), YIGSR-conjugated (●); and proteins combination (Collagen:Fibronectin:Laminin) with a ratio as 1:1:1 (▲) PHBV microspheres. Values represent means $\pm$ SD, n=3. All data were normalized to the ratios of blank microsphere at day 2, which was taken as a benchmark.

The P-450 activities of Hep3B cells grown on blank, peptide-conjugated microspheres and the proteins mixture sample are shown in Figure 4-10, with the P-450 activity at day 2 of the blank microspheres as the benchmark. In general, there was a trend of increasing P-450 activity with time for all samples, which could be

attributed to the increased cell numbers. The cells grown on blank microspheres showed higher P-450 activity over the surface modified samples, and there were no significant difference between the cells grown on peptides conjugated microspheres and the proteins mixture samples. As discussed in section 4.2.6, the surface modification functioned more on improving cell proliferation rather than the differentiated functions. The results for albumin secretion by Hep3B cells showed similar trend (data not shown).

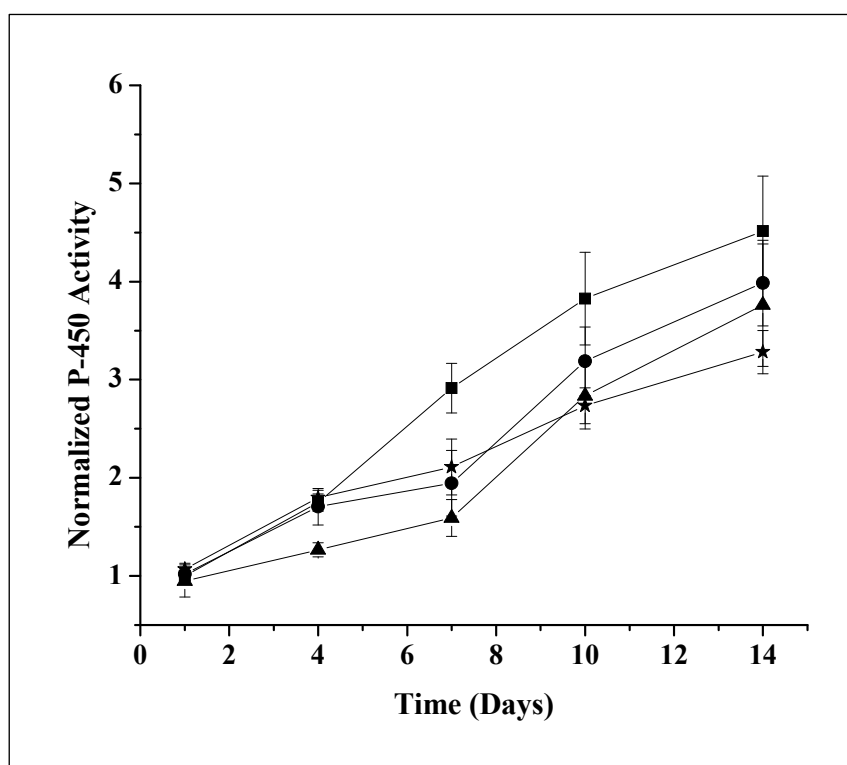


**Figure 4-10.** Cytochrome P-450 activity of Hep3B cells cultured on Blank (■), RGD-conjugated (★), YIGSR-conjugated (●); and proteins combination (Collagen:Fibronectin:Laminin) with a ratio as 1:1:1 (▲) PHBV microspheres. Values represent means $\pm$ SD, n=3. All data were normalized to the ratios of blank microsphere at day 2, which was taken as a benchmark.

### 4.3 Conclusions

In this chapter, the viability of using PHBV microspheres as tissue engineering scaffolds was improved through controlled surface conjugation with extracellular matrix (ECM) proteins, namely collagen, laminin and fibronectin. Successful conjugations of protein molecules were verified by the presence of nitrogen peaks in X-ray photoelectron spectroscopy and fluorescent green surface of microspheres in fluorescence microscopy. The improved proliferation of cells cultured on mixtures of the three types of protein-conjugated microspheres suggested that the proliferation activity of Hep3B did not just depend on single protein, but involved complex interactions between the three ECM components. Therefore, combinations of ECM components is important not just in improving the biocompatibility of tissue engineering scaffolds, but also in enhancing cellular function. Furthermore, hepatocytes with round morphology were found to perform better hepatic functions while having lower proliferation. Conversely, high proliferation would tend to lower cell function. Thus, in the design of a tissue engineering system, a scaffold showing different surface properties at different cell development stages might be necessary. The results in this chapter indicated that surface conjugation of the three ECM proteins on microsphere surfaces has a significant effect in regulating the behavior of Hep3B cells, thus better mimicking the *in vivo* environment for liver tissue engineering.

# **Chapter 5 Delivery of Hepatocyte Growth Factor from Microsphere Scaffold for Liver Tissue Engineering**

The previous two chapters have demonstrated that polymer microspheres with reproducible three-dimensional structures and easily modified surfaces are promising and versatile scaffolds for guiding liver cell growth. In addition to the scaffolds, growth factors also play an essential role in promoting cell proliferation and differentiation, as well as inducing vascularization (Babensee et al., 2000; Tabata, 2000; Chen and Mooney, 2003). Therefore, it would be advantageous if a scaffold that functions as a substrate for cell attachment, could simultaneously deliver suitable growth factors in a controlled manner to stimulate cell growth and new vessel formation within the implantation sites (Saltzman, 2002). However, it is not always possible to encapsulate growth factors directly into scaffolds due to the complex structures and fabrication process. In this regard, use of microspheres is advantageous since the growth factors can be encapsulated into microsphere with controllable

delivery profiles using well-developed techniques (Cao and Shoichet, 1999; Oe et al., 2003).

In this chapter, the encapsulation of hepatocyte growth factor (HGF) into the microspheres and subsequent control-release of the growth factors were investigated to further improve the microsphere scaffold system. HGF, also called scatter factor, is a multiple-function molecule which can interact with various types of cells as well as induce angiogenesis when administered with basic fibroblast growth factor (bFGF) (Marui et al., 2005). More interestingly, HGF is believed to improve the proliferation of primary hepatocytes but inhibit the growth of hepatoma cells. This could be used to test its bioactivity (Shiota et al., 1992; Fukai et al., 2003; Oe et al., 2003).

Poly(3-hydroxybutyrate-*co*-3-hydroxyvalerate) (PHBV) showed excellent biocompatibility to Hep3B and HepG2 cells in previous works. However, PHBV may not be a good candidate for encapsulating proteins such as growth factors since most proteins are hydrophilic while PHBV is quite hydrophobic due to its high crystallinity. Poly(lactic-*co*-glycolic acid) (PLGA) which also shows good biocompatibility, has been shown to be able to encapsulate proteins at higher encapsulation efficiency. In order to preserve the excellent biocompatibility of PHBV, while improving its encapsulation ability of growth factors, PHBV was mixed with PLGA, and investigated as scaffold material for the encapsulation of bovine serum albumin (BSA) and hepatocyte growth factor (HGF). Comparison was made with pure PHBV and pure PLGA microspheres. The release of BSA served as the model for HGF since both proteins have similar molecular weights and hydrophilicity, and the co-encapsulation of BSA with HGF is believed to preserve the bioactivity of the growth factor by

reducing its exposure to organic solvents. The effects of polymers on the morphologies, protein-releases and degradation profiles of the microsphere scaffolds were studied by varying the polymer compositions (PHBV, PLGA and PLGA/PHBV). The bioactivity of released HGF was assessed by Hep3B cell inhibition assay. Furthermore, primary hepatocytes from rats were cultured on the PLGA/PHBV microsphere scaffold for up to 10 days to study the effect of directly delivering the growth factors to the cells.

## **5.1. Materials and Methods**

### **5.1.1 Materials**

Poly(lactide-*co*-glycolide) acid (PLGA, 5050DL 4A) was purchase from Lakeshore Biomaterials (Birmingham, AL, USA), PLGA. Recombinant hepatocyte growth factor (HGF) was from RayBiotech (Norcross, GA, USA). Hepatocyte growth factor detection ELISA kits was purchased from R&D system Inc (Minneapolis, MN, USA). Penicillin, dexamethasone and acetone were purchased from Sigma-Aldrich (St. Louis, MO, USA). Information of the chemicals which were used in this chapter but not listed in this section can be found in section 3.1.1 in Chapter 3. All chemicals were used directly without further purification.

### **5.1.2 Fabrication of protein-encapsulated microspheres**

A water-in-oil-in-water (w/o/w) emulsion solvent evaporation technique was used to fabricate microsphere scaffolds as well as to encapsulate the proteins. Briefly, 500 mg of PHBV (8%) powder was dissolved in 12 mL of chloroform, and 0.5 mL of 50 mg/ml BSA (for a protein loading of 5%) phosphate-buffered saline (PBS, 0.01M, pH=7.4) solution was added. Emulsification was subsequently carried out by

sonication in an ice bath using a probe sonicator (VCX130, SONICS & Materials, CT, USA) at 50% power output for 40s. The homogenized mixture was immediately added into 150 mL of PBS (0.01M, pH=7.4) with 0.05% w/v PVA drop by drop under continuous mechanical stirring (RW20, Ika Labortechnik, Staufen, Germany) at 300 rpm for 4 hours to evaporate the organic solvent. The microspheres produced were washed five times with deionized water to remove as much of the surfactant (PVA) and BSA attached on the surface as possible and freeze dried in a freeze dryer (Alpha 1-4, Martin Christ, GmbH, Germany). PLGA and a blend of PHBV/PLGA (1:1, w/w) microspheres were prepared using the same methodology.

Ten micrograms of HGF was co-encapsulated with BSA in PHBV/PLGA microspheres as described above, using the same BSA loading of 5% w/w. The co-encapsulated BSA might serve to protect HGF through reducing the exposure of the molecules to shear stress and organic solvent during encapsulation as well as to function as a stabilizing agent to prolong the bioactivity of HGF (Cao and Shoichet, 1992). The release of BSA can also serve as a model for HGF release from the microsphere scaffolds and encapsulation efficiency (EE) can be used to estimate the EE of HGF.

### **5.1.3 Characterization of protein-encapsulated microspheres**

The size distributions of all the three types of microspheres were measured by a particle size analyzer (Coulter LS-230, FL, USA). Tween<sup>®</sup>80 was used to disperse microspheres into the water homogeneously. Microspheres were sectioned with a cryostat microtome (Leica CM3050S, Germany) with blade step setting at 30  $\mu$ m and air dried. The intact and cross-sectioned microspheres were mounted onto brass stubs

using double-sided adhesive tape and vacuum-coated with platinum using the Auto Fine Coater (JFC-1300, JEOL, Tokyo, Japan) for 40 seconds. The external and internal morphologies were then characterized by a scanning electron microscope (SEM) (JSM-5600VL, JEOL, Tokyo, Japan). The surface atomic compositions of the three types of microspheres were characterized using an X-ray photoelectron spectroscopy (XPS, VGESCALAB 220I-XL, Thermo VG Scientific, UK) with data processing performed using XPSPEAK (Raymond, W.M. Kwok, Hong Kong). Wide scan (0-1000eV) and high resolution (C1s, O1s and N1s) spectra were acquired respectively.

#### **5.1.4 *In vitro* degradation of microspheres**

Thirty milligrams of microspheres (PHBV, PLGA or PHBV/PLGA) were suspended in an Eppendorf microtube with 1.5 mL of PBS (0.01M, pH=7.4) at 37°C in a circulating water bath (100 rpm), and PBS (0.01M, pH=7.4) was changed every 5 days. At scheduled time, the microspheres were washed with deionized water and freeze-dried for 48 hours. The degradation profiles of the microspheres were characterized by mass loss using a microbalance (Sartorius MC5, Germany). The degraded microspheres were also characterized under SEM to check morphology change.

#### **5.1.5 Encapsulation efficiency assays**

**BSA:** To determine the encapsulation efficiency of BSA in the microspheres, 20 mg of microspheres were dissolved in 2 mL of chloroform to which 5 mL of PBS (0.01M, pH=7.4) was added. The solution was mixed thoroughly using a vortex mixer to extract BSA to the water phase and centrifuged (20 min at 9,000 rpm) to accelerate phase separation. The supernatant was aspirated out and kept in a 50 mL tube. This



process was repeated three times, and the concentration of BSA was measured using a Micro BCA<sup>TM</sup> Protein Assay Kit (Pierce). The encapsulation efficiency was calculated as the ratio of the actual to the theoretical BSA loadings.

**HGF:** Due to the limitations of the assay detection limit (0.5 µg/mL), the Micro BCA<sup>TM</sup> assay is not suitable to measure the EE of HGF. Enzyme-linked immunosorbent assay (ELISA), which is based on antibody-antigen mechanism, is normally used to detect the proteins with very low concentrations. However, the extraction process mentioned above could denature the growth factor according to our preliminary experiments, making ELISA not a feasible method to measure the EE. Therefore, two alternative methods were used to estimate the EE of the HGF: (1) Using the EE of BSA as an indicator to estimate the EE of HGF; and (2) Using the cumulative release of HGF up to three months as the actual HGF loading in the microspheres.

#### **5.1.6 *In vitro* release studies**

**BSA:** Twenty milligrams of each type of BSA-encapsulated microspheres were suspended in 1 mL of PBS (0.01 M, pH=7.4) and incubated at 37°C in a circulating water bath (100 rpm). At set time points, the microspheres were centrifuged (5 min at 13,000 rpm), and the supernatant was collected and stored in a -20°C freezer while the microspheres were re-suspended in 1 mL fresh PBS (0.01 M, pH=7.4). BSA content in the supernatant was analyzed using HPLC (HP1100, Agilent, USA). A size exclusion column for was used as the analytical column (PL Aquagel-OH Mixed, 300mm, Agilent, USA). The mobile phase was PBS (0.01M, pH=7.4) and the flow rate was 1.0

mL/min. The wavelength of UV detector was set as 210 nm and the sample injection volume was 50  $\mu$ L.

**HGF:** For HGF and BSA co-encapsulated microspheres (PHBV/PLGA), 80 mg of microspheres were suspended in 8 mL of serum-free medium and incubated at 37°C. At set time, the microspheres were centrifuged (5 min at 13, 000 rpm), the supernatant was filter-sterilized with a 0.22  $\mu$ m filter and stored in a -20°C freezer prior to concentration and bioactivity analysis. The HGF content in the supernatant was analyzed using an ELISA (Hepatocyte growth factor quantification, R&D System, USA) kit for hepatocyte growth factor.

### **5.1.7 Bioactivity assays for the released proteins**

Hepatoma cell line Hep3B (ATCC) were cultured in a serum-medium which was composed of DMEM supplemented with 10% v/v FBS, 110 mg/L sodium pyruvate and 1% v/v antimycotic solution (100 units/ml penicillin G, 100  $\mu$ g/ml streptomycin sulfate, and 0.25  $\mu$ g/ml amphotericin B). The serum-free (SF) medium was defined the same as the above mentioned serum-medium except FBS was not added. The cells were maintained in T-75 flasks in an incubator at 37°C in the presence of 5% CO<sub>2</sub> and 95% relative humidity. The medium was renewed every three days.

The bioactivity of HGF released from PHBV/PLGA microspheres was assessed using Hep3B cell proliferation inhibition assays (Shiota et al., 1992). Hep3B cells were seeded into a 24-well plate with a concentration of 15,000 cells per well in serum-medium. After being incubated for 4 hours, the medium was aspirated out carefully and replaced with 0.5 mL of the released medium from HGF or BSA loaded microspheres. SF medium and SF medium supplemented with 5 ng/mL and 50 ng/mL HGF were

used as the controls. After the cells were cultured for 24 hours, total DNA quantification assay was used to measure the cell proliferation, while enzyme-linked immunosorbent (ELISA) and EROD assays were used to determine the functionalities of the liver cells. The detailed description of these three assays (total-DNA, ELISA and EROD) can be found at 3.1.6 in Chapter 3.

The degradation products from the polymer may affect the proliferation and function of the cells, and the metabolic activities of the cells may also contribute to the degradation of the polymers. In order to determine these effects, 5 mg of PLGA/PHBV microspheres was put into a 0.22  $\mu\text{m}$  Transwell Insert (Nunc, Denmark). The inserts was then placed in a 24-well plate which has been seeded with Hep3B (15,000 cells per well). The cells seeded on the well without the insert was used as a control. At scheduled time points, the proliferation and albumin secretion of the cells and the degradation of the microspheres were quantitatively measured.

### **5.1.8 Culturing primary hepatocytes on PLGA/PHBV microsphere scaffold**

Primary hepatocytes from rats were obtained from an established liver perfusion method (courtesy of Department of Physiology, National University of Singapore). The culture medium was composed of DMEM supplemented with 10% v/v FBS, 0.1% v/v bovine serum albumin, 100 units/mL penicillin, 5  $\mu\text{g}/\text{mL}$  insulin and 100 nM dexamethasone.

Primary hepatocytes were seeded on the PHBV/PLGA microsphere using previous established method.  $3 \times 10^4$  cells were seeded on every five milligram of microspheres in a 24-well tissue culture plate. Microspheres without growth factors and blank wells were used as controls. To compare the effects of freely administered growth factors to

the cells, cell culture medium supplemented with 50 ng/mL of HGF was used as a third control to culture the cells grown on the wells. At set time points, cell proliferation and functions were quantified with total-DNA, ELISA and EROD assays (rf. 5.1.7). The microspheres and plates were coated with collagen (type IV) before the experiments.

### **5.1.9 Statistics**

All data are presented as mean  $\pm$  standard deviation and were analyzed by a one-way ANOVA followed by Tukey's HSD post hoc analysis, where the "\*" ( $p < 0.05$ ) indicate significant difference of the samples to the positive control (serum free medium). Student's t-test were also carried out for statistical comparisons between pairs of samples, where the "+" indicate significant difference ( $p < 0.05$ ).

## **5.2 Results and Discussion**

### **5.2.1 Characterization of the microspheres**

The size distributions of the three types of microspheres (PHBV, PLGA and PHBV/PLGA) were quantified using Coulter LS-230 and the results were shown in Table 5-1. It can be seen that PHBV microspheres have the largest mean diameter (210.3  $\mu\text{m}$ ), while the mean diameter of PLGA microspheres is the smallest (156.8  $\mu\text{m}$ ). Given that all of the preparation parameters were held constant, this can be attributed to the different molecular weights of PHBV and PLGA which are 575.9 kDa and 61.6 kDa respectively. The longer carbon chains of PHBV could produce a larger microsphere when the polymers entangled together by the force of the surfactant

micelles during the emulsion process. Meanwhile the small standard deviations also indicate narrow distributions of all the microspheres.

**Table 5-1.** PHBV, PLGA and PHBV/PLGA microspheres encapsulated with BSA

<b>Microsphere</b>	<b>Diameter, <math>\mu\text{m}</math> (mean <math>\pm</math> S.D.)</b>	<b>BSA (w/w%)</b>	<b>Encapsulation Efficiency (%)</b>	<b>Initial Burst* (%)</b>
<b>PHBV</b>	210.3 $\pm$ 35.2		32.52 $\pm$ 2.31	59.67
<b>PHBV/PLGA</b>	185.2 $\pm$ 22.5	5	92.36 $\pm$ 3.52	17.66
<b>PLGA</b>	156.8 $\pm$ 23.6		88.65 $\pm$ 1.65	1.12

\* BSA released during the first 24 hour.

The external and internal morphologies of the microspheres were further characterized using SEM. As shown in Figure 5-1, all the three types of microspheres have spherical shapes, but quite different surface morphologies and internal structures. PLGA microspheres have a smooth surface whereas PHBV and PHBV/PLGA microspheres have a rough topography with nano-scale pores which can accelerate the release of proteins from the microspheres. As indicated in Figure 5-1 (A2), PHBV microspheres possess highly porous internal structure with a pore size around 15  $\mu\text{m}$  which could be attributed to the high hydrophobic property of PHBV (water contact angle of PHBV film is around 79°). During the 1<sup>st</sup> emulsification process, water droplets could not mix with the hydrophobic PHBV molecules homogeneously, instead the droplets would coalesce to form bigger droplets among the organic phase, and pores found both internally and on the surface [Figure 5-1 (A3)] were formed by the removal of the water droplets through lyophilization. Compared with PHBV, PLGA molecules are relative more hydrophilic (water contact angle of PLGA is about 60°), therefore the water droplets could be distributed evenly among the polymer solution which resulted in a uniform internal structure [Figure 5-1 (D2)].

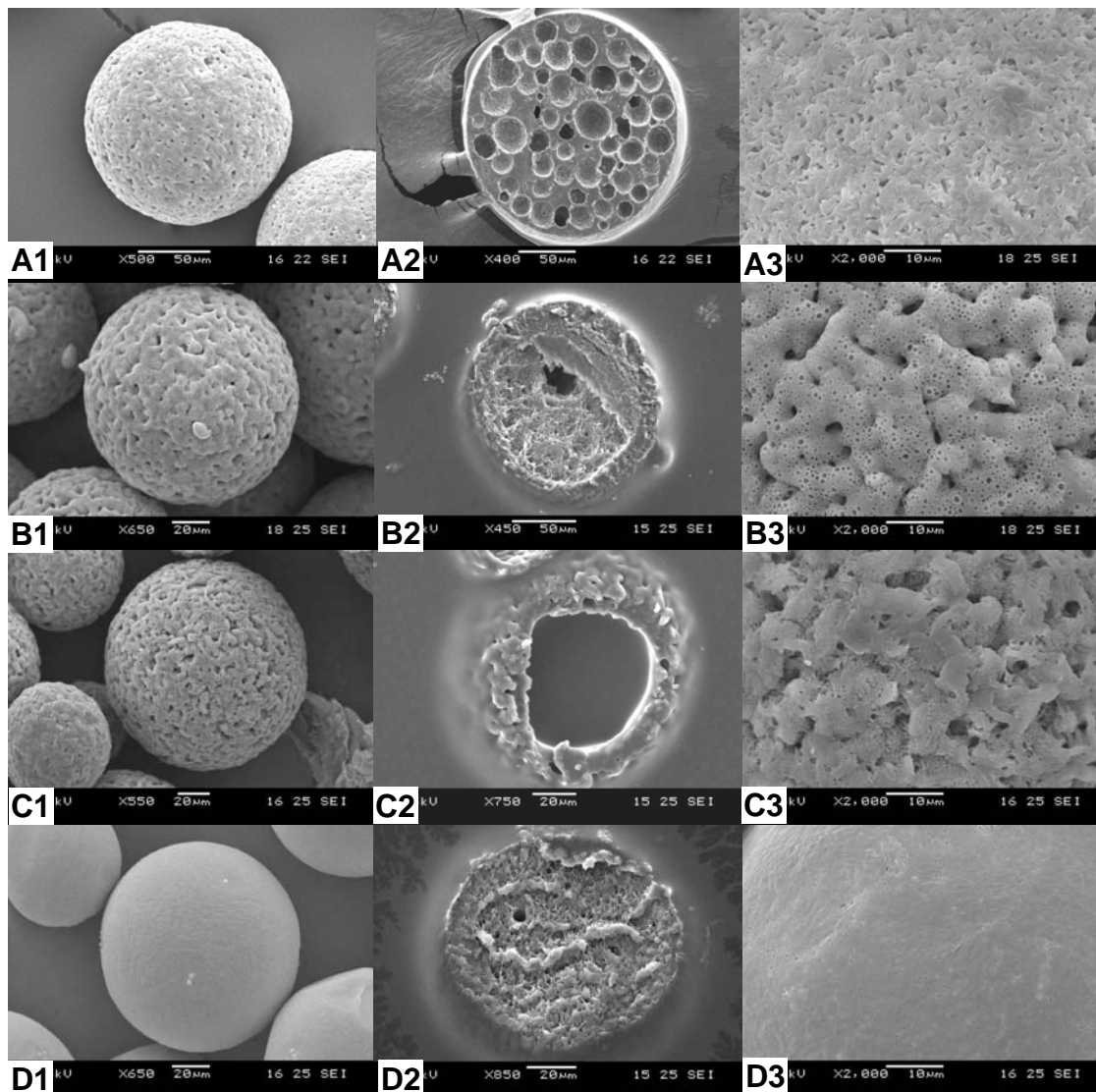


**Figure 5-1.** SEM images of PHBV (A), PHBV/PLGA (B), partially dissolved PHBV/PLGA (C), and PLGA (D) microspheres, where panels labeled with 1, 2 and 3 respectively are the general morphology, cross section and close-up on the surface of the microspheres.

It is interesting to note that the composite PHBV/PLGA microspheres show a core-shell structure, a porous core surrounded by a relative dense shell [Figure 5-1 (B2)]. According to Mathiowitz and colleagues, during the evaporation of the solvent, a two-polymer solution tends to phase separate to achieve the most stable

thermodynamic configuration (Pekarek et al., 1994). The final configuration was affected by the preparation variables, such as the solution concentration, weight ratio and volume ratio of the two polymers, temperature and solvents used (Leach et al., 1999; Yang et al., 2003). In order to determine the distribution of the two polymers within the blend, the PHBV/PLGA microspheres were suspended in acetone for 3 hours followed by washing with deionized water, freeze dried and then observed under SEM. As shown in Figure 5-1 (C2), the cores of the composite microspheres were totally dissolved resulting in a hollow structure. Since PHBV does not dissolve in acetone, the results suggest that the core is mainly PLGA by composition. However, as compared with [Figure 5-1 (B3)], the shell is also partially dissolved forming a porous and rough surface [Figure 5-1 (C3)] which implies that the shell is actually a blend of the two polymers. This was further confirmed by analysis for surface chemical compositions of the microspheres using XPS (Table 5-2).

**Table 5-2.** Surface chemical composition of PHBV, PLGA and PHBV/PLGA microspheres

Microsphere	Atomic concentration %			C/O
	C 1s	O 1s	N 1s	
<b>PHBV</b>	70.32	29.13	0.55	2.41
<b>PHBV/PLGA</b>	68.65	30.62	0.73	2.24
<b>PLGA</b>	66.68	33.12	0.20	2.01
<b>PHBV/PLGA*</b>	69.74	29.85	0.41	2.34

\*After partially dissolved in acetone

Our previous work indicated that either PLGA or PLLA can be located at the core or shell in double-walled microspheres, depending on their respective mass ratio. Specifically, PLGA and PLLA were found to form the shell and core, respectively for mass ratios of PLGA:PLLA > 1:1. In contrast, when PLGA:PLLA is reduced to below

1:1, a phase inversion was observed where the more hydrophobic PLLA was located as the shell to form double-walled microspheres (Tan et al., 2005). Our current findings agree well with the low mass ratio cases mentioned above since the more hydrophilic PLGA occupied the core surrounded by the blended shell of PHBV and PLGA. Given the similar preparation parameters and methods, this can be explained by the different molecular weights. In the present system, the molecular weight of PHBV (575.9 kDa) is significantly greater than PLGA (61.6 kDa). Therefore, besides the mass ratio and hydrophilicity, the molecular weight differences of the two polymers are also an important factor that can affect the final polymer distribution or configuration.

### **5.2.2 Encapsulation efficiency**

The actual protein encapsulated in each type of the polymer microspheres was determined quantitatively by an extraction method. As shown in Table 5-1, the encapsulation efficiency of PHBV microsphere is very low, only 32.52% of BSA has been encapsulated, while PLGA microsphere shows a much higher EE (88.65%). As commonly seen in the double emulsion method for the encapsulation of proteins, EE is highly dependent on the chemical structure, molecular weight and hydrophobicity of the polymers (Cao and Shoichet, 1999). In the present system, hydrophobic PHBV may not be fully compatible with BSA to form a stable emulsion due to the significant difference in hydrophobicity. It can be seen that the EE of composite PHBV/PLGA microsphere is similar to the pure PLGA microspheres although the mass of PLGA is only half of that. As confirmed earlier in section 5.2.1, the PHBV/PLGA microsphere has a core-shell structure. The large PHBV molecules distributed within the shell is hypothesized to prevent the loss of proteins during the fabrication and washing process.



As shown in Table 5-3, HGF was also encapsulated in the composite PHBV/PLGA microspheres with a high efficiency. Since the ELISA assay is based on an antibody-antigen interaction, denatured proteins may not be recognized by the antibodies coated on the plates. Therefore, two methods were used to estimate the EE of HGF (Table 5-3) in this study. The loading of HGF could be quantified accurately by labeling HGF with radioisotope or fluorescent molecules.

**Table 5-3.** PHBV/PLGA microspheres with BSA and HGF co-encapsulated

<b>Microsphere</b>	<b>Diameter, <math>\mu\text{m}</math> (mean <math>\pm</math> S.D.)</b>	<b>Drug Loading (w/w %)</b>	<b>Encapsulation Efficiency (%)</b>
<b>PHBV/PLGA</b>	180.6 $\pm$ 25.6	5 (BSA)	90.88 $\pm$ 2.76*
		0.002 (HGF)	88.62 $\pm$ 3.36**

\* Estimated from co-encapsulated BSA

\*\* Calculated from cumulative release of HGF

### 5.2.3 Degradation of the microspheres

The degradation of the microspheres encapsulated with BSA was characterized with mass loss and SEM. As shown in Figure 5-2, the degradation of PHBV microspheres was very slow, only around 7% of initial mass was lost after 110 days. The slow rate can be attributed to the high crystallinity of PHBV resulting from its repeat units with a short methyl side group. In contrast, PLGA microspheres showed a faster mass loss between 14 and 50 day as indicated by a steep slope, and the microspheres degraded completely after two months. The hydrolysis of ester bonds in the PLGA backbone generated carboxylic acids which can further catalyze the

degradation (autocatalytic hydrolytic degradation) and resulted in the accelerated degradation of PLGA microspheres. Since both PHBV and PLGA are polyesters, their degradation by-products are small molecule acids which are not harmful to the cells. This was verified when Hep3B cells were cultured in the presence of the degradation products of PHBV and PLGA, and no significant differences were observed in the proliferation and albumin secretion of the cells (section 5.1.7, data not shown). However, for *in vitro* cell culture or *in vivo* implantation, the released acids, if not removed timely, may change the local pH value dramatically and affect cell growth or induce inflammatory response (Cao and Shoichet, 1999). In this regard, the PHBV/PLGA composite microspheres, which showed an intermediate degradation rate between PHBV and PLGA of 55% loss of the initial mass by 110 days, would be more suitable since the moderate degradation can allow an effective exchange of acid by-products to the surrounding environment. Since the degradation of PHBV was relatively slow, most of the mass loss here was likely to be resulted from the degradation of the PLGA component.

The presence of metabolically active Hep3B cells were also observed not to have a significant effect on the degradation of the PHBV/ PLGA microspheres as observed by the mass loss (dotted line in Figure 5-2). Therefore, as both PLGA and PHBV are polyesters, the degradation of such polymers is attributed mainly to the hydrolysis of the ester bonds in the backbone. The enzymatic decomposition initiated by the cells, by comparison, would be negligible.

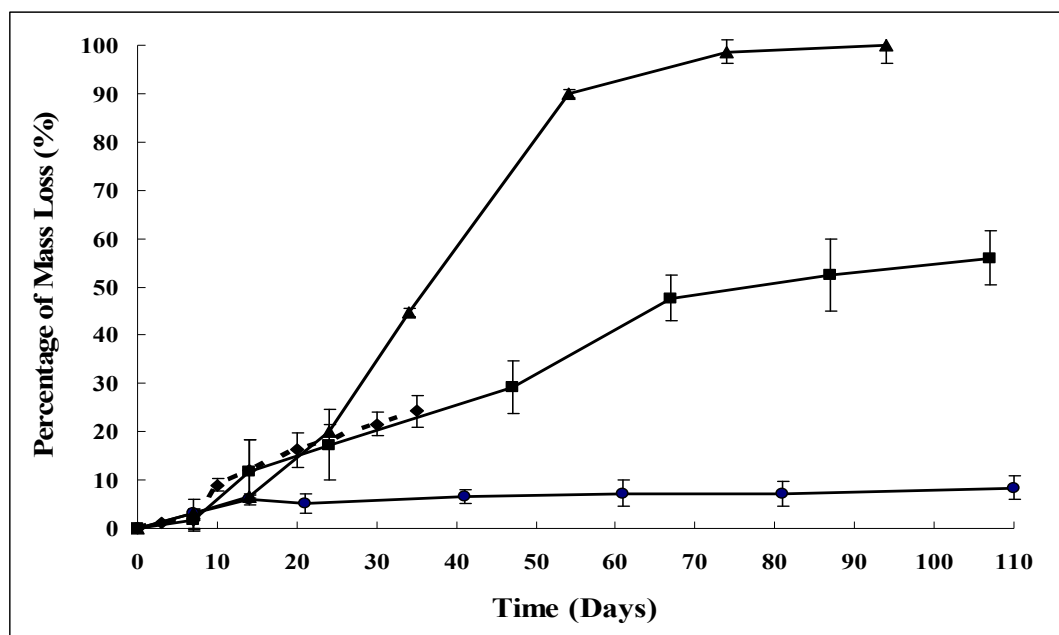


**Figure 5-2.** Degradation profiles of microspheres characterized by mass loss up to 110 days for (●) PHBV, (■) PHBV/PLGA, and (▲) PLGA. Dotted line (◆) shows the degradation profile of PLGA/PHBV microsphere in the presence of Hep3B cells. Values represent means $\pm$ SD, n=3.

The degraded microspheres were observed under SEM to monitor the morphology changes due to degradation (Figure 5-3). After three months of incubation, PHBV microspheres still retained the original spherical shapes and did not show significant changes in surface and internal morphologies. This is consistent with the very slow mass loss observed in Figure 5-2. However, for PLGA microspheres, dramatic morphology changes were observed after one month of incubation. Although the PLGA microspheres still remained spherical, the structure looks quite loose, and the initial smooth surface turned into highly porous structures which probably resulted from the leaching out of the degradation products [Figure 5-3, panel C(3)]. PLGA microspheres degraded almost totally after two months and only aggregated debris was

left (figure not shown). The PHBV/PLGA composite microspheres also showed dramatic morphology changes after three months of incubation. The dense cores totally disappeared and a shell with a hollow core remained. In contrast, the shell was degraded heterogeneously and this resulted in a highly porous surface. This verified again that the core was occupied by PLGA while the shell was the blend of the two polymers (cf. Figure 5-1C).

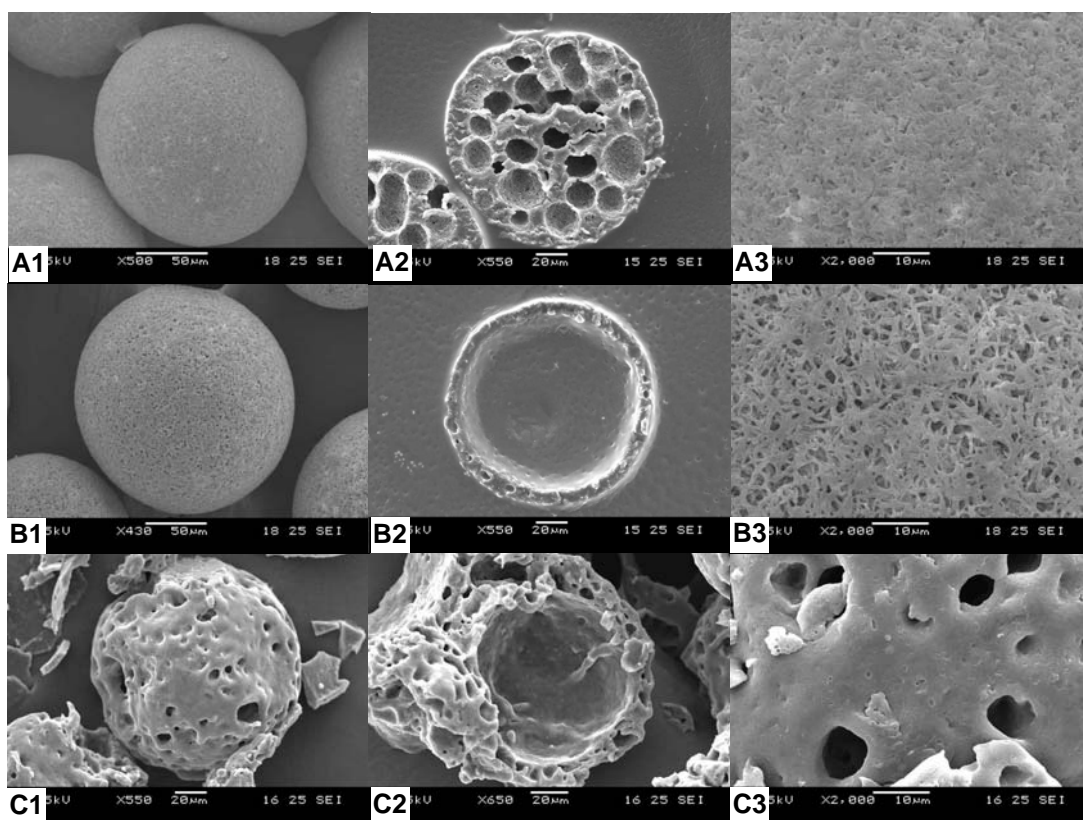


**Figure 5-3.** SEM images of PHBV (A) and PHBV/PLGA (B) microspheres after 90 days of degradation, and PLGA (C) microspheres after 30 days of degradation, where panels labeled with 1, 2 and 3 respectively are the general morphology, cross section and close up on the surface of the microspheres.

### 5.2.4 *In vitro* release profiles of BSA and HGF

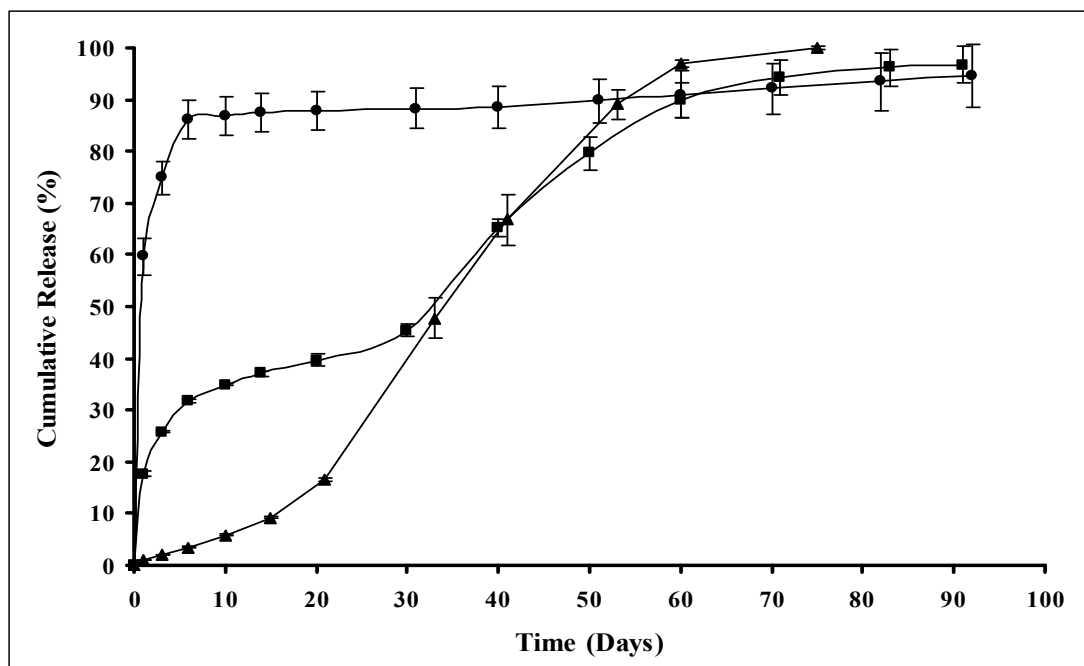


**Figure 5-4.** Cumulative release of BSA from (●) PHBV, (■) PHBV/PLGA, and (▲) PLGA microspheres. Values represent means $\pm$ SD, n=3.

BSA was used as a model protein for HGF because both BSA and HGF have similar molecular weights and BSA is a well-characterized protein with relatively low cost (Cao and Shoichet, 1999). Figure 5-4 shows the release profiles of BSA from the three types of microspheres. The release of BSA from pure PHBV microspheres reached around 88% after 6 days with a substantial initial burst (59.67%). The subsequent release was quite slow and reached around 94% by the end of 3 months. Since PHBV was not compatible with BSA (cf. section 5.2.2), most of the encapsulated proteins might be located near the surface, which could diffuse out very soon during the first week. In contrast, the pure PLGA microspheres provided a slow and linear release profile during the first two weeks. Given that the degradation of

PLGA was insignificant during this period, the released BSA was most by diffusion from areas near the surface. It is interesting to note that the initial amount of BSA released is very small (cf. Table 5-1) which differs from commonly reported protein release profile with a burst more than 10% (Cao and Shoichet, 1999; Tan et al., 2005). This is probably due to the thorough washing process since the initial burst is believed to come from the proteins on the surface. The assumption was supported by surface atomic compositions of the microspheres (Table 5-2), the low nitrogen concentrations indicated small amount of proteins remained on the surface. The less porous surface of PLGA microspheres also reduced the diffusion rate of BSA during this initial period. The accelerated release after the initial diffusion was consistent with the accelerated mass degradation of the microspheres (cf. Figure 5-2). A linear release profile was achieved up to 60 days when microspheres were degraded totally with 100% release of BSA. The initial release (within the first week) of BSA from PHBV/PLGA microspheres is fast followed by a slow release plateau (from 7 days to 30 days), which differs from both pure PLGA and PHBV microspheres. The fast initial release could be attributed to the porous surface which allowed for the easy diffusion of proteins. It is worth noting that the accelerated release phase (from 30 to 70 days) is mainly due the degradation of PLGA, and was delayed as compared with PLGA microspheres (from 20 to 60 days). A possible explanation is that the hydrophobic PHBV shell can slow down the degradation as well as prevent the release.

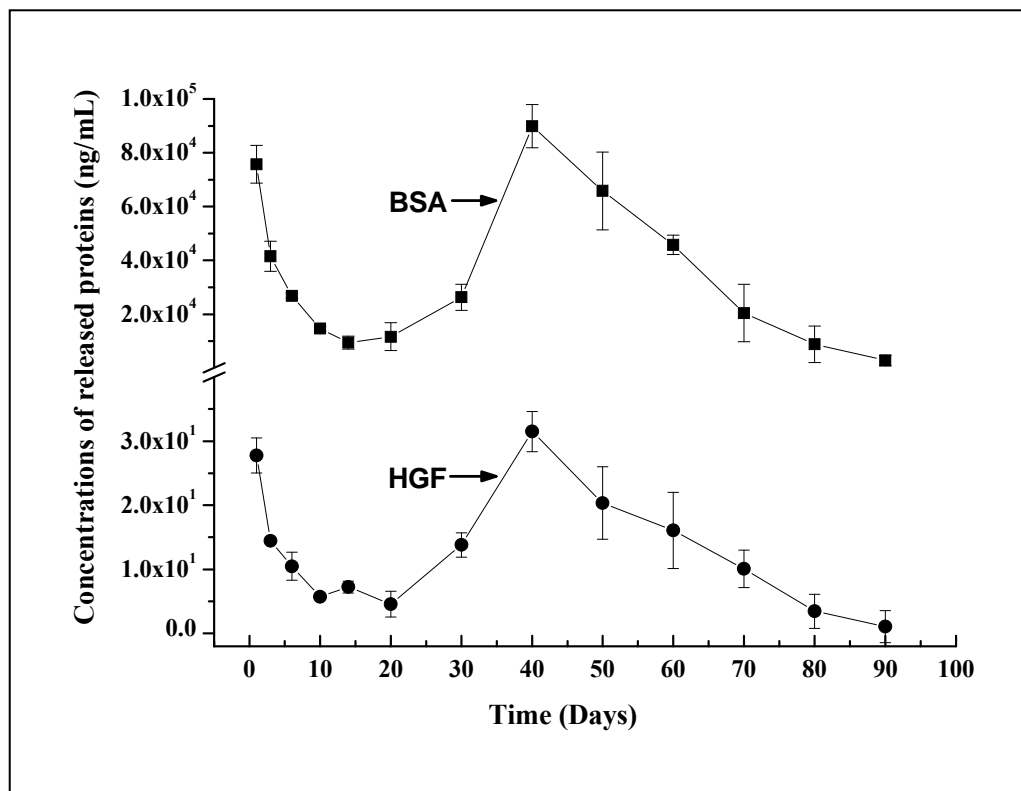


**Figure 5-5.** Actual concentrations of released BSA (■) and HGF (●) from PLGA/PHBV microspheres. Values represent means $\pm$ SD, n=3. Different scales were used to plot HGF and BSA for comparison purposes.

Since the effects of HGF on Hep3B cells are concentration-dependent, the release profile of HGF was plotted in the form of actual concentrations of released proteins versus time for convenience (Figure 5-5). The different scales used here should be noted since the loadings of BSA and HGF were different, and thus the released concentrations were significantly different. As expected, the profile of HGF is similar to BSA released from PHBV/PLGA microspheres. This observation substantiates very well the hypothesis used in the present study that BSA is a reasonably good model protein for HGF. The detection of the growth factor by the ELISA kit also indicated

that the HGF was not denatured and thus reconfirmed the benefits of using BSA co-encapsulated HGF as a protection agent in the double emulsion process.

### **5.2.5 Bioactivity of the released proteins**

The bioactivity of HGF released from PHBV/PLGA microspheres was assessed by culturing Hep3B cells in the medium from the release study. Bioactive HGF is known to improve the proliferation of primary hepatocytes but inhibit the growth of various hepatoma cell lines, such as HepG2 and Hep3B. In previous chapters, Hep3B cell line has been used as a model for tissue engineering, the effects as determined in this section could similarly be used as a model for subsequent works with primary hepatocytes. The cell numbers after 24 hours incubation normalized from cellular DNA, were used as an indicator of bioactivity by comparing to a positive control (SF medium), and two negative controls (SF medium supplemented with 5 ng/mL and 50 ng/mL HGF respectively). The medium from microspheres encapsulated with BSA alone served as a control for both the effects of released BSA on Hep3B cell proliferation and any potential cytotoxicity of the polymer degradation products.



## 5.2.5.1 Total-DNA quantification

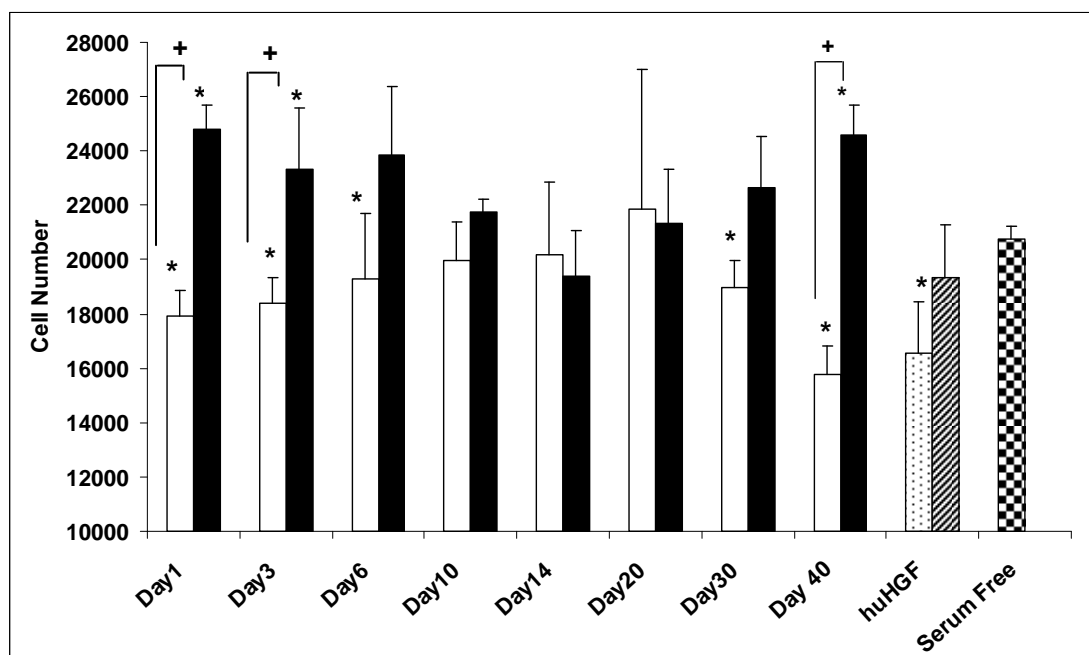


**Figure 5-6.** Hep3B cell proliferations measured by total-DNA assay after incubating the cells in the released HGF (□) and BSA (■) for 24 hrs. SF medium (☒) was used as the positive control, while SF medium containing 5 ng/mL (▨) and 50 ng/mL (▩) HGF were used as negative controls. Values represent means±SD, n=3. Statistical significance (\*  $p < 0.05$ ) was determined by one-way ANOVA with Tukey's HSD post hoc analysis as compared to the positive control, while (<sup>+</sup>  $p < 0.05$ ) was determined by t-test comparison between the two samples.

As was shown in Figure 5-6, the growth inhibition effects of released HGF were significant as compared to the positive controls when cultured in the media from days 1, 3 and 6 ( $P < 0.05$ ), and SF media supplemented with 50 ng/mL HGF showed similar inhibition effect. However, the media from days 10, 14 and 20 showed no inhibition effects which could be attributed to the significantly lower amount of HGF released. In order to verify this assumption, SF medium supplemented with 5 ng/mL HGF (being similar to that released at days 10, 14 and 20) was used to culture Hep3B cells, and no

significant inhibition effect was found. The inhibition effects were observed again when culturing the cells in the media from days 30 and 40, which corresponds to higher HGF released from the microspheres (cf. Figure 5-5). A study by Shiota and colleagues indicated that the inhibition effects of HGF on Hepatoma cells (HepG2 and Hep3B) were dose-dependent up to 50 ng/mL and lower concentrations of HGF did not inhibit the growth of hepatoma cells (Shiota et al., 1992). Our results were consistent with these findings and indicated that the bioactivity of HGF released from PHBV/PLGA microspheres was preserved for at least 40 days. One interesting result was that the BSA released from BSA-alone encapsulated PHBV/PLGA microspheres showed positive effects on the proliferation of Hep3B cells as indicated by the black bars in Figure 5-6. Since the cells were cultured in SF medium, BSA was believed to serve as the nutrient for cell growth (Drumm et al., 2003). While the positive effects may have counteracted the inhibition effects of HGF for Hep3B cells (white bars in Figure 5-6) and which will be addressed, BSA will definitely function as a useful supplement when the scaffold is used to culture primary hepatocytes.

#### **5.2.5.2 Albumin secretion and P-450 activity**

The bioactivity of HGF was also assessed through measuring the human albumin secretion by Hep3B cells, which is one of the important hepatic functions (Figure 5-7). It is worth to note that, when the cells were cultured in HGF-containing media, the human albumin secretion per cell was lower than the cells cultured in the positive control, and the inhibition effects were dose-dependent which was consistent with what have been observed in Figure 5-6. The EROD assay showed a similar inhibition effect on the cytochrome P-450 activity of Hep3B cells by the released HGF (Figure 5-

8). These results indicated that the HGF not only inhibited Hep3B cellular DNA synthesis for proliferation but also suppressed the differentiated function. The cells in this state are most likely related to the G0 phase of a cell cycle. The normal hepatocytes existing in the liver are mostly believed to be in the G0 or so called quiescent phase and they could rapidly respond to *in vivo* signals and re-enter the G1 phase when the liver is damaged (Hansen and Albrecht, 1999). However, this kind of cell cycle is not regulated in cancer, and the cells keep dividing without staying in the quiescent state and will eventually develop into a tumor. Therefore, the release of HGF from the microsphere scaffold can also be used to suppress cancer cell growth.

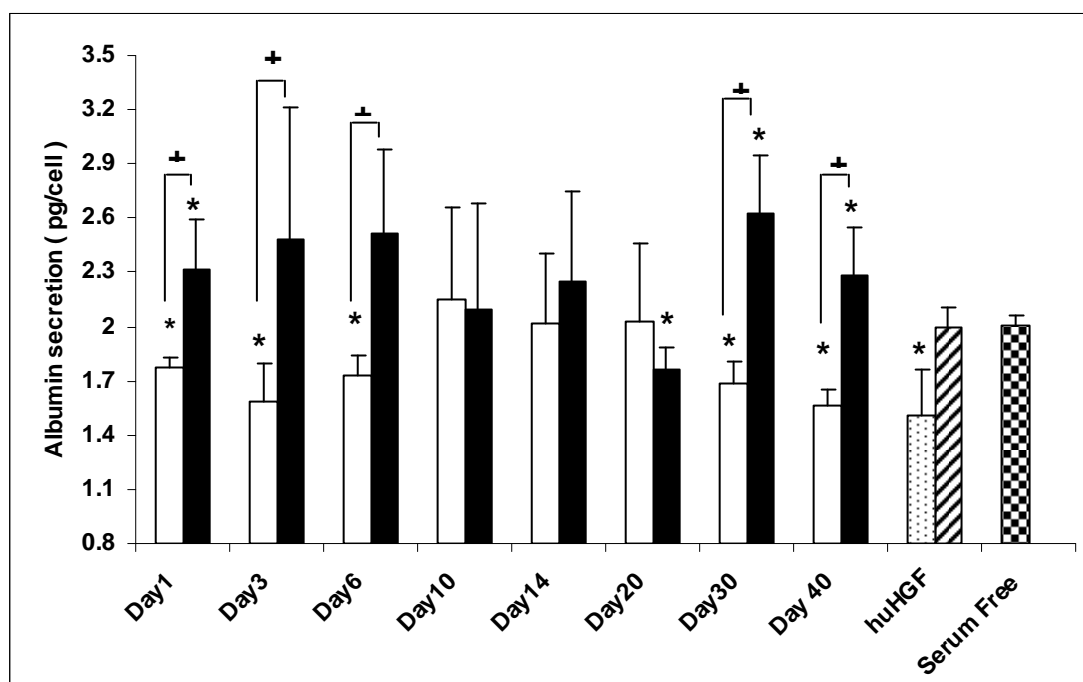


**Figure 5-7.** Albumin secretions by Hep3B cells after incubating the cells in the released HGF (□) and BSA (■) for 24 hrs. SF medium (☒) was used as the positive control, while SF medium containing 5 ng/mL (▨) and 50 ng/mL (▩) HGF were used as negative controls. Values represent means±SD, n=3. Statistical significance (\*  $p < 0.05$ ) was determined by one-way ANOVA with Tukey's HSD post hoc analysis as compared to the positive control, while (<sup>†</sup> $p < 0.05$ ) was determined by t-test comparison between the two samples.

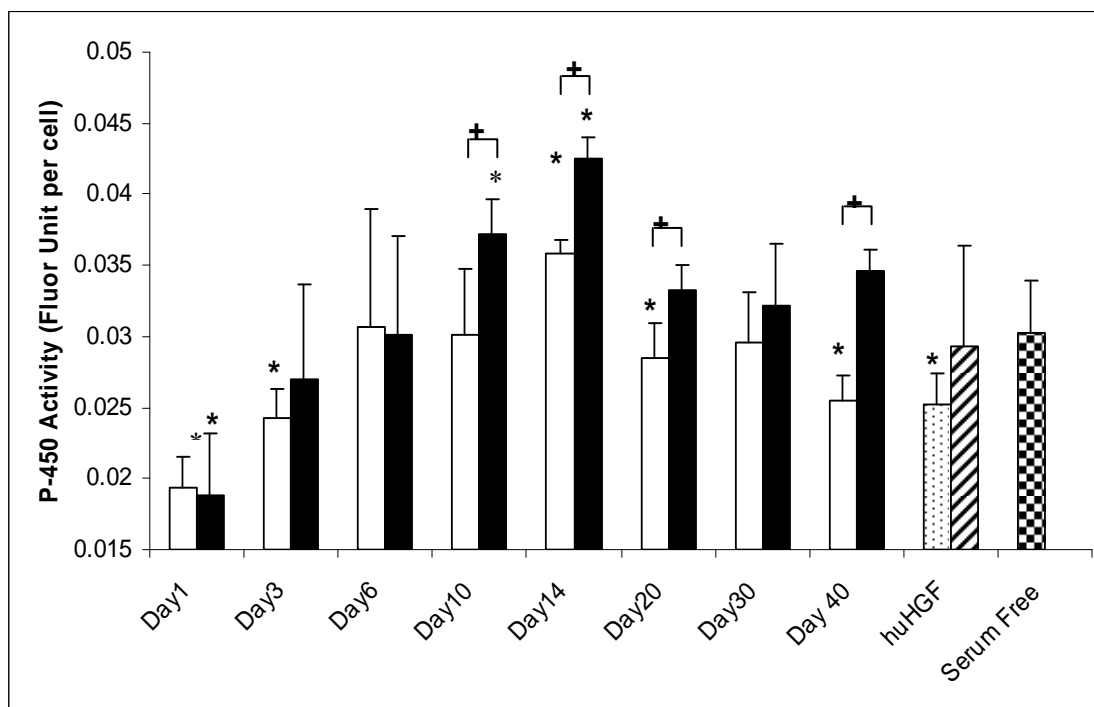


**Figure 5-8.** P-450 activity of Hep3B cells after incubating the cells in the released HGF (□) and BSA (■) for 24 hrs. SF medium (▣) was used as the positive control, while SF medium containing 5 ng/mL (▨) and 50 ng/mL (▤) HGF were used as negative controls. Values represent means±SD, n=3. Statistical significance (\*  $p < 0.05$ ) was determined by one-way ANOVA with Tukey's HSD post hoc analysis as compared to the positive control, while (<sup>+</sup> $p < 0.05$ ) was determined by t-test comparison between the two samples.

### 5.2.6 Culturing primary hepatocytes on PHBV/PLGA microsphere scaffold

Primary hepatocytes were cultured on PHBV/PLGA microspheres for up to 10 days to study the effects of the scaffold as well as the delivery of HGF on the growth of the cells.

### 5.2.6.1 Total-DNA quantification

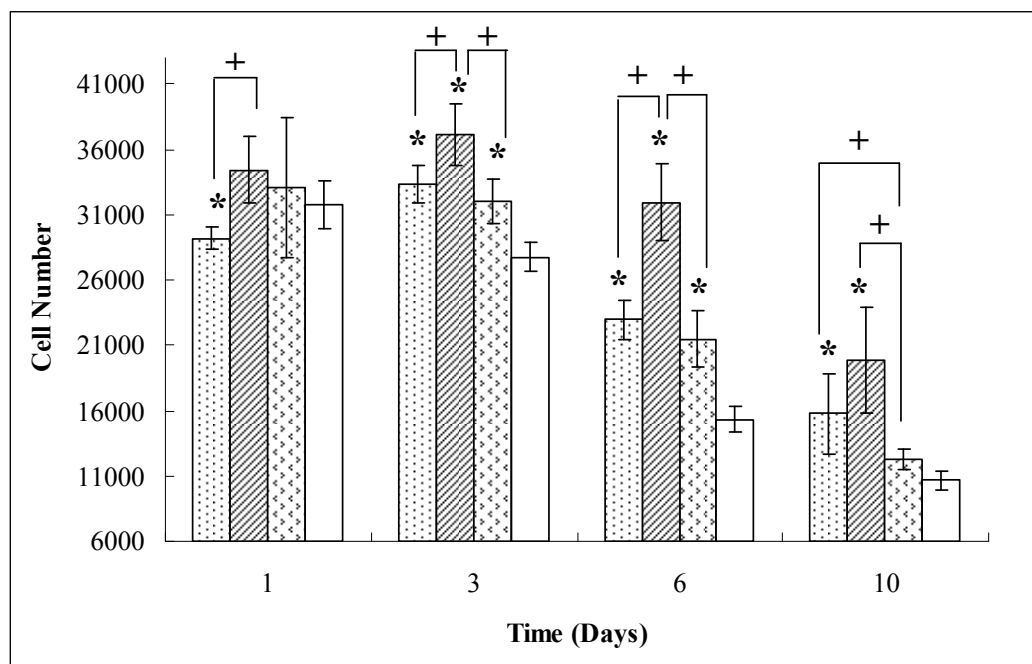


**Figure 5-9.** Proliferation of primary hepatocytes cultured on PHBV/PLGA microspheres and controls as assessed by total-DNA assay. Cells were cultured on microspheres loaded with HGF (▨), blank microsphere (▤), while cell culture medium supplemented with 50 ng/mL of HGF (▩) or without HGF (□) were used as controls. Values represent means  $\pm$  SD,  $n=3$ . Statistical significance (\*  $p<0.05$ ) was determined by one-way ANOVA with Tukey's HSD post hoc analysis as compared to the control, while (+  $p<0.05$ ) was determined by t-test comparison between the two samples.

As was shown in Figure 5-9, the number of cells grown on the microsphere scaffolds remained significantly higher than that of the controls during the period of culture (\* $p<0.05$ ). There was an increase in cell numbers from day 1 to day 3 followed by a slow decrease for the microsphere scaffold. However, the cell numbers decreased sharply from day 1 onwards when the cells were cultured on the controls. By the last day of culture, more than 50% of the original amount of cells remained on the microspheres while only 20-30% cells were found on the controls. It was reported that, when the primary hepatocytes were cultured *in vitro* without appropriate substrates and

stimulus such as growth factors or co-culturing with other types of cells, the viability of the cell number would decrease quickly and the cells tend to de-differentiate and lose their normal functions (Bhandari et al., 2001). Our results are consistent with these findings and indicated that the three-dimensional environment provided by the microspheres can better maintain the viability of the primary hepatocytes. It is of worth to note that the number of hepatocytes cultured on the microspheres loaded with HGF was higher than that of the blank microspheres ( $^+p<0.05$ ), which was also much higher than the control with the media supplemented with 50 ng/mL HGF. As HGF is believed to improve the growth of the primary hepatocytes, we hypothesize that the localized and direct delivery to cells via the microspheres can protect the growth factors from proteolysis as well eliminating the dilution effect of solution delivery.

#### **5.2.6.2 Albumin secretion and P-450 activity of hepatocytes**

Two liver specific functions, cytochrome P-450 activity and albumin secretion were also measured quantitatively (Figure 5-10 and Figure 5-11). It can be seen that the differentiated functions were well preserved when the cells were grown on the microsphere scaffold as compared to the two-dimensional controls ( $*p<0.05$ ). However, in comparing the microsphere loaded with HGF to the blank microspheres, no significant differences in the hepatic functions were observed ( $^+p>0.1$ ), which was also consistent with what was found when the cells were cultured on the two-dimensional controls (tissue culture plates). It is thus hypothesized that the three-dimensional structure of the scaffold plays an important role in preserving the phenotype of primary hepatocytes than the growth factor, while the HGF would more likely improve the cell proliferation.

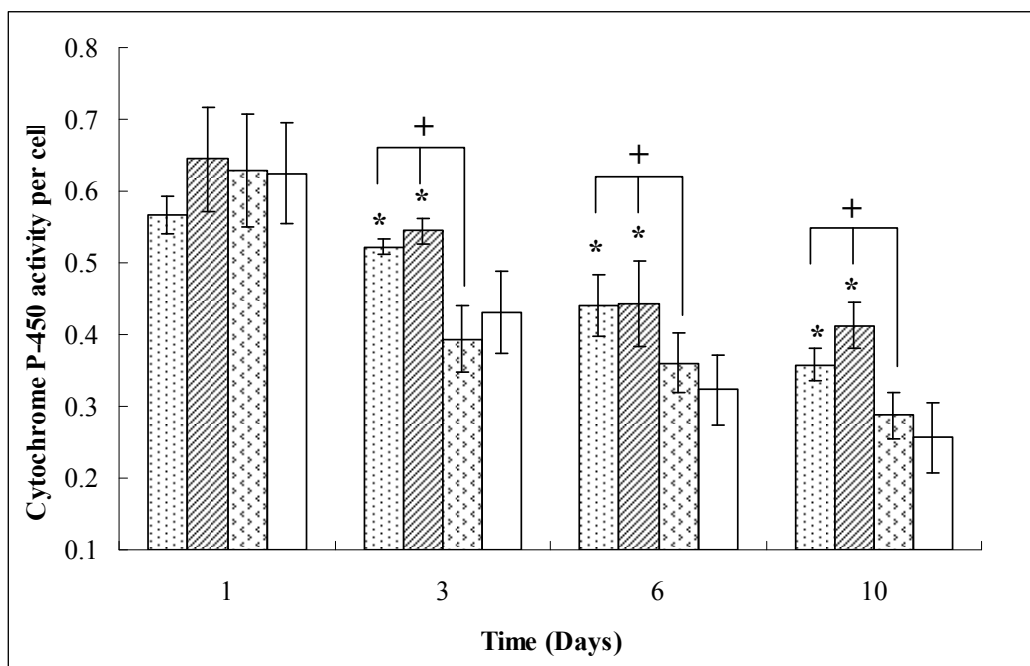


**Figure 5-10.** Cytochrome P-450 activity of primary hepatocytes cultured on PLGA/PHBV microspheres and controls as assessed by total-DNA assay. Cells were cultured on microspheres loaded with HGF (▨), blank microsphere (⋯), while cell culture medium supplemented with 50 ng/mL of HGF (⊠) or without HGF (□) were used as controls. Values represent means  $\pm$  SD,  $n=3$ . Statistical significance ( $*p<0.05$ ) was determined by one-way ANOVA with Tukey's HSD post hoc analysis as compared to the control, while (+  $p<0.05$ ) was determined by t-test comparison between the two samples.

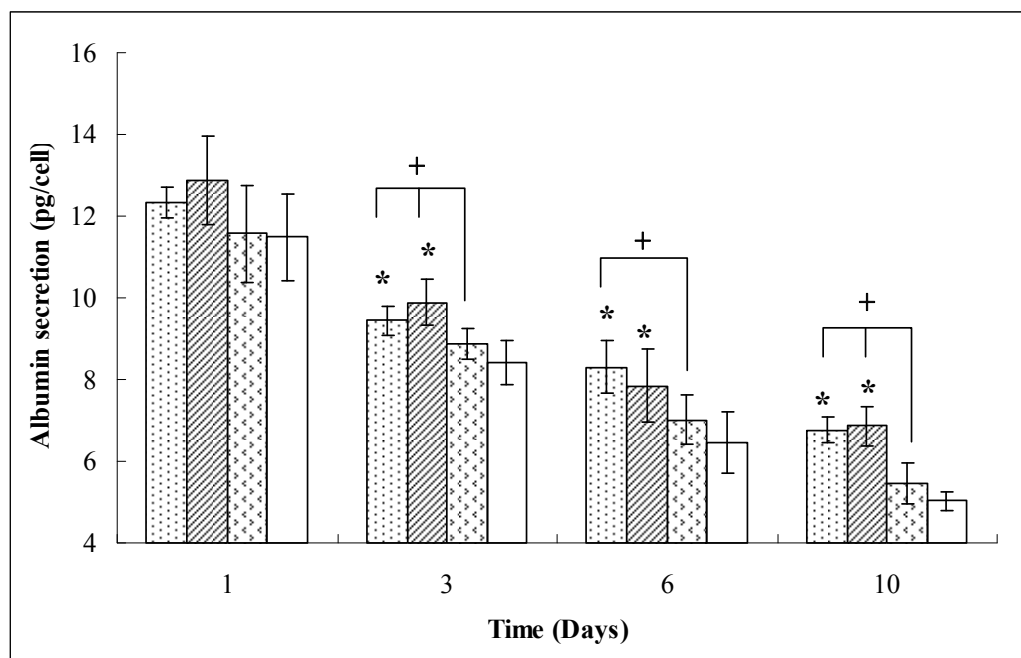


**Figure 5-11.** Albumin secretion by primary hepatocytes cultured on PLGA/PHBV microspheres and controls as assessed by total-DNA assay. Cells were cultured on microspheres loaded with HGF (▨), blank microspheres (▤), while cell culture medium supplemented with 50 ng/mL of HGF (▥) or without HGF (□) were used as controls. Values represent means  $\pm$  SD,  $n=3$ . Statistical significance (\*  $p<0.05$ ) was determined by one-way ANOVA with Tukey's HSD post hoc analysis as compared to the control, while (+ $p<0.05$ ) was determined by t-test comparison between the two samples.

### 5.3 Conclusions

In this chapter, three types of polymer microspheres with distinct release profiles of protein were fabricated for potential application in liver tissue regeneration. Bovine serum albumin was proven to be a suitable model protein for hepatocyte growth factor (HGF) and functioned as a stabilizer to prevent the denaturation of HGF during the fabrication process. The composite microsphere (PHBV/PLGA), which was developed



with a core-shell structure, was shown to possess a moderate degradation rate, well preserved structure and better controlled delivery for HGF during the three months of incubation. The inhibition of Hep3B cells growth indicated that the HGF released from PHBV/PLGA microspheres maintained its bioactivity for at least for 40 days. Furthermore, the three-dimensional microsphere scaffold with the direct delivery of HGF to the cells grown on it was shown to be able to better maintain the viability and phenotype of the primary hepatocytes. This successful controlled release of HGF adds to previous works on using microspheres as scaffolds would push the progress towards a complete engineered liver tissue system.

## Chapter 6 Gelatin Microspheres-based *In Vitro* Vascularization

Microsphere scaffold with bio-mimetic surface and ability to deliver growth factors to the cells in a controlled and localized manner shows great promise for the success of liver tissue regeneration. One of the challenges in successfully applying this scaffolding system is to efficiently provide nutrients and oxygen to the hepatocytes growing in the deeper sections of the scaffold to maintain their viability. Although diffusion is sufficient for thin tissue equivalents, it has not been sufficient to provide nutrients and oxygen to thick and complex tissue equivalents such as the liver (Frerich et al., 2001; Griffith et al., 2005; Levenberg et al., 2005). The lack of sufficient blood supply is believed to be the primary reason for the cell death that occurs in hepatocyte transplantation. Therefore, a vascularized scaffolding system which can provide nutrient and oxygen to maintain the viability of liver cells is a prerequisite for the success of engineering liver tissues.

Although there are many factors affecting the formation of blood vessels *in vitro*, culturing endothelial cells on appropriate three-dimensional scaffolds is believed to be

the basis and premise for the success of vascularization (Nehls and Herrmann, 1996). In a study done by Griffith and his co-workers, human umbilical vein endothelial cells coated microcarrier beads were embedded in fibrin gels and the gel thickness varied to study the formation of capillary network *in vitro* (Griffith et al., 2005). Growth factors such as vascular endothelial cell growth factor (VEGF) and basic fibroblast growth factor (bFGF) and platelet-derived growth factors are also known to stimulate rapid formation of capillary vessels both *in vivo* and *in vitro* (Tabata and Ikada, 1998; Chen and Mooney, 2003; Riley et al., 2006). However, the effects of these factors by direct administration were found to be insignificant because of their poor stability resulting from proteolysis (Tabata and Ikada, 1998). Therefore, a localized delivery system which can maintain the concentration and bioactivity of growth factors for an extended period of time as well as provide the cells with the molecules directly is necessary for the success of vascularization.

In this chapter, the application of microsphere scaffold is extended to *in vitro* vascularization. The strategy is to culture endothelial cells on gelatin microspheres (GMs), followed by incorporation into a fibrin gel. Angiogenic factors (bFGF) were also incorporated into the gelatin microsphere scaffold to further stimulate the vascularization process. The objectives were to examine the effects of cross-linking extent of GMs on the growth of endothelial cells, to investigate the incorporation of bFGF into the microspheres and its release profile, and to study the effects of growth factor on the cell activity and the development of capillary network *in vitro*.

## **6.1 Materials and Methods**

### **6.1.1 Materials**

Acidic gelatin with isoelectric point (IEP) of 5.0 was obtained from Japan (courtesy of Professor Tabata, Kyoto University). Olive oil was purchased from Wako Pure Chemicals (Osaka, Japan). Recombinant basic fibroblast growth factor (bFGF) was purchased from RayBiotech (Norcross, GA, USA). bFGF detection ELISA kit was purchased from Biolegend (San Diego, CA, USA). Ham's F12 K medium, sodium bicarbonate, heparin, endothelial cell growth supplement (ECGS), fibrinogen and thrombin were purchased from Sigma-Aldrich (St. Louis, MO, USA). The information of the chemicals which were used in this chapter but not listed in this section can be found in section 3.1.1 in Chapter 3. All chemicals were used directly without further purification.

### **6.1.2 Fabrication of gelatin microspheres**

The GMs were fabricated according to an established method (Tabata et al., 1999). Briefly, 4 g of gelatin was dissolved in 20 mL of water and heated up to 60°C. 200 mL of olive oil was heated up to 40°C. Gelatin was then added drop-wise into the olive oil, while stirring at 420 rpm with a mechanical stirrer (RW20, Ika Labortechnik, Staufen, Germany). The water-in-oil (w/o) emulsion was stirred for 10 minutes before being immersed into an ice bath to maintain the temperature at 10°C and stirred for a further 30 minutes. 60 mL of chilled acetone was then added and the mixture was stirred for another 1 hour. The GMs were extracted from the olive oil by a series of centrifuging and washing with chilled acetone. Cross-linking was carried out by immersing the microspheres in 150 mL of three different concentrations of glutaraldehyde solution

(5mM, 10mM and 20 mM) and stirred at 420 rpm for 12 hours at 4°C. Cross-linked microspheres were washed with deionized water and then suspended in glycine solution (50 mM) to block the un-reacted aldehyde groups for 2 hours in room temperature. The microspheres were then washed with acetone and dried with a freeze-dryer (Alpha 1-4, Martin Christ, GmbH, Germany) for 24 hours to remove any remaining solvent.

### 6.1.3 Characterization of the GMs

The sizes of gelatin microspheres were estimated using a light microscope (Leica DMIL, GmbH, Germany). Dried and wet (saturated with deionized water for 3 hours) microspheres were observed under the microscope. The images were captured by a digital camera (QICAM Fast 1394, QIMAGING, Canada) and analyzed using built-in software to measure the diameter of individual microsphere. The swelling ratios were then calculated using the following formula,

$$\text{Swelling Ratio} = \frac{\text{Volume of wet microsphere}}{\text{Volume of dry microsphere}}$$

The external morphologies of GMs were characterized by a scanning electron microscope (SEM) (JSM-5600VL, JEOL, Tokyo, Japan). The microspheres were mounted onto brass stubs using double-sided adhesive tape and vacuum-coated with platinum using the Auto Fine Coater (JFC-1300, JEOL, Tokyo, Japan) for 40 s.

The chemical structures (functional groups) of cross-linked GMs were examined with a Fourier transform infrared (FTIR) spectrometer (Excalibur Series, BioRad Laboratories, FTS, 135, USA). Briefly, 4 mg of the 10 mM microspheres was mixed with 96 mg of potassium bromide. The mixture was then grounded with a mortar and

pestle after which it was compressed into pellets under a pressure of 10,000 kg/inch<sup>2</sup> for 10 min prior for IR examination. The IR frequency range of interest is 4000 cm<sup>-1</sup> to 400 cm<sup>-1</sup>.

#### **6.1.4 bFGF incorporation and *in vitro* release from GMs**

The bFGF was incorporated into GMs according to previously established method (Tabata and Ikada, 1998). Briefly, 5 µL of the bFGF solution (60 ng/µL, pH 7.4 ) was added to per mg of freeze-dried GMs cross-linked with GTA, followed by standing at 4°C overnight. The microspheres absorbed all of the bFGF solution during the swelling process since the volume was much less than the theoretical swelling saturation volume (Tabata and Ikada, 1998; Holland et al., 2005). Therefore, the incorporation efficiency of bFGF into GMs was considered as 100%.

To determine the release profile, the bFGF-loaded microspheres were suspended in 2 mL of PBS and incubated at 37°C. At set time points, the supernatant was collected and replaced with fresh PBS. The concentrations of bFGF in the supernatant were analyzed using an ELISA kit (Biolegend).

#### **6.1.5 Cell and cell culture**

Human umbilical vein endothelial cells (ATCC) were cultured in a serum-medium which was composed of Ham's F12K medium supplemented with 10% v/v FBS, 1.5 g/L sodium bicarbonate, 0.1 mg/mL heparin and 0.05 mg/mL ECGS. The cells were maintained in T-75 flasks in an incubator at 37°C in the presence of 5% CO<sub>2</sub> and 95% relative humidity. The medium was changed every three days.

### **6.1.5.1 Morphology of cell-microsphere constructs**

**Light microscope:** The morphologies of cells and cell-microspheres constructs were observed under optical microscope ((rf. 3.1.5 in Chapter 3).

**Scanning Electron Microscope (SEM):** Clear and more detailed images of cell-microsphere constructs were obtained by fixing the cells with 2.5 v/v% glutaraldehyde and observed under SEM (rf. 3.1.5 in Chapter 3).

**Confocal Laser Scanning Microscope (CLSM):** The nucleus and actins of the HUVEC were stained and observed under CLSM (rf. 3.1.5 in Chapter 3).

### **6.1.5.2 Cell metabolic activity by MTT assay**

The proliferations of the cells growth on GMs were quantified by using MTT assay. The detailed description of the assay can be found at 3.1.6 in Chapter 3.

### **6.1.6 Culturing HUVEC on GMs cross-linked with different concentrations of GTA.**

GMs cross-linked with 5 mM, 10 mM and 20 mM GTA respectively, were sterilized with 70% ethanol followed by complete washing with sterilized PBS. The microspheres were then transferred into a 24-well plate (2 mg per well). Cells were subsequently seeded at  $3 \times 10^4$  cells/well, or approximately  $1.5 \times 10^4$  cells/mg of microsphere. Every half an hour, the plate was shaken gently for 2 minutes to improve the adhesion of the cells onto the microspheres (Wissemann and Jacobson, 1985). A blank well coated with gelatin (0.5%) was used as the control. After three hours, the plates were put into the incubator.

### 6.1.7 Culturing HUVEC on GMs incorporated with bFGF

Six hundred ng of bFGF were incorporated into 2 mg of sterilized GMs (rf. 6.1.4). HUVEC were then seeded onto the microspheres as described above. Microspheres without incorporating growth factors and blank well coated with gelatin were used as controls. To compare the effects of free administration of the growth factors to the cells, cell culture medium supplemented with 60 ng/mL of bFGF was used a third control to culture the cells grown on gelatin-coated wells. GMs cross-linked with 10 mM GTA were used in this assay.

### 6.1.8 An *in vitro* model of vascularization

In each well of a 24-well plate,  $3 \times 10^4$  HUVEC cells were grown on 0.5 mg GMs confluence. The cells coated GMs were then suspended in 200  $\mu$ L of fibrinogen solution (2 mg/mL in PBS, pH=7.6, filter-sterilized). 10  $\mu$ L of thrombin solution (25 U/mL, in PBS, pH=7.6, filter-sterilized) was added in before the plate was incubated for 30 min at 37 °C. After the fibrin gel was formed, 0.8 mL of cell culture medium was added to each well. The migration of cells into the fibrin matrix was observed under optical microscope.

### 6.1.9 Statistical Analysis

All data were presented as mean  $\pm$  standard deviation and were analyzed by a one-way ANOVA followed by Tukey's HSD post hoc analysis, where the "\*" ( $p < 0.05$ ) indicate significant differences of the samples to the control (Tissue culture plate coated with gelatin). Student's t-test were also carried out for statistical comparisons between pairs of samples, where the "†" indicate significant difference ( $p < 0.05$ ).



## 6.2 Results and Discussion

One of the major obstacles in engineering thick tissues such as the liver is the lack of sufficient supply of nutrients and oxygen to the cells. The potential solution is to encourage the development of a vascular network within the three-dimensional tissue engineering matrices before it can be used for implantation. In this work, gelatin microspheres were used to guide human umbilical vein endothelial cells adhesion and proliferation as a potential system for vascularization. The choice of gelatin as the scaffold material is justified by the fact that gelatin is one of the most commonly used natural polymer for biomedical applications (Goodstone et al., 2004; Layman et al., 2007). More important, gelatin is a denatured form of collagen with all of its cell-adhesive properties and also with different isoelectric points obtained by acid or alkaline processing. Therefore, the positively or negatively charged gelatin can interact with growth factor molecules with opposite charges to form ionic complexation for a sustained release system (Tabata and Ikada, 1998; Tabata et al., 1999; Holland et al., 2005).

### 6.2.1 Fabrication and characterization of the GMs

GMs were fabricated using a water-in-oil process, and further cross-linked with glutaraldehyde of different concentrations, namely 5 mM, 10 mM and 20 mM respectively. Cross-linking was achieved by the reactions between aldehyde groups of GTA and the  $\epsilon$ -amino groups of the lysine residues in gelatin to form aldimine linkages which induced a color change.

As shown in Figure 6-1, all of the GMs have spherical shapes with uniform sizes, and the surfaces were very smooth (see the Insert in Figure 6-1C). It can be seen from

the light micrographs [Figure 6-1(E) and 6-1 (F)] that the translucent microspheres tend to swell when immersed in water and turn transparent. Although the overall morphologies and sizes of the dried GMs were not significantly affected by the concentrations of the cross-linker, the microspheres cross-linked with higher concentrations of GTA showed smaller swelling ratios, which indicated a relatively more rigid structure. The degradation of GMs can also be tuned by changing the cross-linking extent (data not shown) to fit the regeneration profiles required for the particular tissue.

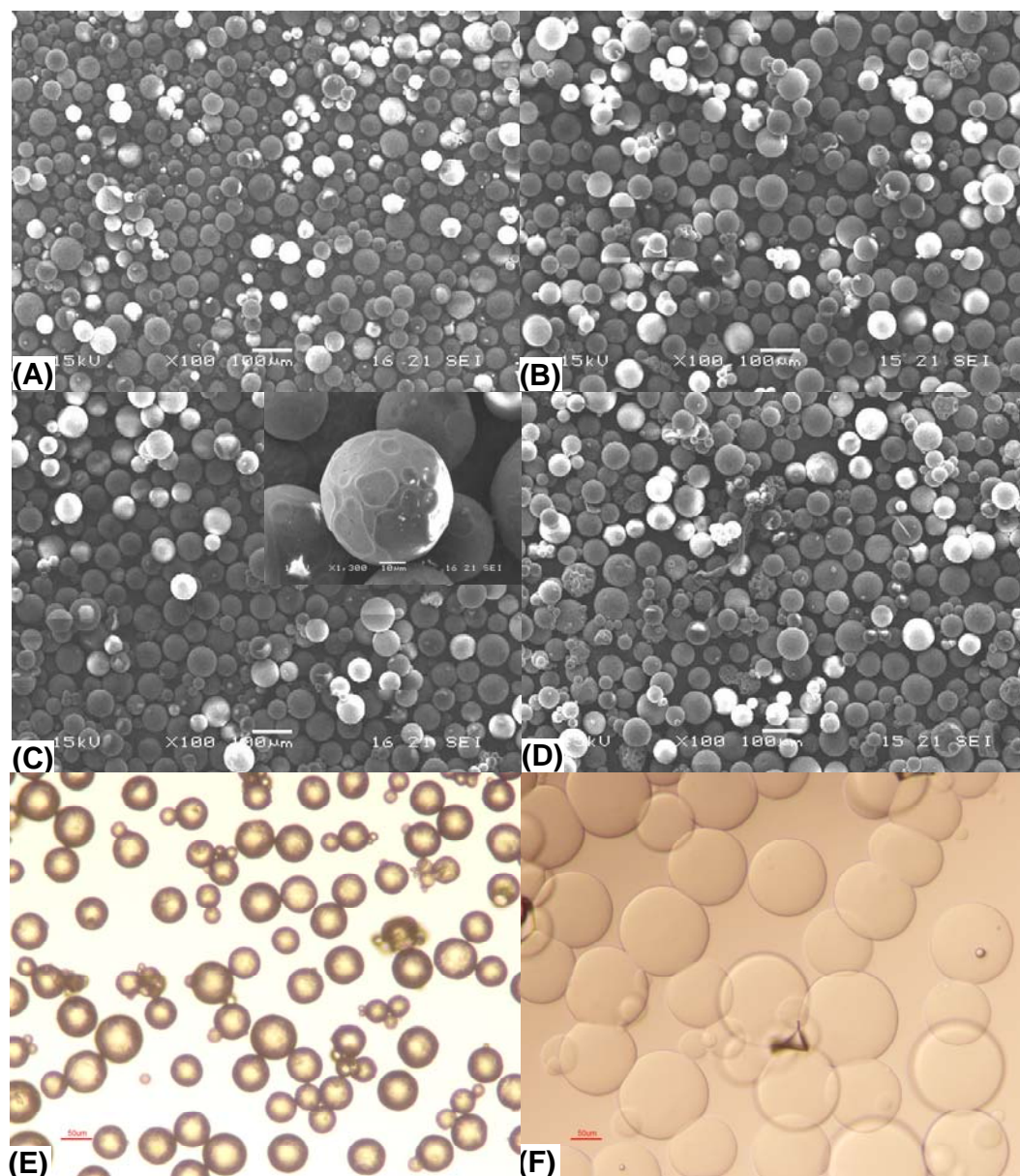


**Figure 6-1.** SEM images of GMs. (A) Non-cross-linked, and cross-linked with GTA at the concentrations of (B) 5 mM, (C) 10 mM and (D) 20 mM. Light micrographs of (E) Dry and (F) Wet gelatin microspheres cross-linked with 10 mM GTA.

The mean diameters of dry microspheres were 60.2, 59.2, 60.6, and 61.3  $\mu\text{m}$  respectively with small standard deviations (SD), and the wet diameters were 108.5, 100.1, 98.2 and 96.7  $\mu\text{m}$  (Table 6-1). Swelling ratios based on volume indicate that with higher cross-linking extent, the GMs tend to absorb less water, and therefore had

a smaller swelling ratio. The colors of the microspheres also changed from pale to deep orange with increasing cross-linking.

**Table 6-1.** Size and swelling ratio of gelatin microspheres

<b>Gelatin Microsphere</b>	<b>Dry Diameter ±S.D. (µm)</b>	<b>Wet Diameter ±S.D. (µm)</b>	<b>Swelling Ratio (volume)</b>
<b>Non-crosslink</b>	60.2 ± 6.3	108.5 ± 8.3	5.85
<b>5 mM</b>	59.5 ± 5.6	100.1 ± 5.2	4.76
<b>10 mM</b>	60.6 ± 5.1	98.2 ± 6.5	4.26
<b>20 mM</b>	61.3 ± 8.3	96.7 ± 3.6	3.93

The FTIR spectrum (Figure 6-2) showed two common absorption bands for proteins, the C=O stretching at  $1650\text{ cm}^{-1}$  and the NH stretching at  $3300\text{ cm}^{-1}$ . The characteristic absorptions of the backbone of gelatin molecules occurring at  $1540\text{ cm}^{-1}$  and  $1650\text{ cm}^{-1}$  were also observed. Pale GMs changed color to deep orange due to the establishment of aldimine linkages (CH=N), between the free amino groups of protein and glutaraldehyde. The aldimine absorption peak at  $1450\text{ cm}^{-1}$  which represents cross-linked gelatin was present but weak compared with other's work. This could be due to the significantly lower concentrations of glutaraldehyde used in this work.

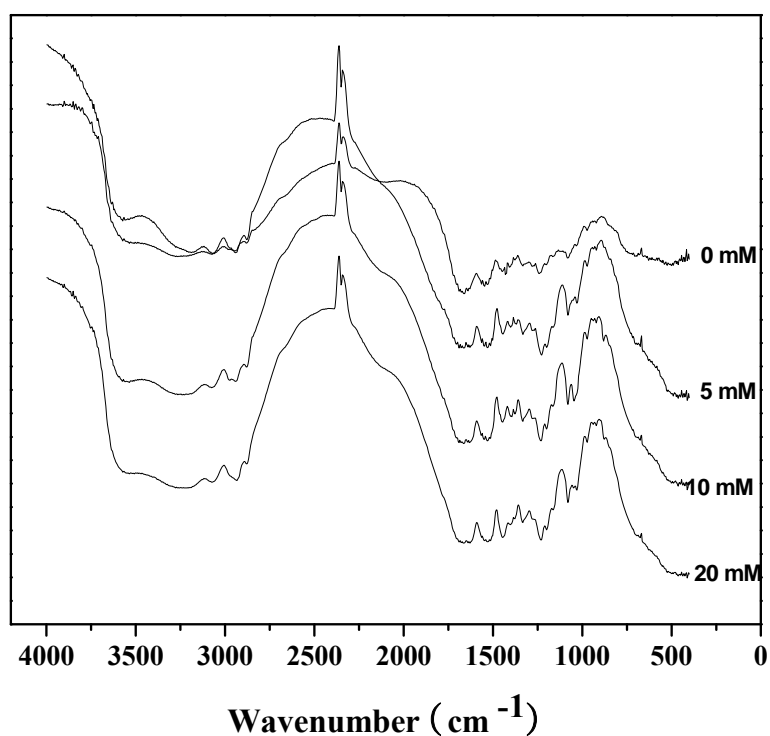


**Figure 6-2.** FTIR spectrum of gelatin microspheres cross-linked with glutaraldehyde.

## 6.2.2 Culturing HUVEC on GMs cross-linked with different concentrations of GTA

### 6.2.2.1 Light microscope images

Light micrographs of HUVEC cultured on GMs cross-linked with 10 mM GTA are shown in Figure 6-3. It can be seen that the cells with round shapes were mainly attached to the microspheres with less spreading on the initial adhesion stage [Figure 6-3 (A)], which indicated very good biocompatibility of the GMs for the HUVEC cells. After one day, the cells spread over the surface of single microspheres and began to bridge adjacent microspheres together [Figure 6-3 (B)]. By one week of culture, cells

were seen to become confluent on the scaffolds and stretched to fill the gaps between the microspheres to form large cell-microsphere clusters [Figure 6-3 (C)]. Compared to two-dimensional cultures on the blank wells, the cells showed more elongated shapes and strong interactions with adjacent cells and substrates. The interactions would not only improve the proliferation of the cells but could also stimulate the differentiation of the cells to develop into blood vessels. The cell-microspheres clusters formed after one week of culture could be ideal since during early angiogenesis *in vivo*, angiogenic cells form cluster processes which then coalesce to form blood vessels (Buschmann and Schaper, 2000). After the degradation of the GMs, the remaining blank spaces will enable the cells to develop into vascular networks.

In order to get clearer view on how the cell grew on the scaffold, individual microsphere was isolated after the initial adhesion stage, and the results are shown in the right column of Figure 6-3 [(D), (E) and (F)]. The cells grown on GMs cross-linked with 5 and 20 mM GTA showed a similar profile (Data not show).

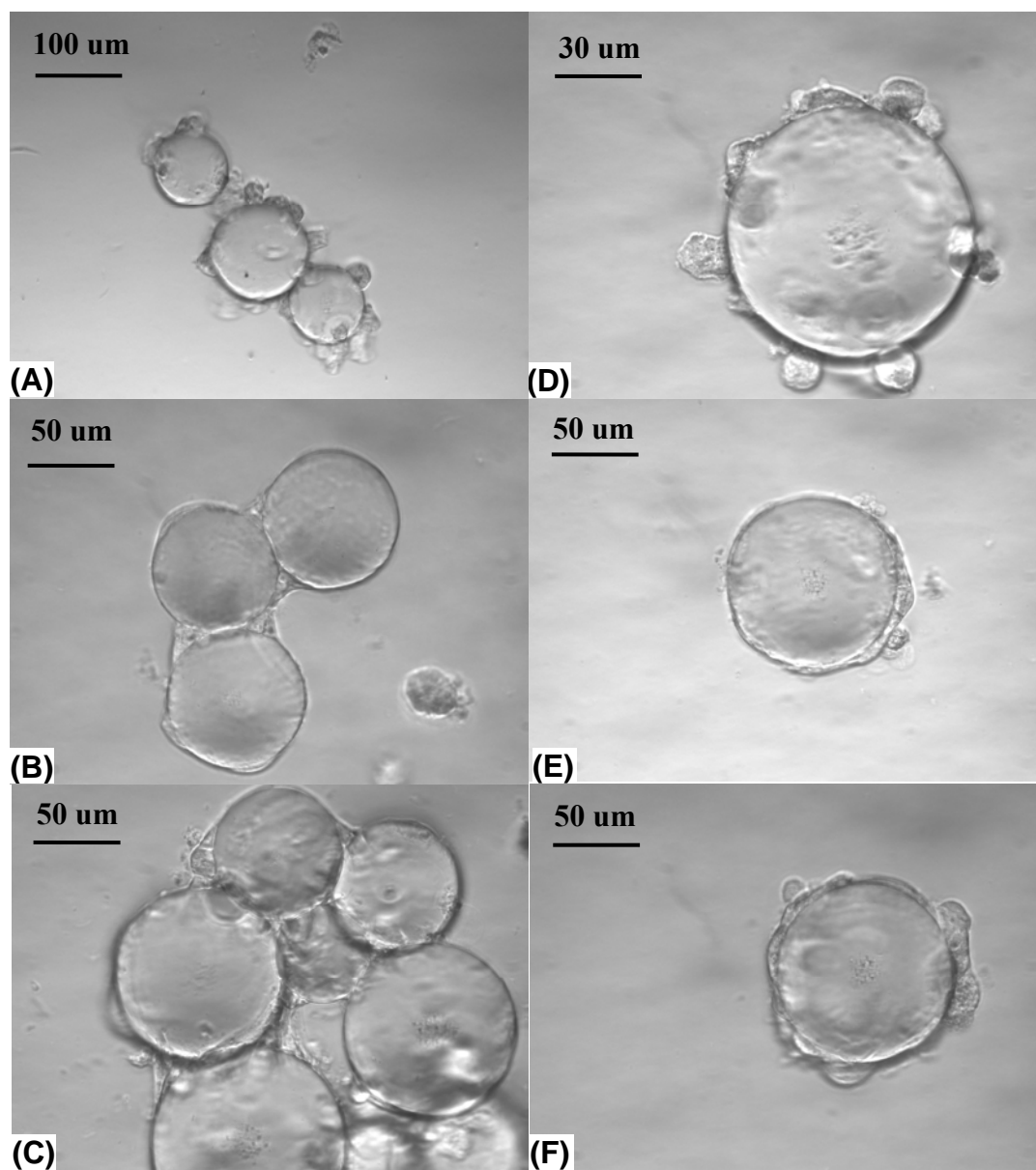


**Figure 6-3.** Optical micrographs of the morphologies of HUVEC cells grown on GMs after (A, D) Three hours (initial adhesion), (B, E) 1 days, and (C, F) 7 days of culture. The right column indicated the cells grown on individual microspheres, while the left column indicated the cell-microsphere clusters. The microspheres were cross-linked with 10 mM GTA.

### **6.2.2.2 SEM and CLSM images**

Clearer and more detailed images of cell-scaffold morphologies can be obtained by using SEM and CLSM. Images in Figure 6-4 were taken after one week of culture. The SEM images showed that the surface of microspheres was covered by cells which deposited an abundant amount of extracellular matrix proteins, and there existed strong cell-cell interaction and cell-substratum interaction between cells and the microspheres. In the confocal images, the cell nucleus were dye with DAPI (blue color), and the actins were dye with phalloidin-FITC (green color). It can be seen that the cells evenly spread and covered the surfaces of the microspheres. The extensively elongated cells with stretched actins bridged the adjacent microspheres together and indicated very strong cell-microsphere interactions.



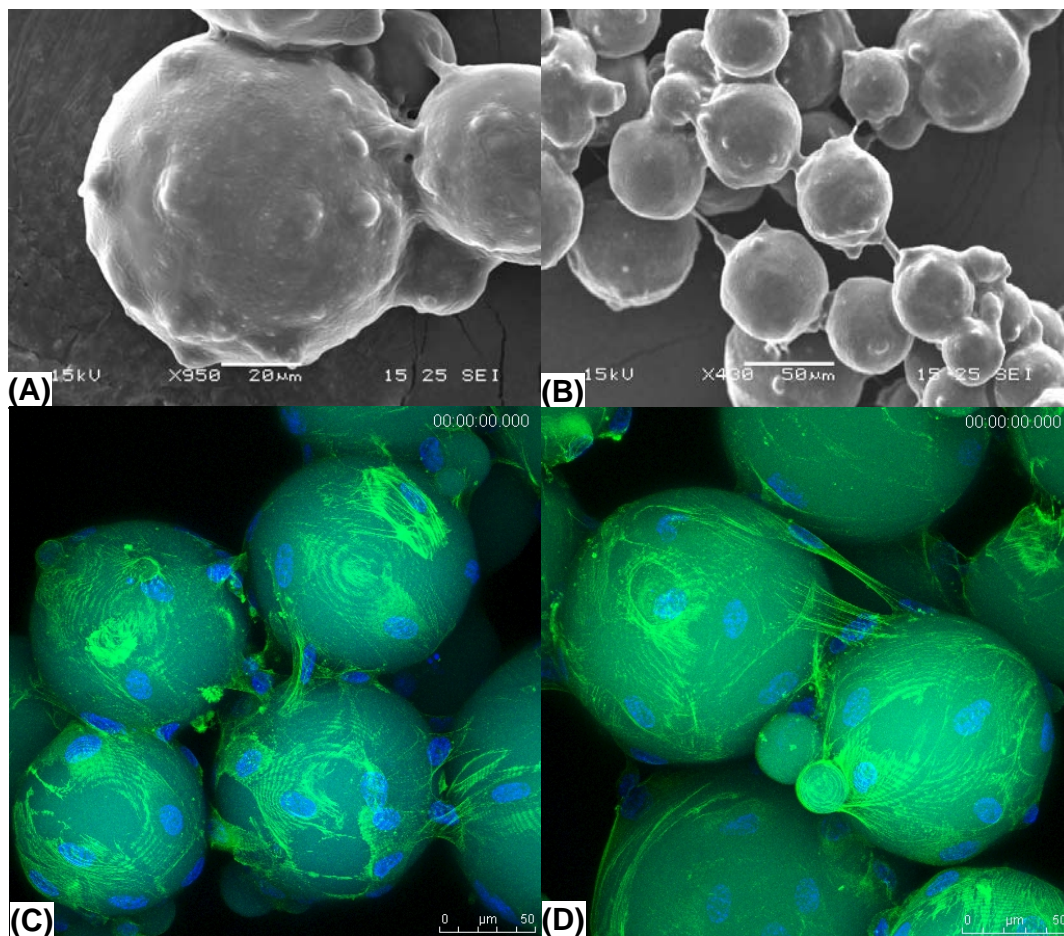


**Figure 6-4.** SEM (A, B) and CLSM (C, D) images of HUVEC grown on GMs after one week. Cell actin was dyed with Phalloidin-FITC, and the nucleus was dyed with DAPI. The microspheres were cross-linked with 10 mM GTA.

### 6.2.2.3 Cell proliferation measured by MTT assay

The proliferation rates of HUVEC cultured on the GMs as well as on the control were quantitatively evaluated by MTT assay during the 10 days of culture as shown in Figure 6-5. It can be seen that the cell proliferation rates on the three types of microspheres were much higher than that of the control ( $*p < 0.05$ ). From day 3 to day 6, there was a sharp increase in cell proliferation and confluence was reached by day

10. The cells grown on GMs with higher cross-linker concentration also showed higher proliferation rate than that of the microspheres cross-linked with lower concentration of GTA ( $\dagger p < 0.05$ ).

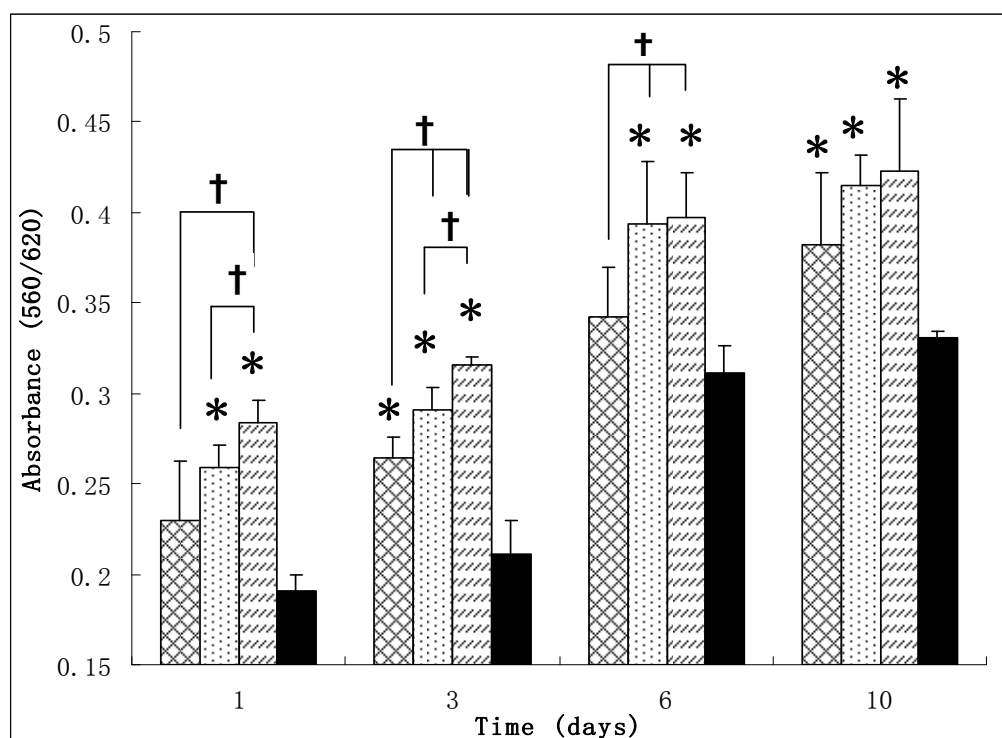


**Figure 6-5.** Proliferation of HUVEC cells cultured on gelatin microspheres cross-linked with different concentrations of GTA as assessed by MTT assay. 5 mM ( $\boxtimes$ ), 10 mM ( $\boxdot$ ), 20 mM ( $\boxminus$ ). Blank well was used as the control ( $\blacksquare$ ). Values represent means  $\pm$  SD,  $n=3$ . Statistical significance ( $*p < 0.05$ ) was determined by one-way ANOVA with Tukey's HSD post hoc analysis as compared to the control, while ( $\dagger p < 0.05$ ) was determined by t-test comparison between the two samples.

It was believed that the rigidity of the substrate has an affect on the gene expression of cytoskeletal proteins and therefore can regulate the morphology and proliferation of the cells (Mooney et al., 1992). Our results were consistent with this finding as higher proliferation rates were observed with cells grown on GMs with

higher cross-linking extent and therefore high rigidity (Figure 6-5). Figure 6-5 also dictated higher cell proliferation on GMs as compared to blank wells of a tissue culture plate. One reason for this is that as compared to two-dimensional tissue culture plates, microspheres have a larger surface area providing for larger number of cells to grow. More importantly, it is believed that the shape of the scaffold affects cell adhesion, proliferation and function greatly (Malda et al., 2003; Barrias et al., 2005). As shown in Figure 6-3 and Figure 6-4, microspheres scaffold improved cell-cell interaction and cell-substrate interactions which may stimulate cell proliferation. The cells would also be more active in aggregate forms.

### 6.2.3 bFGF incorporation and *in vitro* release from GMs

As hydrogel beads, the GMs used in this work have high swelling ratios (Table 6-1). 5  $\mu$ L of bFGF aqueous solution is much less than the theoretical volume for 1 mg GMs to absorb. The incorporation efficiencies therefore can be assumed to be 100%. Shown in Figure 6-6 are the *in vitro* release profiles of bFGF from GMs cross-linked with 5 mM, 10 mM and 20 mM GTA respectively. Irrespective of the microsphere type, there was an initial burst release of bFGF (24 hour) at a certain amount followed by small amount of protein release for up to two weeks. However, for the microspheres cross-linked with different concentrations of GTA, namely, 5 mM, 10 mM and 20 mM GTA, the initial bursts were also significantly different at 23.9%, 13.3% and 8.2% respectively. Up to two weeks of incubation, the accumulated releases were 41.4%, 26.1% and 12.9% respectively, and a plateau was observed thereafter.

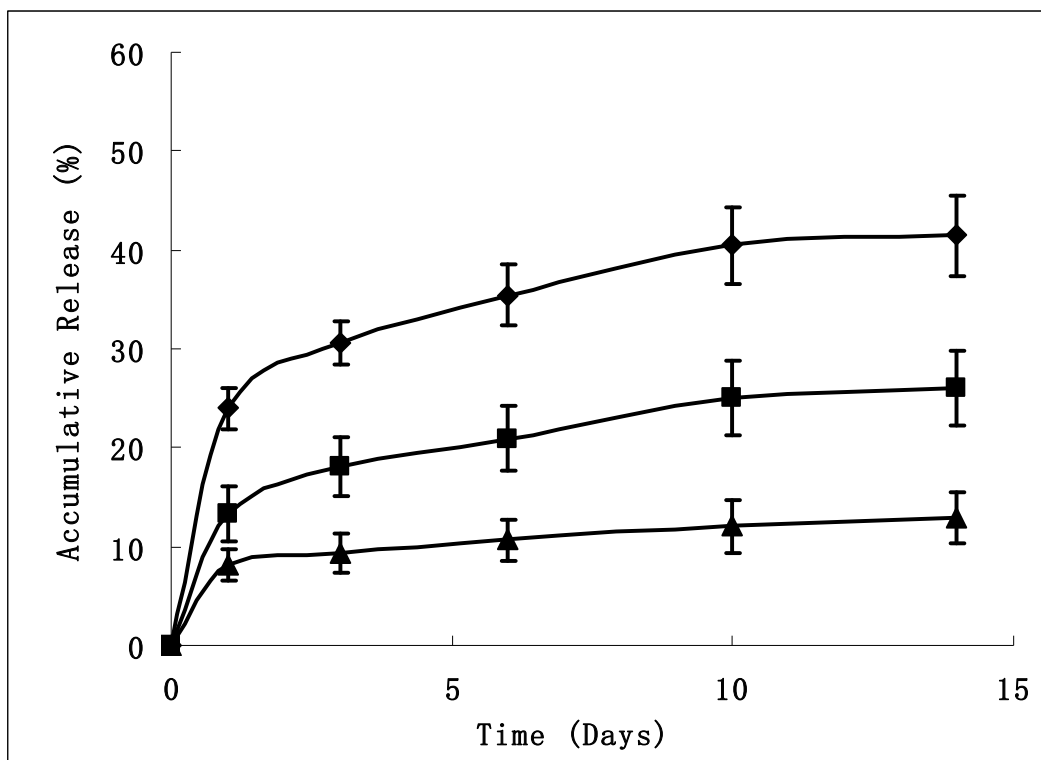


**Figure 6-6.** Cumulative release of bFGF from gelatin microspheres cross-linked with different concentrations of GTA. 5 mM (◆), 10 mM (■), 20 mM (▲). Values represent means $\pm$ SD, n=3.

The results indicated that highly cross-linked microspheres released less cumulative bFGF as well as having a lower initial burst compared to mildly cross-linked microspheres which could be attributed to the cross-link networks. The incorporation of growth factors into GMs are based on ionic complexation between positively charged bFGF (IEP of 9) and negatively charged acidic gelatin molecules (IEP of 5.0). Since cross-linking is achieved by the reaction between glutaraldehyde and the  $\epsilon$ -amino group of the lysine residue of the protein chains, this process could change the charges of the GMs and therefore change the complexation process.

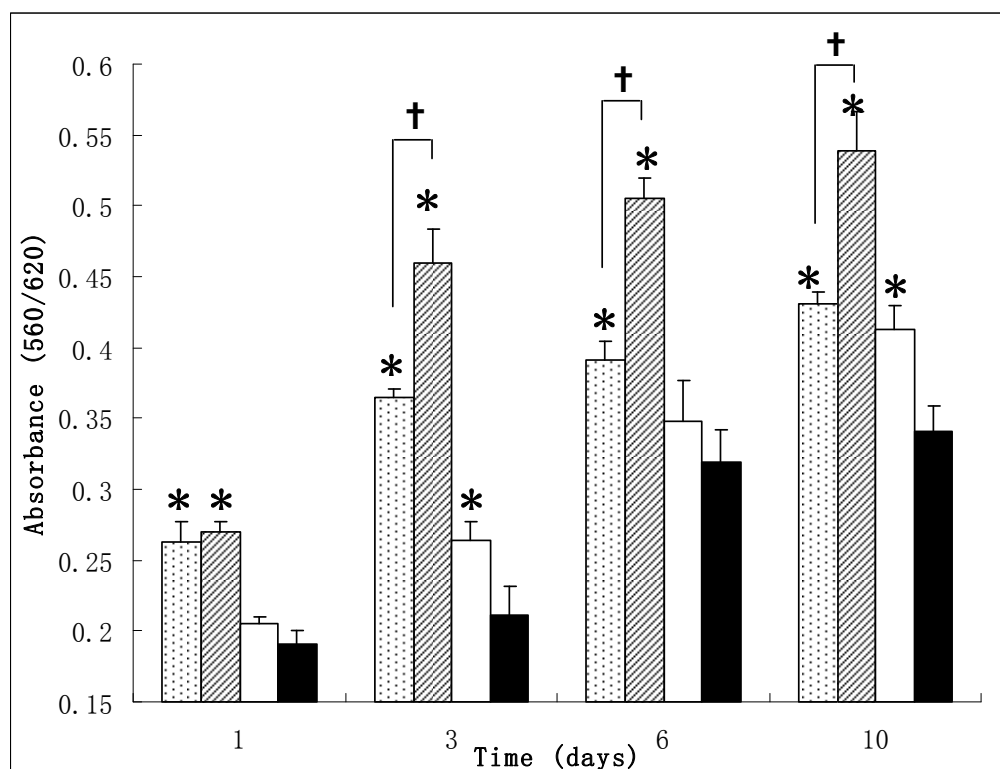


**Figure 6-7.** Proliferation of HUVEC cells cultured on gelatin microspheres and controls as assessed by MTT assay. Microspheres loaded with bFGF (▨), blank microsphere (▤). Cell culture medium supplement with 60 ng/mL of bFGF (□) or without bFGF (■) were used as controls. Values represent means±SD, n=3. Statistical significance (\*p<0.05) was determined by one-way ANOVA with Tukey's HSD post hoc analysis as compared to the control, while (†p<0.05) was determined by t-test comparison between the two samples

#### 6.2.4 Culturing HUVEC on GMs incorporated with bFGF

The bioactivity of bFGF released from GMs cross-linked with 10 mM GTA was assessed by culturing HUVEC on the microspheres and controls. Bioactive bFGF is known to stimulate *in vivo* angiogenesis and to improve the proliferation of various types of cells, such as endothelial cells and fibroblasts. As shown in Figure 6-7, the proliferation rate of HUVEC culturing on GMs loaded with bFGF was improved significantly as compared to the control (blank well) by about two times (\*p<0.05)

during the 10 days of culture which indicated that the bioactivity of bFGF was well maintained during the incorporation and release process by GMs.

It is also of worth to note that the cells showed improved activity in cultures with bFGF released directly from the GMs as compared to the media supplemented with 60 ng/mL bFGF. This could be due to the poor stability of the free growth factors resulted from proteolysis. It is also hypothesized here that the localized and controlled delivery directly to cells grown on the GMs can protect the growth factors from proteolysis as well provide the cells with the molecules without the dilution effect in solution. By comparing microspheres loaded with bFGF to microspheres without bFGF, there was also significant improvement of the proliferation from day 3 onwards ( $\dagger p < 0.05$ ).

### **6.2.5 Gelatin microsphere-based *in vitro* vascularization model**

HUVECs coated GMs were embedded into a fibrin gel to stimulate the formation of capillary network *in vitro*. As was shown in Figure 6-8, after one day of culture, the cells which were grew on blank GMs just migrated into the gel, they did not form any capillary networks. On the contrary, capillary networks were developed when the cells grew on GMs incorporated with bFGF [Figure 6-8 (C)] and the bFGF was added as a supplement of the cell culture medium [Figure 6-8 (B)], which indicated that bFGF played an essential role in stimulating the remodeling of endothelial cells in the fibrin gel to develop into blood vessels. However, it was also found that the freely administered bFGF only gave strong angiogenic response initially, but failed in long-term stabilization. After five days of culture, the bFGF added as a supplement to the cell culture medium did not further stimulate the development of the capillary network in the fibrin gel [Figure 6-8 (E)], while the cells growing on GMs incorporated with

bFGF continued to remodel, developing an extensive capillary network among neighboring beads [Figure 6-8 (F)]. As discussed in previous section (6.2.4), the localized and controlled delivery of the growth factors directly to cells via the substrate might be more efficient in stimulating the *in vitro* vascularization since the bioactivity of the growth factor can be well maintained and provided to the cells without any dilution effect.

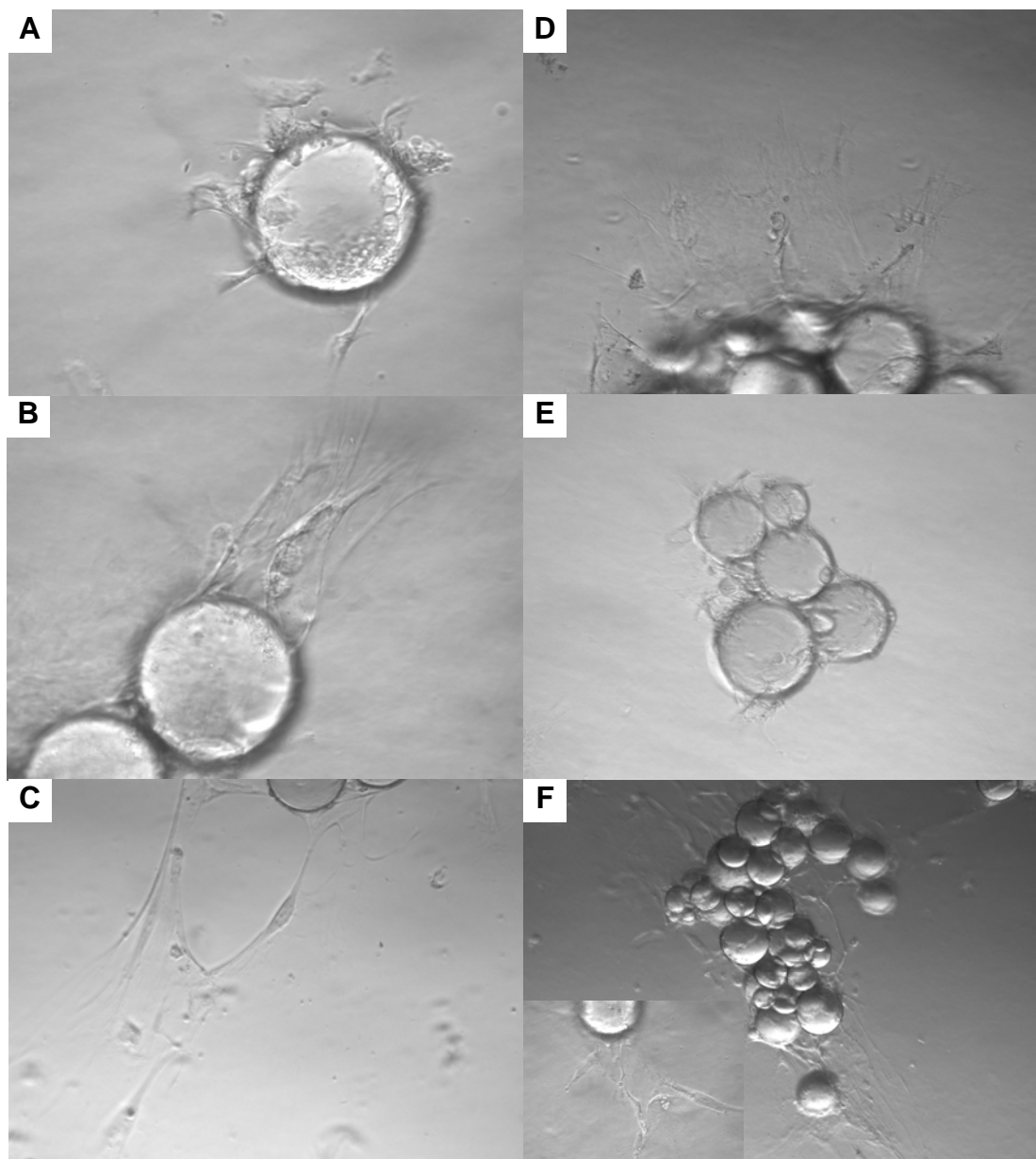


**Figure 6-8.** *In vitro* formation of capillary network using HUVEC-coated GMs embedded into a fibrin gel. (A, D) HUVEC grown on blank GMs, (B, E) HUVEC grown on blank GMs with bFGF as supplement of the cell culture medium and (C, F) HUVEC grown on GMs incorporated with bFGF. The left column indicated the cells grew in the gel for 1 day, while the right column indicated the cell grew in the gel for 5 days. The microspheres were cross-linked with 10 mM GTA.



### 6.3 Conclusion

In this study, gelatin microspheres fabricated using a water-in-oil emulsion technique were studied as a scaffold for culturing human umbilical vein endothelial cells for the application of *in vitro* vascularization. As compared to cells cultured on tissue culture plates, cells grown on microsphere scaffold showed much higher proliferation rates and elongated morphologies. The cells also showed higher proliferation rate when cultured on gelatin microspheres cross-linked with higher concentrations than lower concentrations of glutaraldehyde. Basic fibroblast growth factor was subsequently incorporated into the gelatin microspheres based on ionic complexation. The improved cell proliferation with controlled release of bFGF, compared to blank microspheres indicated that the bioactivity of bFGF was well maintained during the incorporation and release. In the presence of bFGF, capillary networks were developed when HUVECs coated gelatin microspheres were embedded in a fibrin gel, and the controlled and localized delivery of bFGF to the cells further stabilized the network *in vitro*.

## Chapter 7 Conclusions and Recommendations

This study investigated the viability of using a novel polymer microsphere as scaffolds for liver tissue regeneration. First, the sizes of the microsphere were optimized to guide the growth of liver cells. The viability of the scaffold was further improved through surface conjugation with extracellular matrix proteins and encapsulation of growth factors.

### 7.1 Conclusions

Polymeric microspheres fabricated from poly(3-hydroxybutyrate-co-3-hydroxyvalerate) (PHBV, 8% PHV) using emulsion solvent evaporation method, were investigated as novel scaffolds for liver tissue regeneration. Compared with cells cultured on two-dimensional controls, cells grown on microsphere scaffold showed higher proliferation as well as improved hepatic functions. This could be attributed to the large surface area provided by the microspheres, which allowed for larger cell populations. More importantly, it is believed that the spherical shape of the scaffold affects cell adhesion, proliferation and function greatly. Smaller microspheres improved cell-cell interaction and cell-substrate interaction which can stimulate cell proliferation and function. It was found that PHBV microspheres with the size range between 100-300 $\mu$ m were the most suitable to support growth of the liver cells. The

microspheres were assembled by the cells into various shapes after two weeks of culture, which would be desirable for the defects with irregular structures or organs with complex architecture. Although multilayers of cells was formed among the cell-scaffold constructs, the viability of the cells was well preserved as confirmed by live/dead assay.

We have also demonstrated that the biocompatibility of the PHBV microsphere scaffolds can be improved through surface conjugation with extracellular matrix (ECM) proteins, namely collagen, laminin and fibronectin. Successful conjugations of protein molecules were verified by the presence of nitrogen peaks in X-ray photoelectron spectroscopy (XPS) and fluorescence microscope. The improved proliferation of cells cultured on the combination of three protein-conjugated microspheres suggested that the proliferation activity of Hep3B did not just depend on single protein, but rather, involved complex interactions with all of the ECM components. Therefore, combinations of ECM components is important not just in improving the biocompatibility of tissue engineering scaffolds, but also in enhancing cellular function. Furthermore, hepatocytes with round morphology were found to possess better hepatic functions while having lower proliferation. Conversely, high proliferation would tend to lower cell function. Thus, in the design of a tissue engineering system, a scaffold showing different surface properties at different cell development stages might be necessary.

One advantage of using microspheres as scaffold is that growth factors can be encapsulated into the scaffold directly. Three types of polymer microspheres with distinct release profiles of protein were fabricated. The composite microspheres

(PHBV/PLGA), which were developed with a core-shell structure, were shown to possess a moderate degradation rate, well preserved structure and better controlled delivery for hepatocyte growth factor (HGF) during three months of incubation. The inhibition of Hep3B cells growth indicated that the HGF released from PHBV/PLGA microspheres maintained its bioactivity for at least for 40 days. Furthermore, the three-dimensional microsphere scaffold, with direct delivery of HGF to the cells grown on it, was shown to better maintain the viability and phenotype of the primary hepatocytes. Bovine serum albumin was also proven to be a suitable model protein for HGF and functioned as stabilizer to prevent the denaturation of HGF during the fabrication process.

Vascularization of the scaffold system to provide the cells with nutrients and oxygen efficiently is a prerequisite for the success in engineering large tissues such as the liver. Gelatin microspheres based three-dimensional vascularization *in vitro* was studied. As compared to cells cultured on tissue culture plates, human umbilical vein endothelial cells (HUVECs) grown on gelatin microspheres showed much higher proliferation rates and elongated morphologies. The cells also showed higher proliferation rate when cultured on gelatin microspheres cross-linked with higher concentrations than lower concentrations of glutaraldehyde. Basic fibroblast growth factor (bFGF) was subsequently incorporated into the gelatin microspheres based on ionic complexation. The improved cell proliferation with controlled release of bFGF, compared to blank microspheres, indicated that the bioactivity of bFGF was well maintained during the incorporation and release process. In the presence of bFGF, capillary networks were developed when HUVECs coated gelatin microspheres were

embedded in a fibrin gel, and the controlled and localized delivery of bFGF to the cells further stabilized the network *in vitro*.

In summary, we have developed a novel and versatile tissue engineering system using polymeric microspheres as the scaffold. This versatility includes not just the ease of scaffold assembly into various shapes suitable for different tissue applications, but also offers easy and controllable surface modification and growth factor encapsulation properties as well as *in vitro* vascularization. This system has great potential for regeneration of liver tissue or any other large tissue to reduce the cost of implantation and solve the shortage of organ donors.

## **7.2 Recommendations for Future Works**

### **7.2.1 In vivo animal test**

The present work focuses on demonstrating the viability of using microspheres as tissue engineering scaffold. *In vitro* cell culture is believed to be adequate to achieve this purpose. However, *in vivo* animal tests can further verify this viability and give us better understanding of the interactions between the engineered liver tissue and the host. This is also the necessary step before it can be applied for human liver tissue regeneration. Therefore, implantation of the engineered liver tissue with microsphere scaffold into animal models (rats or mice) is suggested for future work. For convenient surgical operation, the cell-microsphere constructs could be embedded into biocompatible gel before implantation. Sodium alginate which is polysaccharide, could be a good candidate due to its hydrophilicity and biocompatibility. Soluble sodium alginate is water soluble, and it can be cross-linked with divalent cations such as calcium, to form an insoluble alginate gel (Marijinissen et al., 2002; Wang et al., 2003).

### 7.2.2 Co-culturing hepatocytes with nonparenchymal cells

A major challenge in constructing an engineered functional liver tissue is the short-term survival and rapid de-differentiation of hepatocytes in *in vitro* culture. Cell-cell interactions (homotypic and heterotypic) have been proved to play an important role in modulating and preserving the phenotype of primary hepatocyte. Many researches have shown that co-culturing hepatocytes with nonparenchymal cells such as fibroblast can preserve hepatocyte morphology and the synthetic, metabolic and detoxification functions of the liver (Bhatia et al., 1997; Bhandari et al., 2001). Similar conclusions have also been obtained by co-culturing hepatocytes with liver-derived cells such as Ito cells and epithelial cells (Mesnil et al., 1987; Loreal et al., 1993;). Therefore, co-culturing primary hepatocyte with fibroblast and endothelial cells is suggested for future work. The three types of cells could be firstly cultured on different sets of microspheres. After the cells grow to confluency, different cells attached microspheres could be then mixed in different ratios to form a co-culture system. The heterotypic interactions between different cell types could be studied by changing the ratios of the microspheres.

### 7.2.3 Dual growth factor delivery system

PHBV/PLGA composite microsphere with core-shell structure can encapsulate different growth factors in its core and shell separately. In this case, the release of different growth factors could be controlled in a time and spatial sequence which could be useful in simulating the *in vivo* environment of human body. For example, in skin wound healing, platelet-derived growth factor is applied as the early mediator of inflammatory process, and then basic fibroblast growth factor is applied as an

angiogenic factor to accelerate healing and improve the healing quality. Due to time constrain, this is not covered in this thesis. Future work could involve encapsulating two growth factors or even multiple growth factors and releasing them in a desired sequence. This would be very useful not only for tissue regeneration but also for growth factor therapies.

#### **7.2.4 Other tissue regeneration using microsphere scaffold**

Small microspheres can be self-assembled into various shapes which could be fitted into irregular shaped implantation sites without arousing inflammatory response. For regeneration of large organ such as heart and kidney, it is not always feasible to fabricate a big polymer scaffold with the same shape as the organs due to limitations of experimental conditions. The self-assembly ability of microspheres may address this difficulty since small scale tissue units are formed initially *in vitro*. Large organ might eventually be regenerated by implanting these tissue units. Therefore, besides regeneration of liver tissue, regeneration of other tissue could be attempted by using the microsphere scaffolding system discussed in this thesis.

## List of Publications

### Journal Publications:

1. **X.H. Zhu**, C-H Wang, Y.W. Tong. Growing tissue-like constructs with Hep3B/HepG2 liver cells on PHBV microspheres of different sizes. *J Biomed Mater Res: Appl Biomater*, 82B: 7-16, **2007**.
2. **X.H. Zhu**, S.K. Gan, C-H Wang, Y.W. Tong. Proteins combination on PHBV microsphere scaffold to regulate Hep3B cells activity and functionality: a model of liver tissue engineering system. *J Biomed Mater Res Part A*, 83A:606-616, **2007**.
3. **X.H. Zhu**, C-H. Wang, Y.W. Tong. *In vitro* characterization of hepatocyte growth factor release from PHBV/PLGA microsphere scaffold. *J Biomed Mater Res Part A*. **2008 (In press)**
4. S.T. Khew, **X.H. Zhu**, Y.W. Tong. An integrin-specific collagen-mimetic peptide (CMP): a biomolecular approach for optimizing cell adhesion, proliferation, and cellular functions. *Tissue Eng.* 13 (10): 2451-2463, **2007**
5. **X.H. Zhu**, L. Y. Lee, J. S. Hong (Jackson), Y. W. Tong, C-H Wang. Characterization of porous poly (D,L-lactic-co-glycolic) acid sponges fabricated by supercritical CO<sub>2</sub> gas-foaming method as a scaffold for three-dimensional growth of Hep3B cells. *Biotechnology and Bioengineering*, **2008 (In press)**
6. **X.H. Zhu**, Y. Tabata, C-H. Wang, Y.W. Tong. Delivery of basic fibroblast growth factor from gelatin microsphere scaffold for the growth of human umbilical vein endothelial cells. *Tissue Eng.* **2008 (In press)**

### Conference Presentations:

1. **X.H. Zhu**, C-H. Wang, Y.W. Tong. PHBV microspheres as scaffold for liver tissue engineering. ICMAT2005, Suntec City, Singapore, July 3-8, **2005**.
2. **X.H. Zhu**, C-H. Wang, Y.W. Tong. Growing tissue-like constructs with Hep3B/HepG2 liver cells on PHBV microsphere scaffold. AIChE 2006 annual meeting, San Francisco, USA, Nov. 12-16, **2006**
3. **X.H. Zhu**, C-H. Wang, Y.W. Tong. Combination of proteins on PHBV microsphere scaffold to regulate Hep3B cells activity and functionality for an in vitro model of liver tissue engineering. AIChE 2006 annual meeting, San Francisco, USA, Nov. 12-16, **2006**



4. S.T. Khew, **X.H. Zhu**, Y.W. Tong. Collagen-mimetic peptide (CMP) for integrin-specific cellular recognition and tissue engineering. AIChE 2006 annual meeting, San Francisco, USA, Nov. 12-16, **2006**
5. **X.H. Zhu**, C-H. Wang, Y.W. Tong. Primary hepatocyte culture on polymeric microsphere scaffold with human hepatocyte growth factor release. SFB 2007, Chicago, USA, April 18-21, 2007.
6. Y.W. Tong and **X.H. Zhu**. Engineering liver tissue with microsphere scaffold. ICMAT 2007, Suntec City, Singapore, July 2-6, **2007**.
7. **X.H. Zhu**, C-H. Wang, Y.W. Tong. Culturing liver cells on gelatin microspheres versus PHBV microspheres. WACBE 2007, Bangkok, Thailand, July 9-11, **2007**.

## References

- Avella M., Martuscelli E., Raimo M. Review: Properties of blends and composites based on poly(3-hydroxy)butyrate (PHB) and poly(3-hydroxybutyrate-hydroxyvalerate) (PHBV) copolymers. *J. Mater. Sci.*, 35, pp. 523– 545. 2000
- Babensee J.E., McIntire L.V., Mikos A.G. Growth factor delivery for tissue engineering. *Pharm. Res.*, 17, pp. 497-504. 2000
- Barrias C.C., Ribeiro C.C., Lamghari M., Miranda C.S., Barbosa M.A. Proliferation activity and osteogenic differentiation of bone marrow stromal cells cultured on calcium titanium phosphate microspheres. *J. Biomed. Mater. Res.*, 72A, pp. 57-66. 2005.
- Bartolo L.D., Morelli S., Lopez L.C., Giorno L. et al. Biotransformation and liver-specific functions of human hepatocytes in culture on RGD-immobilized plasma-processed membranes. *Biomaterials*, 26, pp. 4432–4441. 2005.
- Benzeev A., Robinson G.S., Bucher N.L.R., Farmer S.R. Cell-cell and cell-matrix interactions differentially regulate the expression of hepatic and cytoskeletal genes in primary cultures of rat hepatocytes. *Proc. Natl. Acad. Sci.*, 85, pp. 2161-2165. 1998.
- Bhadriraju K. and Hansen L.K. Hepatocyte adhesion, growth and differentiated function on RGD-containing proteins. *Biomaterials*, 21, pp. 267-272, 2000.
- Bhandari R.N.B., Riccalton L.A., Lewis A.L., Fry J.R., Hammond A.H., Tendler S.J.B., Shakesheff K.M. Liver tissue engineering: A role for co-culture systems in modifying hepatocyte function and viability. *Tissue Eng.*, 7(3), pp. 345-357. 2001.
- Bhatia S.N., Yarmush M.L., Toner M. Controlling cell interactions by micropatterning in co-cultures: hepatocytes and 3T3 fibroblasts. *J. Biomed. Mater. Res.*, 34, pp.189-199. 1997.

- Biltresse S., Attolini M., Marchand-Brynaert J. Cell adhesive PET membranes by surface grafting of RGD peptidomimetics. *Biomaterials*, 26, pp. 4576–4587. 2005.
- Bissell D.M., Arenson D.M., Maher J.J., Roll F.J. Support of cultured hepatocytes by a laminin-rich gel. *J. Clin. Invest.*, 79, pp. 801-812. 1987.
- Brieva T.A., Moghe P.V. Engineering the hepatocyte differentiation–proliferation balance by acellular cadherin micropresentation. *Tissue Eng.*, 10, pp. 553-564. 2004.
- Buschmann I., Schaper W. The pathophysiology of the collateral circulation (arteriogenesis). *J. Pathol.*, 1990, pp. 338-342. 2000
- Caldwell K.D. Surface modifications with adsorbed poly(ethylene oxide)-based block copolymers. In *Poly(ethylene glycol) chemistry and biological applications*, ACS Symposium Series 680, ed by Harris J.M. and Zalipsky S. Washington, DC: American Chemical Society. c1997
- Cao X.D. and Shoichet M.S. Delivering neuroactive molecules from biodegradable microspheres for application in central nervous system disorders. *Biomaterials*, 20, pp. 329-339. 1999.
- Carlisle E.S., Marinappan M.R., Nelson K.D., Thomes B.E. Enhancing hepatocyte adhesion by pulsed plasma deposition and polyethylene glycol coupling. *Tissue Eng*, 6(1), pp. 45-52. 2000.
- Chen R., Curran S.J., Curran J.M., Hunt J.A. The use of poly(L-lactide) and RGD modified microspheres as cell. *Biomaterials*, 27, pp.4453-4460. 2006.
- Chen R.R. and Mooney D.J. Polymeric growth factor delivery strategies for tissue engineering. *Pharmaceut. Res.*, 20(8), pp. 1103-1112. 2003.
- Chua K.N., Lim W.S., Zhang P.C., Lu H.F. et al. Stable immobilization of rat hepatocyte spheroids on galactosylated nanofiber scaffold. *Biomaterials*, 26, pp. 2537–2547. 2005.

Clement B., Loreal O., Rescan P.Y., Levavasseur F., Diakonova M., Rissel M., L'Helgoualch A., Guillouzo A. Cellular origin of the hepatic extracellular matrix. In Proc. International Falk Symposium, Molecular and cell biology of liver fibrinogenesis, ed by Gressner A.M. and Ramador G., 1992, Marburg, Germany, pp. 85-98.

Coombes A.G.A., Rizzi S.C., Williamson M., et al. Precipitation casting of polycaprolactone for applications in tissue engineering and drug delivery. *Biomaterials*, 25, pp. 315-325. 2004.

Curtis A.S.G. (ed) and Lackie J.M (ed). *Measuring cell adhesion*. New York: Wiley. c1991

Davis M.W., Vacanti J.P. Toward development of an implantable tissue engineered liver. *Biomaterials*, 17, pp. 365-372. 1996.

DeFail A.J., Chu C.R., Izzo N., Marra K.G. Controlled release of bioactive TGF- $\beta$ 1 from microspheres embedded within biodegradable hydrogels. *Biomaterials*, 27, pp. 1579-1585. 2006.

Deuel T.F. and Zhang N. Growth factors. In *Principles of tissue engineering*, 2<sup>nd</sup> edition, ed by Lanza R.P., Langer R., Vacanti. J, pp.553-557. California: Academic Press. 2000.

Doyle C., Tanner E.T., Bonfield W. In vitro and in vivo evaluation of polyhydroxybutyrate and of polyhydroxybutyrate reinforced with hydroxyapatite. *Biomaterials*, 12(9), pp. 841-847. 1991.

Drumm K., Lee E., Stanners S., Gassner B., Gekle M., Poronnik P., Pollock C.A. Albumin and glucose effects on cell growth parameters, albumin uptake and Na/H exchanger isoform 3 in OK cells. *Cell. Physiol. Biochem.*, 13, pp. 199-206. 2003.

- Dvir-Ginzberg M., Gamlieli-Bonshtein I., Agbaria R., et al. Liver tissue engineering within alginate scaffolds: effects of cell-seeding density on hepatocyte viability, morphology, and function. *Tissue Eng.*, 9(4), pp. 757-766. 2003.
- Freed L.E., Vunjak-Novakovic G. Culture of organized cell communities. *Adv. Drug Deliver. Rev.* 33, pp.15-30. 1998.
- Frerich B., Lindemann N., Hoffmann J.K., Oertel K. In vitro model of a vascular stroma for the engineering of vascularized tissue. *J. Oral Maxillofac Surg.*, 30, pp. 414-420. 2001.
- Fukai K., Yokosuka O., Chiba T., Hirasawa Y., Tada M., Imazeki F., Kataoka H., Saisho H. Hepatocyte growth factor activator inhibitor 2/Placental bikunin (HAI-2/PB) gene is frequently hypermethylated in human hepatocellular carcinoma. *Cancer Res.*, 63, pp. 8674-8679. 2003.
- Gan L., Gomez R.D., Powell C.J., McMichael R.D., Chen P.J., Egelhoff W.F. Thin Al, Au, Cu, Ni, Fe and Ta films as oxidation barriers for Co in air. *J. Appl. Phys.*, 93(10), pp. 8731-8733. 2003.
- Glicklis R., Shapiro L., Agbaria R., Merchuk J.C., Cohen S. Hepatocyte behavior within three-dimensional porous alginate scaffolds. *Biotechnol. Bioeng.*, 67(3), pp. 344-353. 2000.
- Goodstone N.J., Cartwright A., Ashto B. Effects of high molecular weight hyaluronan on chondrocytes cultured within a resorbable gelatin sponge. *Tissue Eng.*, 10, pp. 621-631. 2004.
- Griffith C.K., Miller C., Sainson R.C.A., Calvert J.W., Jeon N.L., Hughes C.C.W., George S.C. Diffusion limits of an in vitro thick prevascularized tissue. *Tissue Eng.*, 11, pp. 257-266. 2005

Gumucio J.J., Berkowitz C.M., Webster S.T., Thornton A.J.. Structural and Functional Organization of the Liver. In *Liver and Biliary Diseases*, 2<sup>nd</sup> edition, ed by Kaplowitz N. pp.3-20. Baltimore: Williams & Wilkins. c1996.

Gürsel İ., Korkusuz F., Türesin F., Alaeddinoğlu N.G., Hasırcı V. In vivo application of biodegradable controlled antibiotic release systems for the treatment of implant-related osteomyelitis. *Biomaterials*, 22, pp. 73-80. 2001.

Hansen L.K. and Albrecht J.H. Regulation of the hepatocyte cell cycle by type I collagen matrix: role of cyclin D1. *J. Cell Sci.*, 112, pp. 2971-2981. 1999.

Hersel U., Dahmen C., Kessler H. RGD modified polymers: biomaterials for stimulated cell adhesion and beyond. *Biomaterials*, 24, pp. 4385–4415. 2003.

Holland T.A., Tabata Y., Mikos A.G. Dual growth factor delivery from degradable oligo(poly(ethylene glycol) fumarate) hydrogel scaffolds for cartilage tissue engineering. *J. Cont. Rel.*, 101, pp. 111-125. 2005.

Hong Y., Gao C.Y., Xie Y., Gong Y.H., Shen J.C. Collagen-coated polylactide microspheres as chondrocyte microcarriers. *Biomaterials*, 26, pp. 6305-6313. 2005.

Hu S.G., Jou C.H., Yang M.C. Protein adsorption, fibroblast activity and antibacterial properties of poly(3-hydroxybutyric acid-co-3-hydroxyvaleric acid) grafted with chitosan and chitooligosaccharide after immobilized with hyaluronic acid. *Biomaterials*, 24, pp. 2685–2693. 2003.

Hubbell JA. Matrix Effects. In *Principles of tissue engineering*, 2<sup>nd</sup> edition, ed by Lanza R.P., Langer R., Vacanti. J, pp. 237-250. California: Academic Press. 2000.

Hubbell J.A. and Langer R. Tissue engineering. *Chem. Eng. News.*, 73(11), pp. 42-54. 1995.

Hynes R.O.(ed). *Fibronectins*. Pp. 188-189, New York: Springer-Verlag. 1990.

Ishihara M., Obara K., Ishizuka T., Fujita M. Controlled release of fibroblast growth factors and heparin from photocrosslinked chitosan hydrogels and subsequent effect on in vivo vascularization. *J. Biomed. Mater. Res.*, 64A, pp. 551-559. 2003.

Jacobson B.S., Ryan U.S. Growth of endothelial and HeLa cells on a new multipurpose microcarrier that is positive, negative or collagen coated. *Tissue Cell*, 14(1), pp. 69-83. 1982.

Jagur-Grodzinski J. Polymers for tissue engineering, medical devices, and regenerative medicine: concise general review of recent studies. *Polym. Adv. Technol.*, 17, pp. 395-418. 2006.

Jun H.W. and West J. Development of a YIGSR-peptide-modified polyurethaneurea to enhance endothelialization. *J. Biomater. Sci. Polymer Edn*, 15 (1), pp. 73–94. 2004.

Khang G., Choe J.H., Rhee J.M., Lee H.B. Interaction of different types of cells on physicochemically treated poly(L-lactide-co-glycolide) surfaces. *J. Appl. Polym. Sci*, 85, pp.1253-1262. 2002.

Kim K., Yu M., Zong X., Chiu J., Fang D., Seo Y., Hsiao S., Chu B., Hadjiargyrou M. Control of degradation rate and hydrophilicity in electrospun non-woven poly(D,L-lactide) nanofiber scaffolds for biomedical applications. *Biomaterials*, 24, pp. 4977–4985. 2003.

Köse G.T., Kenar H., Hasırcı N., Hasırcı V. Macroporous poly(3-hydroxybutyrate-co-3-hydroxyvalerate) matrices for bone tissue engineering. *Biomaterials*, 24, pp. 1949–1958. 2003.

Ku Y., Chung C.P., Jang J.H. The effect of the surface modification of titanium using a recombinant fragment of fibronectin and vitronectin on cell behavior. *Biomaterials*, 26, pp. 5153–5157. 2005.

Langer R. Selected advances in drug delivery and tissue engineering. *J. Control. Release.*, 62, pp. 7-11. 1999.

Langer R. and Vacanti J.P. Tissue engineering. *Science*, 260, pp. 920-926. 1993.

Layman H., Spiga M.G., Brooks T., Pham S., Webster K.A, Andreopoulos F.M. The effect of the controlled release of basic fibroblast growth factor from ionic gelatin-based hydrogels on angiogenesis in a murine critical limb ischemic model. *Biomaterials*, 28, pp. 2646-2654. 2007.

Leach K., Noh K., Mathiowitz E. Effect of manufacturing conditions on the formation of double-walled polymer microspheres. *J Microencapsul.*, 16, pp.153-167. 1999.

Lee K.B., Kim D.J., Lee Z.W., Woo S.I., Choi I.S. Pattern generation of biological ligands on a biodegradable poly(glycolic acid) film. *Langmuir*, 20, pp.2531-2535. 2004.

Levenberg S., Rouwkema J., Macdonald M., Garfein E.S., Kohane D.S, Darland D.C, Marini R., Blitterswijk C.A.V., Mulligan R.C., D'Amore R.A., Langer R. Engineering vascularized skeletal muscle tissue. *Nature Biotechnol.*, 23, pp. 879-884. 2005.

Levick J.R. (ed). *An introduction to cardiovascular physiology*. Pp.118-238, London: Arnold. 2000.

Li J.L., Pan J.L., Zhang L.G., Yu Y.T. Culture of hepatocytes on fructose-modified chitosan scaffolds. *Biomaterials*, 24, pp.2317–2322. 2002.

Lin H.R., Yen Y.J. Porous Alginate/Hydroxyapatite Composite Scaffolds for Bone Tissue Engineering: Preparation, Characterization, and In Vitro Studies. *J. Biomed. Mater. Res.*, 71B, pp. 52-65. 2004.

Loreal O., Levavasseur F., Fromaget C., Gros D. Cooperation of Ito cells and hepatocytes in the deposition of an extracellular matrix in vitro. *Am. J. Pathol.*, 143, pp. 538-544. 1993.



- Majima T., Funakosi T., Iwasaki N., Yamane S., Harada K. Alginate and chitosan polyion complex hybrid fibers for scaffolds in ligament and tendon tissue engineering. *J. Orthop. Sci.*, 10, pp.302–307. 2005.
- Malda J., Kreijveld E., Temenoff J.S., Van Blitterswijk C.A., Riesle J. Expansion of human nasal chondrocytes on macroporous microcarriers enhances redifferentiation. *Biomaterials*, 24, pp.5153-5161. 2003.
- Malm T., Bowald S., Karacagil S., Bylock A., Busch C. A new biodegradable patch for closure of atrial septal defect- An experimental study. *Scand J Thorac Cardiovasc Surg*, 26(1), pp.9-14. 1992.
- Marijijnissen W.J.C.M, Osch G.J.V.M.V., Aigner J., Veen S.W.V.D., Hollander A.P., Verwoerd-Verhoef H.L., Verhaar J.A.N. Alginate as a chondrocyte-delivery substance in combination with a non-woven scaffold for cartilage tissue engineering. *Biomaterials*, 23, pp.1511-1517. 2002.
- Marler J.J., Upton J., Langer R., Vacanti J.P. Transplantation of cells in matrices for tissue regeneration. *Adv. Drug Deliver. Rev.*, 33, pp.165-182. 1998.
- Marui A., Kanematsu A., Yamahara K., Doi K., Kushibiki T., Yamamoto M., Itoh H., Tabata Y., Komeda M. Simultaneous application of basic fibroblast growth factor and hepatocyte growth factor to enhance the blood vessels formation. *J. Vasc. Surg.*, 41, pp.82-90. 2005.
- Massia S.P. and Stark J. Immobilized RGD peptides on surface-grafted dextran promote biospecific cell attachment. *J. Biomed. Mater. Res.*, 56, pp.390-399. 2001.
- Merrett K., Griffith C.M., Deslandes Y., Pleizier G., Sheardown H. Adhesion of corneal epithelial cells to cell adhesion peptide modified pHEMA surfaces. *J. Biomater. Sci. Polym. Edn.*, 12, pp. 647–671. 2001.

Mercier N.R., Costantino H.R., Tracy M.A., Bonassar L.J. Poly(lactide-co-glycolide) microspheres as a moldable scaffold for cartilage tissue engineering. *Biomaterials*, 26, pp.1945-1952. 2005.

Mesnil M., Fraslin J., Piccoli C., Yamasaki H.Y., Gugen-Guillouzo C. Cell contact but not junctional communication (dye coupling) with biliary epithelial cells is required for hepatocytes to maintain differentiated functions. *Exp. Cell Res.*, 173, pp. 173:524-533. 1987.

Mooney D.J., Hansen L., Vacanti J., Langer R., Farmer S., Ingber D. Switching from differentiation to growth in hepatocytes: controlled by extracellular matrix. *J. Cell. Physiol.*, 151, pp.497-505. 1992.

Murohara T. Therapeutic vasculogenesis using human cord blood-derived endothelial progenitors. *Trends Cardiovasc Med.*, 11, pp.303-307. 2001.

Nehls V., Herrmann R. The configuration of fibrin clots determines capillary morphologies and endothelial cell migration. *Microvasc Res.*, 51, pp.347-364. 1996.

Nerem R.M. The challenge of imitating nature. In *Principles of tissue engineering*, 2<sup>nd</sup> edition, ed by Lanza R.P., Langer R., Vacanti. J, pp.9-15. California: Academic Press. 2000.

Newman K.D. and McBurney M.W. Poly(D,L lactic-co-glycolic acid) microspheres as biodegradable microcarriers for pluripotent stem cells. *Biomaterials*, 25, pp.5763-5771. 2004.

Oe S., Fukunaka Y., Hirose T., Yamaoka Y. A trial on regeneration therapy of rat liver cirrhosis by controlled release of hepatocyte growth factor. *J. Control. Release*, 88, pp.193–200. 2003.

Pachence J.M., Kohn J. Biodegradable Polymers. In Principles of tissue engineering, 2<sup>nd</sup> edition, ed by Lanza R.P., Langer R., Vacanti. J, pp.263-277. California: Academic Press. 2000.

Peirce S.M., Skalak T.C. Microvascular remodeling a complex continuum spanning angiogenesis to arteriogenesis. *Microcirculation*, 10, pp.99-111. 2003.

Pekarek K.J., Jacob J.S., Mathiowitz E. Double-walled polymer microspheres for controlled drug release. *Letters to Nature*, 367, pp. 258-260. 1994.

Perets A., Baruch Y., Weisbuch F., Shoshany G. Enhancing the vascularization of three-dimensional porous alginate scaffolds by incorporation controlled release basic fibroblast growth factor microspheres. *J. Biomed. Mater. Res.*, 65A, pp.489-497. 2003.

Peters M.C, Isenberg B.C, Rowley J.A., Mooney D.J. Release from alginate enhances the biological activity of vascular endothelial growth factor. *J. Biomater. Sci. Polymer Edn*, 9(12), pp.1267-1278. 1998.

Rago R., Mitchen J., Wilding G. DNA fluorometric assay in 96-well tissue culture plates using Hoechst 33258 after cell lysis by freezing in distilled water. *Anal Biochem.*, 191, pp.31-34. 1990.

Rana B., Mischoulon D., Xie Y., Bucher N.L.R., Farmer S.R. Cell-extracellular matrix interactions can regulate the switch between growth and differentiation in rat hepatocytes: reciprocal expression of C/EBP $\alpha$  and immediate-early growth response transcription factors. *Mol Cell Biol.*, 14(9), pp.5858-5869. 1994.

Rezania A. and Healy K.E. The effect of peptide surface density on mineralization of a matrix deposited by osteogenic cells. *J. Biomed. Mater. Res.*, 52, pp.595–600. 2000.

Riley C.M., Fuegy P.W., Firpo M.A., Shu X.Z., Prestwich G.D., Peattie R.A. Stimulation of in vivo angiogenesis using dual growth factor-loaded crosslinked glycosaminoglycan hydrogels. *Biomaterials*, 27, pp.5935-5943. 2006.

Rodriguez-Lorenzo L.M. and Ferreira J.M.F. Development of porous ceramic bodies for applications in tissue engineering and drug delivery systems. *Mater. Res. Bull.*, 39, pp.83-91. 2004.

Sahoo S.K., Panda A.K., Labhasewar V. Characterization of porous PLGA/PLA microparticles as a scaffold for three-dimensional growth of breast cancer cells. *Biomacromolecules*, 6(2), pp.1132-1139. 2005.

Saltzman W.M., Olbricht W.L. Building drug delivery into tissue engineering. *Nature Review*, 1, pp.177-186. 2002.

Saltzman W.M. Cell interactions with polymers. In *Principles of tissue engineering*, 2<sup>nd</sup> edition, ed by Lanza R.P., Langer R., Vacanti J, pp.221-236. California: Academic Press. 2000.

Sanchez A., Alvarez A.M., Pagan R., Roncero C., Vilaro S., Benito M., Fabregat I. Fibronectin regulates morphology, cell organization and gene expression of rat fetal hepatocytes in primary culture. *J. of Hep.*, 32, pp.242-250. 2000.

Sendil D., Gursel I., Wise D.L., Hasircı V. Antibiotic release from biodegradable PHBV microparticles. *J. Control. Release*, 59, pp.207-217. 1999.

Shiota G., Rhoads D.B., Wang T.C., Nakamura T., Schmidt E.V. Hepatocyte growth factor inhibits growth of hepatocellular carcinoma cells. *Proc. Natl. Acad. Sci.*, 89, pp.373-377. 1992.

Stevens M.M., Qanadilo H.F., Langer R., Shastri V.P. A rapid-curing alginate gel system: utility in periosteum-derived cartilage tissue engineering. *Biomaterials*, 25, pp.887-894. 2004.

Tabata Y. The importance of drug delivery systems in tissue engineering. *PSTT*, 3, pp.80-89. 2000.

- Tabata Y., Hijikata S., Muniruzzaman M., Ikada Y. Neovascularization effect of biodegradable gelatin microspheres incorporating basic fibroblast growth factor. *J. Biomater. Sci. Polymer Edn.*, 10(1), pp.79-94. 1999.
- Tabata Y., Ikada Y. Protein release from gelatin matrices. *Adv Drug Deliver Rev.*, 31, pp.287-301. 1998.
- Tabata Y., Ikada Y., Morimoto K., Katsumata H., Yabuta T., Iwanaga K., Kakemi M. Surfactant-free preparation of biodegradable hydrogel microspheres for protein release. *J. Bioact. Compat. Pol.*, 14, pp.371-383. 1999.
- Tabata Y., Miyao M., Yamamoto M., Ikada Y. Vascularization into a porous sponge by sustained release of basic fibroblast growth factor. *J. Biomater. Sci. Polymer Edn.*, 10(9), pp.957-968. 1999.
- Tan E.C., Lin R., Wang C.H. Fabrication of double-walled microspheres for the sustained release of doxorubicin, *J. Colloid Interf Sci.*, 291, pp.135-143. 2005.
- Thomson R.C., Shung A.K., Yaszemski M.J., Mikos A.G. Polymer Scaffold Processing. In *Principles of tissue engineering*, 2<sup>nd</sup> edition, ed by Lanza R.P., Langer R., Vacanti. J, pp.251-262. California: Academic Press. 2000.
- Thwin C.S. Fabrication, characterization and degradation of PHB and PHBV microspheres for liver cell growth. Master Thesis, National University of Singapore. 2004.
- Tomomura A., Sawada N., Sattler G.L., Kleinman H.K., Pitot H. The control of DNA synthesis in primary cultures of hepatocytes from adult and young rats: interactions of extracellular matrix components, epidermal growth factors, and the cell cycle. *J Cell Physiol.*, 130, pp.221-227. 1987.
- Wallace D.G. and Rosenblatt J. Collagen gel systems for sustained delivery and tissue engineering. *Adv. Drug Deliver Rev.*, 55, pp.1631– 1649. 2003.

- Wan Y.Q., Yang J., Yang J.Q., Bei J.Z., Wang S.G. Cell adhesion on gaseous plasma modified poly-(l-lactide) surface under shear stress field. *Biomaterials*, 24, pp.3757–3764. 2003.
- Wang P.P., Frazier J., Brem H. Local drug delivery to the brain. *Adv. Drug Del. Rev.*, 54, pp.987-1013. 2002.
- Wang W.J., Wang X.H., Feng Q.L., Cui F.Z. Sodium alginate as a scaffold materials for hepatic tissue engineering. *J. Bioact. Compat. Pol.*, 18, pp.249-257. 2003.
- Watanabe Y., Liu X., Shibuya I., Akaike T. Functional evaluation of poly-(N-r-vinylbenzyl-O-b-Dgalactopyranosyl-[1-4]-D-gluconamide) (PVLA) as a liver specific carrier. *J. Biomater. Sci. Polymer Edn*, 11(8), pp.833–848. 2000.
- Wayne J.S., McDowell C.L., Shields K.J., Tuan R.S. In vivo response of polylactic acid-alginate scaffolds and bone marrow-derived cells for cartilage tissue engineering. *Tissue Eng.*, 11, pp.953-963. 2005.
- Wisseman K.W. and Jacobson B.S. Pure gelatin microcarriers: synthesis and use in cell attachment and growth of fibroblast and endothelial cells. *In Vitro Cell Dev-An.*, 21, pp.391-401. 1985.
- Yang Y.Y., Chia H.H., Chung T.S. Effect of preparation temperature on the characteristics and release profiles of PLGA microspheres containing protein fabricated by double-emulsion solvent extraction/evaporation method *J Control. Release*, 69, pp.81-96. 2000.
- Yang Y.Y., Shi M., Goh S.H., Moochhala S.M., Ng S., Heller J. POE/PLGA composite microspheres: formation and in vitro behavior of double walled microspheres. *J Control. Release*, 59, pp.201-213. 2003.
- Yang X.S., Zhao K., Chen G.Q. Effect of surface treatment on the biocompatibility of microbial polyhydroxyalkanoates. *Biomaterials*, 23, pp.1391–1397. 2002.